STUDY OF THE CLAY EFFECT ON CRUDE OIL COMBUSTION USING THERMOGRAVIMETRIC ANALYZER (TGA) AND DIFFERENTIAL SCANNING CALORIMETER (DSC)

BY

Youssef M. T. El-Shoubary

B.S., Cairo University, 1977

Submitted to the Department of Chemical and Petroleum Engineering and the Faculty of the Graduate School of the University of Kansas in partial fulfillment of the requirements of the degree of Master of Science.

Thesis Committee:

_____
Chairman

_____

_____

December, 1981

ACKNOWLEDGEMENTS

The author wishes to express his sincere thanks and gratitude to the following:

Dr. Shapour Vossoughi, who contributed generously of his time, advice, understanding and encouragement during this study.

Dr. Paul Willhite, Who contributed extensive time and effort in assisting the author throughout the course of this study and giving valuable advice and encouragment.

The Tertiary Oil Recovery Project at the University of Kansas, which provided the funding for this project.

Laurel Mueller, Ruth Sleeper and Nancy Prohaska for typing and reviewing this thesis.

My colleagues in Room 4021, who provided constant encouragement, and were always stimulating company.

ABSTRACT

The effects of clay on the crude oil combustion were studied using thermal analysis techniques (Thermogravimetric Analyzer (TGA) and Differential Scanning Calorimeter (DSC)). TGA and DSC thermograms were obtained for combustion of crude oil, crude oil in the presence of sand, clay, silica powder, different mixtures of each, and burned clay. In all obtained TGA thermograms, three distinct peaks were observed in the derivative curve. The first peak was identified as distillation peak while the second and the third were identified as cracking and burning peaks.

TGA thermograms were interpreted by using Arrhenius type kinetic model and ratio method to generate kinetic parameters (activation energy and reaction order). The DSC thermograms were evaluated to obtain heat values of the crude oil.

From the TGA runs, the activation energy of the first DTG peak, i.e., distillation, was unaffected by clay or silica powder, remaining in the range of 6000-7000 cal/gm-mole. However, there was a definite indication of clay catalytic effect on the second and third DTG peaks, i.e., combustion/cracking peaks. Activation energy for the second peak of the thermograms generated for crude oil and crude oil/sand mixtures was in the range of 41000-42000 cal/gm-mole while that of the clay mixture reduced to the level of 16000-18000 cal/gm-mole. Silica powder had a similar effect at higher weight fraction (80%) but its effect diminished when its weight fraction was reduced to 40%. Activation energy of around 46000-48000 cal/gm-mole was obtained for the third peak of the crude oil and the crude oil sand mixture; 39000 cal/gm-mole for

the crude oil/silica mixture; 19000 cal/gm-mole for the crude oil-clay mixture; and remained at around 48000 cal/gm-mole for the 40% silica mixture. The reaction order was always equal to 2.2 for the distillation peak and between 1 and 2 for the combustion/cracking peaks. A significant reduction of activation energy due to the addition of clay to the crude oil is a definite indication of catalytic and surface area effect on crude oil combustion/cracking reactions.

For the DSC thermograms, the addition of clay or silica powder to the crude oil mixture shifted a portion of the the total heat of the combustion reactions from a higher to a lower temperature range.

TABLE OF CONTENTS

TABLE OF CONTENTS (Cont.)

TABLE OF CONTENTS (Cont.)

LIST OF FIGURES

LIST OF FIGURES (cont.)

LIST OF FIGURES (cont.)

LIST OF FIGURES (Cont.)

LIST OF FIGURES (Cont.)

Figures Page

LIST OF TABLES

LIST OF TABLES (Cont.)

To my parents

CHAPTER 1

INTRODUCTION

Energy is a major problem in our world today. Crude oil is one of the most important sources of energy supply. Crude oil is found in porous sedimentry rocks like sandstone or limestone. On drilling a well through the porous rocks, primary methods such as gas drive and secondary methods such as water flooding, recover only one-third of the original oil in place[1]. The rest of the oil is trapped in the rocks as discontinuous droplets or in regions not swept by the displacing fluid. To recover this trapped oil new enhanced methods of oil recovery are required.

Enhanced oil recovery methods can recover at least 20% of the oil left in the reservoir[1], which is a significant portion. These methods could be used in addition to or beyond water flooding. They involve the injection of chemicals, such as carbon dioxide - micellar - polymer, or the use of thermal energy, such as steam - hot water - in-situ combustion.

Thermal recovery methods deal with producing high viscous (low ^{o}API gravity) crude oils. They can be divided into two major groups:

1- External power input: in these methods heat is produced first then injected into the reservoir. These are hot water flooding, cyclic steam stimulation, continuous steam flood, and steam slug flood.

2- Heat produced in-situ by burning a portion of the oil in place. These include forward and reverse in-situ combustion.

In-situ combustion as a thermal recovery method appears to be quite promising. In-situ combustion basically consists of injecting compressed air, with or without recycled gases, and igniting oil in porous reservoir rock with a suitable ignitor. The driving force of air and produced gases cause the oil bank to move through the reservoir toward producing wells. In the field, the ignition starts either by electrical means or by a gas burner and in some cases auto-ignition can be achieved. The fuel is a "coke like" residual material. A heat wave will be generated and whether the combustion can be sustained or not depends on the rate at which the fuel "coke" is formed from the original oil and the rate at which this fuel is burned. The economics of this process mostly depends on the amount of air to be injected and, consequently, upon the price of compressors.

Kinetics of the process play a dominant role in determining whether or not a self-sustained burning zone can be established. The in-situ combustion process has been widely studied in laboratory[2-8] as well as field operations[9-12,5] Most laboratory studies have been carried out to determine the effect of overall kinetic parameters on the combustion tube as a preparation for field tests. Different mathematical models[13-20,7] have also been developed to predict the related characteristics. In in-situ combustion tube runs, the combustion reaction occurs in a relatively narrow zone and heat wave starts to flow through the tube. The chemical reaction can be studied by itself, without a travelling heat wave, by applying the technique of thermal analysis or by using a combustion cell where a duplication of burning crude oil in the combustion tube can be obtained. No significant thermogravimetric

study has been carried out to study the crude oil oxidation behavior in porous media.

Thermogravimetry may be defined as a technique whereby the weight of a substance is recorded as a function of time or temperature isothermally or in an environment heated or cooled at a controlled rate.

Present day thermal analysis instruments are the result of a long period of development. The first crude instruments were manually controlled in that the data, e.g., temperature, was recorded point by point by the operator. With the advent of various recording techniques this tedious task was eliminated by the use of the new equipment. Further sophistication of this new equipment included automatic temperature programming and control, controlled furnance and sample environment, and data manipulation (differentiation and integration).

The objective of this investigation was to study the effects of clay on the burning of crude oil. The differential scanning calorimetry (DSC) and the thermogravimetric analyzer (TGA) were used to further demonstrate the catalytic and-or surface area effects of clay on crude oil combustion.

CHAPTER 2

LITERATURE SURVEY

In this chapter a historical review of thermogravimetric analysis as well as differential scanning calorimetry will be presented. Also, a review of the thermo-oxidative behavior of crude oils using thermal analysis techniques and the applications of kinetic models to interpretate the thermograms obtained will be presented.

2-1 Historical review of thermal analysis technique

2-1-1 Thermogravimetric analyzer

The art of weighing was known in ancient Egypt as early as 2800 B.C.[21] But, perhaps the earliest example of the use of weighing to follow a reaction was in the early fifteenth century[21] when gold was refined in Egypt by amalgamation with mercury. The amalgam was then kept in the molten state for 24 hours or so after which time the product was weighed in order to confirm the complete removal of mercury and impurities.

Probably one of the earliest appreciations of thermogravimetry was in 1780 when Dr. Bryan Higgins[22] realized that not only could information be obtained by weighing materials after heating, but that additional information could be derived by weighing the sample during heating. Higgins studied the effect of heating chalk and limestone at different temperatures with a view to improving the quality of quick lime. Further, he compared the melting points of mixtures with the melting point of known materials. Also, Higgins heated his samples in

static and flowing air and studied their effects on the properties of the end materials.

In 1886 Ellis Lovejoy published the weight losses of clays at the melting points of different metals and found that, Kaolin decomposed near the melting point of antimony (624^{o}C).

The world's first thermobalance was introduced into the science by Honda[22] in 1915. He designed and put into use the first apparatus worthy of this name. The work of Honda did indeed lay the foundation for practically all of the future work in thermogravimetry. His thermobalance enabled the investigator to continuously weigh the sample as it was heated and also, to employ the feature of quasi-isothermal heating.

In 1923 Guichard[22], assisted by his students, carried out a comprehensive series of systematic investigations. After several years of experience with the apparatus and technique, Guichard was prompted to warn workers of the care necessary in interpreting thermogravimetric curves because the shape was due to several factors, viz, partial pressure, amount of sample, diffusion of gas through the sample, and heating rate. Mass-loss curves recorded on this balance agreed well with the results obtained by Duval[23] some forty years later.

No less than fifty thermobalances had been described by 1961, and ten of these were commercially available[24]. At the present time there are books written on thermobalances and how to use them[23-25] Today thermal analysis is one of the fastest growing methods and computerized thermobalances are available. In recent years, new thermobalances have

appeared in the literature which enable working under pressure[26] or controlled humidity.[27]

2-1-2 Differential Scanning Calorimeter (DSC)

The measurement in the differential scanning calorimetry is based on the "null-balance" principle, in which heat energy adsorbed or evolved by the sample is compensated by adding or removing an equivalent amount of electrical energy to a heater located in the sample holder. In practice this is achieved by comparing the signal from a platinum resistance thermometer in the sample holder with that from an identical sensor in a reference holder. The continuous and automatic adjustment of heater power (energy per unit time) necessary to keep the temperature of the sample holder identical to that of the reference holder provides a varying electrical signal, opposite but equivalent to the varying thermal behavior of the sample. By recording the variable part of the electrical signal or differential power, a record of the sample behavior is obtained in power units and expressed in millicalories per second. The peak area is a true electrical energy measurement and its direction will determine whether the reaction is exothermic or endothermic.

The idea of the DSC was started by Le Chatelier. His work on clays and minerals consisted of thermal analysis determination employing a single thermocouple immersed in the sample. The thermocouple was embedded in the clay sample which was heated at about 100° C/min. Response from a galvanometer was measured by reflection of flashes from an induction coil from the galvanometer mirror to a photographic plate. The temperature of the sample was then displayed on the developed

photographic plate as a series of lines, each of which corresponded to a spark discharge which occured at 2 sec. An endothermic reaction was indicated by closely spaced lines, while wider spacing indicated an exothermic reaction.

In 1899 Robert Austin[24] came with the idea of using two thermocouples, one of the thermocouples was placed in the sample while the other in a reference block in the furnace. Thus, the differential temperature reading, which was more sensitive to small terperature changes in the sample than the single thermocouple method, was recorded or plotted as a function of time or temperature.

In 1908, Burgerss[24] discussed the difference between one or two thermocouples as applied to cooling curve data. He obtained a plot of sample temperature, T, verses time, t, also, a plot of T verses dT/dt. The first application of the differential scanning calorimeter to the study of a chemical problem was made by Houldsworth and Cobb in 1913 who studied phase transitions in silicate minerals. They also studied the behavior of fire clays and bauxite on heating, a field of investigation in which DSC has become an important tool.

The pioneering efforts of the clay mineralogists and metallurgists kept the technique of DSC alive, both experimentally and theoretically. As far as chemistry is concerned, the renaissance of DSC development and application occured during the early 1950's as a result of the work of Stone[28-29], Borchardt and Daniels.[30] Stone is credited with the development of the first modern, high quality commercial DSC instrumentation which served as a stimulus to further developments in this area.

In the 1960's, due to the availability of commercial instrumentation, the DSC technique was applied with great vigor to problems in polymer chemistry. DSC has become successful in measurement of small reactions and therefore is becoming more widely used to obtain analytical and calorimetric effects under extreme conditions.

2-2 Interpretation of data

In this section a description of the thermograms obtained with the Thermogravimetric analyzer (TGA) and the differential scanning calorimeter (DSC) will be presented. Also, the application of the thermogravimetric technique to study the kinetic parameters involved in a reaction will be discussed.

2-2-1 Explanation of thermograms obtained from TGA runs

Results from the programmed operation of a thermobalance (TGA) may be presented in two ways:

i- A plot of weight loss versus temperature (or time), which is called a TG curve. The weight is plotted on the ordinate, with weight decreasing downwards and temperature (T) or time (t) on the abscissa increasing from left to right.

ii- A plot of the rate of weight loss versus temperature (or time) which is called a derivative thermogravimetric curve (DTG). The DTG curve is plotted on the ordinate, with rate of weight loss decreasing from top to bottom and temperature T (or time t) on the abscissa increasing from left to right.

Figure 2-1 presents typical TG and DTG curves. From this figure one can distinguish three regions:

i- Plateau A on the TG curve indicates a constant weight region. The DTG curve corresponds to this portion of the TG curve with a straight line A', which indicates that the rate of weight loss with respect to time is zero. In other words, there is no weight change occuring in this temperature range.

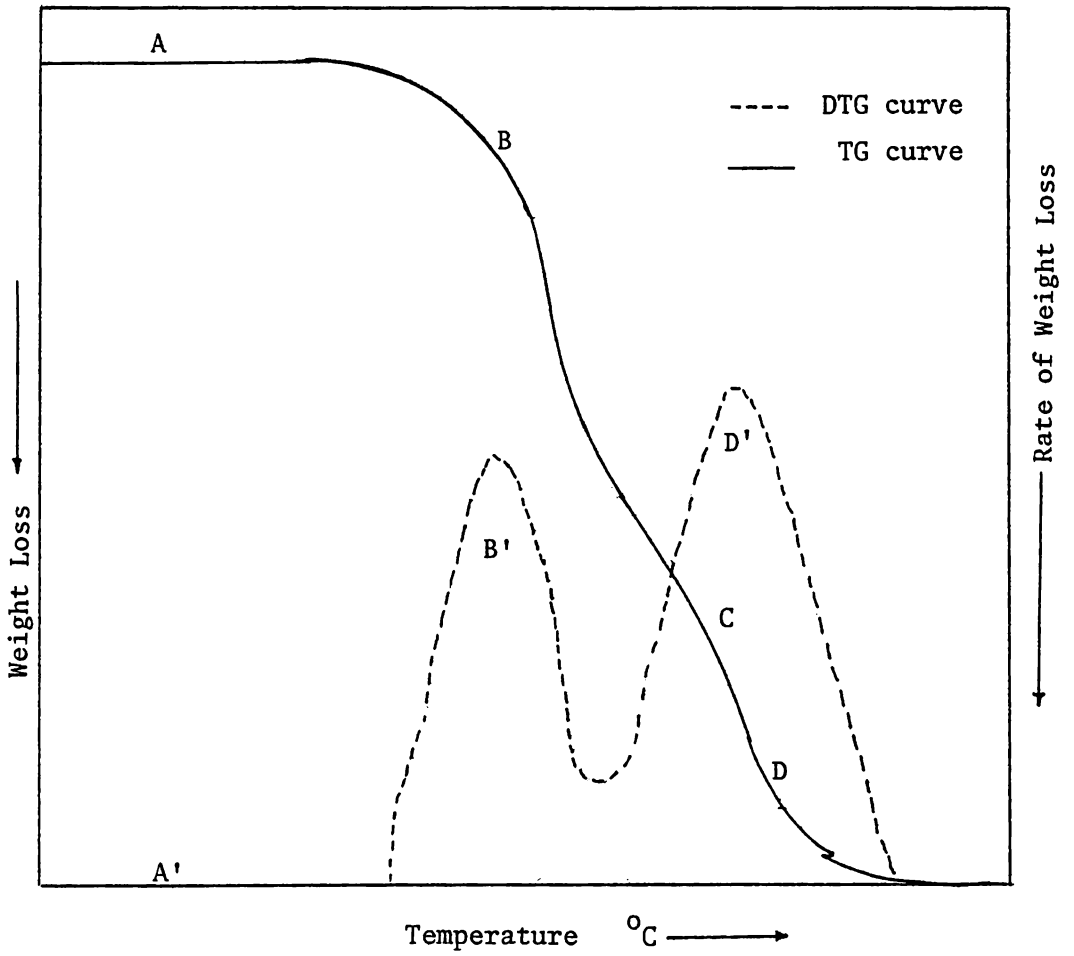

Figure 2-1 Typical TG and DTG curves

ii- The steepness of the curved portion B in the TG curve indicates weight loss with respect to temperature. The distinguished peak B' on the DTG curve corresponding to this portion of the DTG curve indicates that there is a weight change taking place at this range of temperature. The maximum rate of weight loss corresponds to the peak of the DTG curve.

iii- The C portion of the TG curve showed some weight gain which might be due to the addition of gaseous phase to the sample by adsorption or even by chemical reaction.

iv- The D portion of the TG curve showed weight loss with respect to temperature. The TG curve goes to zero at the end of portion D , i.e., there is no sample left on the sample pan at this temperature. The distinct peak D' on the DTG curve corresponds to this portion of the TG curve, indicating that at this range of temperature there is a reaction taking place which is different from other reactions took place before.

The DTG curve has certain advantages over the TG curve. For example, two overlapping reactions which often present a rather ill-defined TG curve will produce two distinguished peaks in DTG curves. Moreover, DTG curves often bear a strong resemblance to differential thermal analysis (DTA) curves and permit comparisons to be made.

2-2-2 Explanation of thermograms obtained from DSC runs

Results from the programmed operation of a differential scanning calorimeter (DSC) may be presented as follows:

A plot of rate of heat flow in cal/sec (Δq) versus temperature T (or time t) is given in Figure 2-2. The rate of heat flow (Δq) is plotted on the ordinate, with rate of heat flow decreasing from top to bottom and temperature T (or time t) on the abscissa increasing from left to right.

An endothermic peak is indicated by a peak in the downward direction (decrease in enthalpy) (peak A), while an exothermic peak is recorded in the opposite direction (peak B).

In DSC curves the peak areas are found between the themogram peak and the base line. The base line corresponds to the portion of the DSC curve for which heat flow rate (Δq) is approximately zero. Base line shifting occures due to the change in specific heat as well as bulk density of the sample. The peak area then is measured from the point where the thermogram departs from the base line to the point where it returns.

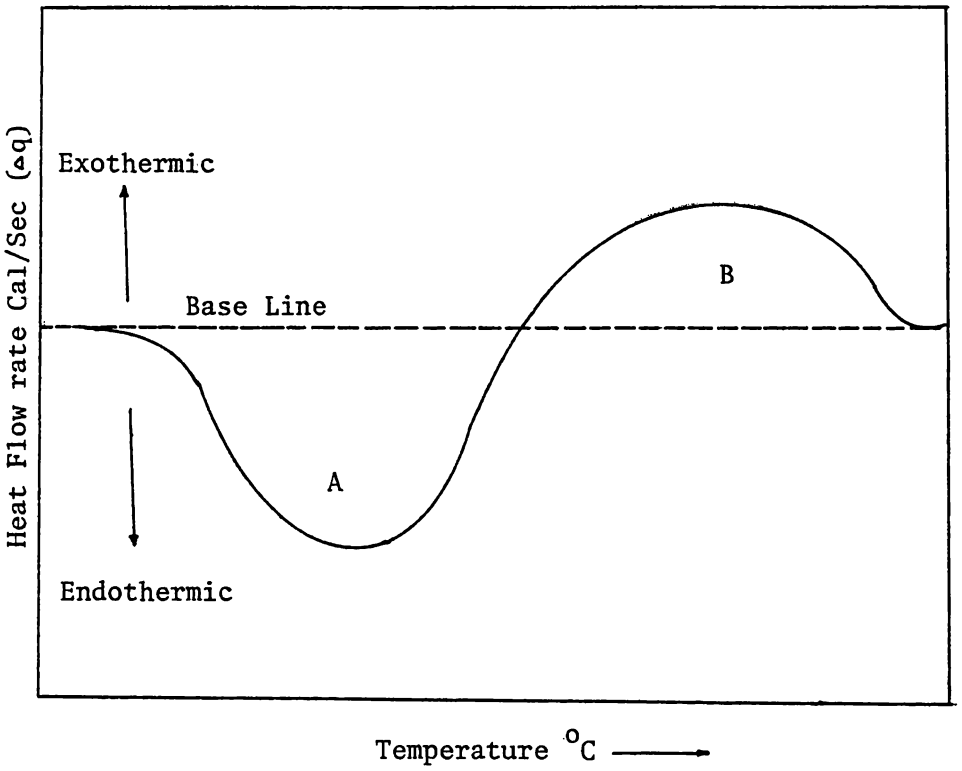

Figure 2-2 Typical DSC curve

2-2-3 Review of the application of thermogravimetric technique to study the kinetic parameters involved in a reaction

Several methods have been used to interpret the thermogravimetric curves. Some of these methods are very simple, while some others are complicated and involve a trial and error procedure.

Newkirk[31] made several runs using the TGA module to investigate the effect of heating rate on the decomposition reactions. From a single TG curve, Newkirk obtained rate constants for the decomposition reaction under study. He obtained the reaction rate by drawing tangents to the TG curve at several locations.

Coats and Redfern[32] investigated the thermogravimetric data to evaluate the kinetic parameters of solid state reactions involving weight loss (or gain). They measured the sample temperature by means of a thermocouple immersed directly in the sample. They fitted the data to linear equation, assuming the validity of Arrhenius' equation, to calculate the activation energy of the reaction in study. Their equation depended on the choice of the order of the reaction. The best straight line obtained will correspond to the right reaction order. The slope of the line will yield a value for the activation energy.

Freeman and Carroll[33] studied the kinetic parameters involved in a reaction under nonisothermal conditions. The advantage of this method is that considerably less experimental data is required than in the isothermal method, and that the kinetics can be obtained over an entire range of temperatures in a continuous manner without missing any region. They fitted the data to linear equation assuming the validity of Arrhenius' equation. A plot of the straight line will yield a value for

the reaction order (from the intersection with the Y axis) and a value for the activation energy (from the slope of the line). An explanation of this method is presented in Appendix A.

Horowitz and Metzger[34] studied the cases in which the rate constant involves concentration expressible as mole fractions with the total number of moles constant and derived an equation similar to Freeman and Carroll.[33]

Mickelson and Einhorn[35] studied the rate of decomposition of any material with respect to time and the fraction remaining at any temperature. He assumed the validity of Arrhenius' equation. He used a simple straight line equation to generate the kinetic data involved in a reaction. His method depended on the accuracy of the readings obtained from the thermogram derivative curve. Also, in this method the entire thermogram or a portion of it can be used to determine the kinetic parameters. This model will be presented in Appendix A.

Doyle[36] studied in detail the kinetics of volatilization of polymers using thermogravimetric techniques. He investigated the evaporation of octamethylcyclotetrasiloxane and polytetrafluorothylene in dry nitrogen atmosphere. His method of investigation depended on the choice of an equation that represents the portion of the thermogram under investigation.

Ozawa[37] and Satava[38] generated two approximate integral methods similar to Doyle's method. They reported that their methods had a wider range of application than Dolye's method. The only difference between Doyle's[36] method and these methods was in the choice of empirical equation representing the thermogram.

Zsako[39] also attempted to simplify Doyle's[36] trial and error method. The main modification was how to choose the best equation for the thermogram in study. His equation depended only upon the nature of the compound studied and upon the heating rate, but not temperature.

Wieckowsko and Bogdemaw[40] used Zsako's[39] model to investigate the mathematical description of the kinetics of the thermal decomposition of residue remaining after vaccum-distillation of Romashkino crude oil. To determine a function presenting the thermogram curve, they used polynomials of various degrees. They reported that Zsako's[39] model worked well except at high temperatures (above 723^{o}K) where the reaction occured so quickly.

Carroll[41] used the TGA, DSC, and DTA to describe the treatment of experimental data under non-isothermal conditions in order to obtain the kinetic parameters of chemical reactions. Carroll generated a model to get kinetic parameters from DSC curves. He also generated two models to get kinetic parameters from TGA curves, integral method and differential method. The models in all cases are straight line equations. When plotted the slope of the line will yield a value for the activation energy while the intersect with the Y axis will yeild a value for the order of the reaction.

Sharp[42] modfied Carroll's[41] method for the TGA models. His method is a differential one and applies to all reaction mechanism provided that the correct mechanism is known. This model also, produces a straight line equation from which activation energy, E, can be calculated.

Ellerstein[43] used Carroll's[41] method for DSC data to investigate the kinetics of thermal degradation of several synthetic polymers. He reported satisfactory results.

Vachuska and Vobori[44] evaluated the kinetic parameters from the thermogravimetric curves when a non-linear temperature rise is used. They provided a computer program to calculate the constants involved in their equation. This method took into account the thermal effects of reactions which result in a deviation of the sample temperatures from the programmed values of heating. The model is a straight line equation. Plotting this straight line, the intersection with the Y axis will yield a value of the activation energy and the slope will yield a value for the reaction order.

All these data treatment methods depend on the choice of an emperical model and fitting the data into it. Usually kinetic data generated using these methods has a small error ($\pm$ 10%) due to the accuracy in reading data from thermograms. The Freeman and Carroll[33] method, as well as the Mickelson and Einhorn[35] method, was used to analyze the data obtained in this study. The main reason for selecting these methods was in the simplicity of the two models.

2-3 Errors of kinetic data obtained from thermogravimetric technique curves at increasing temperature

In a thermoanalytic method, continuous changes of some physical properties such as weight, enthalpy, length or volume of the investigated sample are measured with temperature under a chosen temperature rise program. Computed kinetic data from such thermograms are influenced by:[45]

A- The accuracy of the data measurement (weight, temperature of sample, time, ...etc.)

B- The accuracy of maintaining conditions defined in advance during the reaction (linearity of temperature increase, constancy of aerodynamic conditions and composition of gaseous medium) and removing the influence of disturbing effects.

C- The accuracy in reading data from the produced thermoanalytic curves to fit into the chosen kinetic mode.

2-3-1 Accuracy of weight change and temperature measurements

Weight and temperature measurments mainly depend on the TGA apparatus, the sensitivity of its balance and the thermocouple and its position. It should be noted here that the thermocouples of both DuPont 951 thermogravimetric analyzer (TGA) and DuPont 910 differential scanning calorimeter (DSC) are not immersed in the sample so they measure the temperature of a point close but outside the sample which might be different from the actual temperature of the sample. Figures

2-3 and 2-4 present the positions of the thermocouples in both equipments used in this study.

2-3-2 Accuracy in maintaining conditions and reducing disturbances

Sestak[45] discussed this topic and found that the arrangement of the experiment is the most important aspect for accuracy. The rate of the investigated reaction must be kept from distortion by eliminating disturbing effects. The major disturbing effects are usually found to be those of transport which consist of heat and mass transfer.[45]

To reduce the heat transfer disturbing effects, a suitable heating rate must be selected. It should be noted that the slower the heating rate, the greater the degree of decomposition and thus it follows that the shape of the thermogravimetric techniques curves can be profoundly influenced by the heating rate.[31] Also, it has been shown[25] that for exothermic reactions the slower the heating rate, the smaller the difference between the sample temperature and the furnace temperature.

The influence of mass transfer cannot be eliminated in a simple way[45] because it is very hard to find out in advance how important this influence will be and, consequently, general conclusions cannot be formulated. The most frequent disturbing transport effect is the removal of gaseous reaction product from the reaction interface. Sestack considered this to be consisted of two consecutive effects

1- Migration of the reactant gases through the sample.

2- The removal of gaseous products from the surface of the sample.

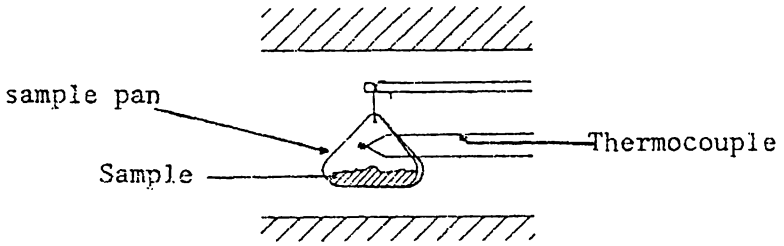

Figure 2-3 Location of temperature-detection thermocouple in DuPont 951 thermogravimetric analyzer (TGA)

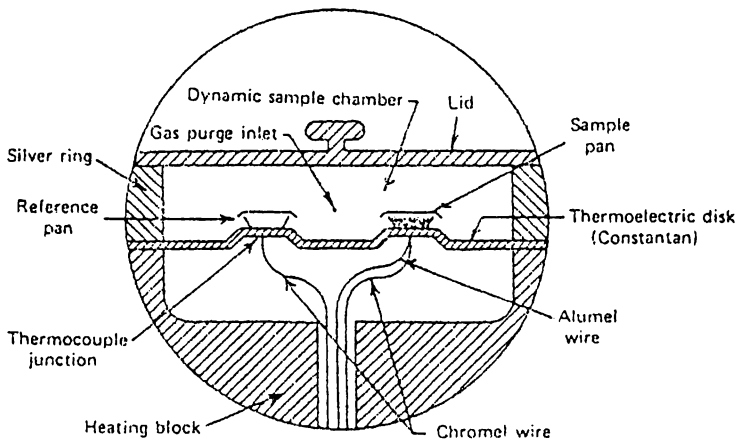

Figure 2-4 Location of temperature-detection thermcouple in Dupont 910 differential scanning calorimeter (DSC)

He called the first internal and the second external diffusion. When the diffusion rate is small it is evident that local concentration of gaseous products might occur, thus changing the equilibrium conditions.

2-3-3 Accuracy of reading data from the thermogravimetric technique curves

Each kinetic model needs different readings from the produced thermal curves. Setak[45] compared the kinetic results calculated by five different methods for a system corresponding to the dehydration of γ-$CaSO_4.0.5H_2O$. The five methods evaluated mathematically were:

a- Freeman and Carroll[33]

b- Doyle[36]

c- Coats and Redfern[32]

d- Horowitz and Metzger[34]

e- Van Krevelen et al[45]

He found that the computed values of activation energy did not deviate from the actual value more than 10 percent, therefore, all the methods seem to be satisfactory for the computation of kinetic data within the limits of required accuracy ($\pm$ 10%). Sestak[45] also calculated the errors due to the inaccuracy of reading values from thermograms for each method. He reported that the magnitude of this error depends considerably on the position of the point on the thermogravimetric curve in which the kinetic analysis is being performed. Sestak[45] showed only the results of three methods and ignored the other

two. Table 2-1 shows these results.

Although there were enough publications on the factors affecting the accuracy of kinetic data obtained from thermogravimetric techniques, there was no mention of how much each factor affected the accuracy and how to be definitly sure that their effects were eliminated.

Table 2-1 Accuracy of using different kinetic models to analyize thermogravimetric curves. (45)

Method	Activation Energy Accuracy %	Reaction Order Accuracy %
Freeman and Carrol[33]	4%	12%
Doyle[36]	4%	Correct value of n assumed
Horowitz and Metzger[45]	9%	Correct value of n assumed

2-4 Review of the thermo-oxidative behavior of crude oils using thermal analysis techniques

Studies on the quantitative and/or qualitative description of the kinetics involved in burning crude oil using thermal analysis thecniques have been very limited.

Tadema[3] used differential thermal analysis to study the thermal effects of mixtures of various oils and sands. His study showed that two distinct combustion reactions occured in general, namely at about 270° and 400°C. Analysis of the exhaust gas showed that oxygen was taken up near the 270°C peak and a coke like residue was formed. Only a small part of the oxygen could be found as carbon dioxide or carbon monoxide, a samll percentage is taken up by the residue and the major part forms water. During the high temperature peak, Tadema found out that mainly CO_2 and some CO are formed and little water was produced, and no residue was left. Tadema concluded that during the first reaction (270°C) mainly hydrogen was burned off, leaving a coked residue. This residue could only burn near 400°C and gives mainly carbon oxides. Also, he reported that the atomic H/C ratio of the burned fuel decreased with increasing peak temperature in agreement with the findings of Martin, Alexander, and Dew.[6]

Figure 2-5 presents examples of his curves. The top curve of the figure presents the two peaks obtained in air atmosphere. The bottom curve presents the results obtained by heating oil first in air atmosphere to a temperature above the first reaction peak (300°C). The air was then replaced by nitrogen and the sample cooled to room temperature. Then, air was admitted again and the heating of the sample was repeated.

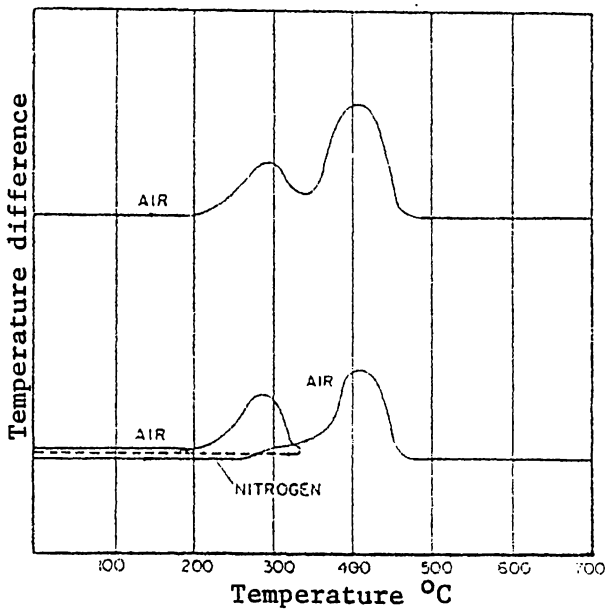

Figure 2-5 Differential thermal analysis of an oil sand obtained by Tadema (3).

The reaction peak at 270°C did not reappear. Upon further heating to 400°C, the second peak was recorded as before. Tadema concluded that the substance reacted at 400°C was different from the one that developed heat at 270°C.

Burger and Sahuquet[46] studied the kinetics of oxidation reactions involved in burning oil by different thermal analysis techniques. Through analyzing the exhaust gases they reported that three successive oxidation reactions are occuring:

1- Low temperature partial oxidation.

2- Combustion of crude oil fractions.

3- Combustion of coke.

They reported that the last step corresponds to the predominant reaction during dry forward combustion of crude oil in porous media. They observed significant differences in oxidation of crude oil in the presence of porous medium consisting of natural rock (containing clays) and porous medium composed only of ground silica. DTA technique was successful in demonstrating how the properties of both oil and porous media influenced the oxidation process.

J.H. Bae[47] studied the thermo-oxidative behavior of crude oils using differential thermal analysis and thermogravimetric instruments. He ran his experiments using 15 different crude oils ranging from 6 to 38 °API gravity under pressure (50-500-1000 psig). The experiments were conducted in both nitrogen and air atmosphere. The gas flow rate was 10 ml/min and the sample weight was 20 mg. He used a heating rate of 6°F/min up to a maximum temperature of 1000°F.

In the curves from the DTG runs, two peaks usually occured. The first peak started just below 400°F, signaling the onset of low temperature oxidation. The second peak appeared around 700°F and by the time the temperature reached 900°F the reaction was completed.

In the curves obtained from the TGA runs, Bae found that two types of crude oil (type L and I) gained weight in relation to the distillation curve obtained in nitrogen atmosphere at both low (200-330°F) and high (500-750°F) temperature ranges. Figure 2-6 presents his results for type L crude oil. He concluded that the availability of oxygen at low temperature drastically changed the quantity and the quality of the lay-down fuel. Bae also believed that the heat generated by low temperature oxidation reactions might be significant in fire flooding. No attempt was carried out to determine reaction order or heat values in his study, in other words, no quantitative study was provided.

Hardy, et. al[48] conducted DTA studies on crushed core obtained from Bartlesville-Allen county, Kansas and a synthetic porous matrix saturated with oil. Crude oil combustion in a synthetic porous matrix containing 95-5% quartz-kaolinite produced a thermogram closely similar to the mixture of natural core and crude.

Adonyi[49] investigated the evaporation of pure components, as well as mixtures, by thermogravimetric technique. He used mixtures of 50% benzene , or 50% cyclohexane , and 50% refined residue oil. His results showed that for evaporation of pure component, the reaction order is zero, while the apparent reaction order of mixtures were between 1-2.5 for different regions of the DTG curve, which is significantly different than zero. Adonyi made some TGA runs using light crude oil. The reac-

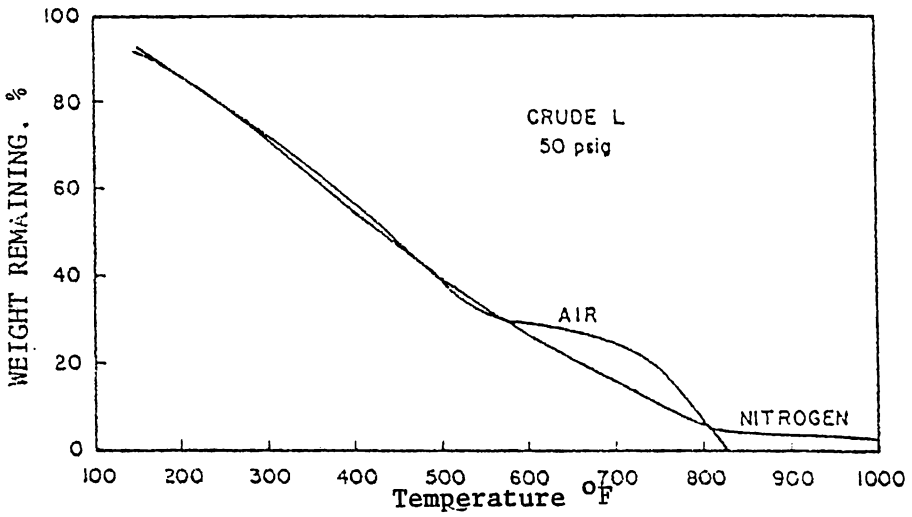

Figure 2-6 Typical TGA thermograms for type L crude obtained by J. Bae (47)

tion order of evaporation was also zero. It should be mentioned here that Adonyi did not define what he meant by light crude oil or refined residue oil in his study.

Susan[50], using the TGA module, developed a method termed "finger printing" to determine the country of origin of crude oil. He used twenty nine crude oil samples from various sources. He based his method on comparison of the thermogravimetric data, both graphically (through curve comparison) and numerically (by calculating weight loss at each temperature). The main purpose of Susan's study was to distinguish Alaskan crude oil from other crudes.

Lonvik and Rajeshwar[51] performed a thermogravimetric study on the green river oil shales using a DSC module. They noticed two exothermic peaks, one between 100-300^{o}C and the other between 400-500^{o}C. They believed that these peaks corresponded roughly to the amount of organic materials in the shale. Johnson and Smith[61] also ran similar experiments using both TGA and DSC modules on oil shales and other solids. Their results agreed with the Lonvik and Rajeshwar[51] study.

CHAPTER 3

Role of Clay in Combustion Process

In this chapter the definition of a catalyst and a review of the significance of clay in oil reservoirs and its possible catalytic effect on crude oil burning will be presented.

3-1 Clay importance in reservoirs and its physical characteristics

Many oil producing formations contain significant amounts of clay. Clay possesses a very large surface area with many active sites. Therefore, various oil recovery methods may be affected by the presence of clays. Clays, especially after various treatment such as acid treatment, are known to be active as catalysts in many hydrocarbon reactions.[52] Clays are composed of alumina, silica, and water, with iron, alkalies and earths in varying amounts. Clay minerals hold water at relatively low temperatures which is driven off by heating to about 100 to 150°C. When the clay minerals are heated to just above room temperature they begin to lose pore water and absorbed water. Between 400°C and 700°C the hydroxyl structure of the clay is lost. Within this same temperature interval the structure of clay minerals may be somewhat disrupted or altered. At a higher temperature (900°C) the structure of clay minerals is destroyed which is followed in some instances by the fusion of the mineral. More often, following the loss of the structure of the clay minerals, there is a considerable temperature interval in which new crystalline structure develops prior to the vitrification and fusion of the minerals.[52]

Clay can be activated to increase its catalytic nature by acid treatment.[53,54] The presence of traces of iron or vanadium would increase the amount of coke make of the catalyst.[52]

3-2 Definition of a catalyst

The rates and the activation energy of many reactions are affected by materials which are neither reactants nor products. Such materials, called catalysts, may slow down reactions in which case they are called negative catalysts or they may speed up the reactions, in which case they are called positive catalysts. Positive catalysts reduce the value of the activation energy while negative catalysts increase the value of the activation energy.

3-3 Clays - Possible influence on crude oil burning

Dart et al[55] studied the combustion rate for oxidation of carbonaceous residues on clay catalyst pellets. They found second order reaction with respect to carbon concentration and first order with respect to oxygen partial pressure. Their reactor contained carbon concentration less than two weight percent of the catalyst weight. Dart also, reported that hydrogen in the hydrocarbon residue appeared to react faster than the carbon.

Bousaid[56] studied the carbon burning rate for two types of crude oil. He coked the oil-sand mixture by heating the sample to a high temperature in nitrogen atmosphere. He burned a thin layer of coked sand in a combustion cell in air atmosphere. He showed that the combustion reaction was first order with respect to both carbon concentration and oxygen partial pressure. He also reported that the specific reaction

rate constants were related to combustion temperature by the Arrhenius type equation. The activation energy appeared to be insensitive to the gravity of the crude oil for the two oils studied. Bousaid also found that the activation energy decreased from 26600 BTU/lb mole (14782 cal/gm mole) to about 20,000 BTU/lb mole (11114 cal/gm mole) when 20% clay was added to the sand matrix. Bousaid believed that his activation energy was artificially low and he blamed that on the diffusion effects.

Burger and Sahuquet[46] using differential thermal analysis, studied the kinetics of oxidation reactions involved in crude oil burning. They found significant differences between burning crude oil in a porous media consisting of natural rock containing clay and porous media composed only of ground silica. In the natural matrix higher oxidation temperature was obtained, and larger amounts of oxygen were consumed, and larger amounts of CO and CO_2 were produced. Figures 3-1 and 3-2 present their results. They believed that these differences were due to the catalytic effect of clays, or the large surface area, or both.

Hardy et al[48] studied burning crude oil mixed with crushed cores containing clays and crude oil mixed with synthetic matrix by DTA technique. Hardy reported that the type and the amount of clay minerals present in the rock affected the combustion process. Unfortunately he did not elaborate on what the effects were.

Dabbous[57] studied the kinetics of low temperature oxidation reactions (LTO) of crude oils in porous media. He analyzed the isothermal as well as integral reactor data and obtained the overall rate equations for the partial oxidation reactions occuring at temperatures below $500^{o}F$. The reaction order with respect to oxygen was found to be

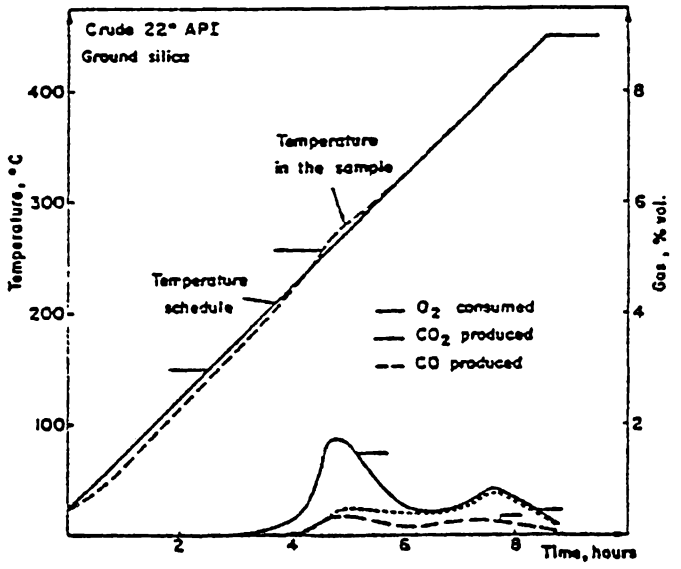

Figure 3-1 DTA thermograms of the oxidation of a crude oil in ground silica (46)

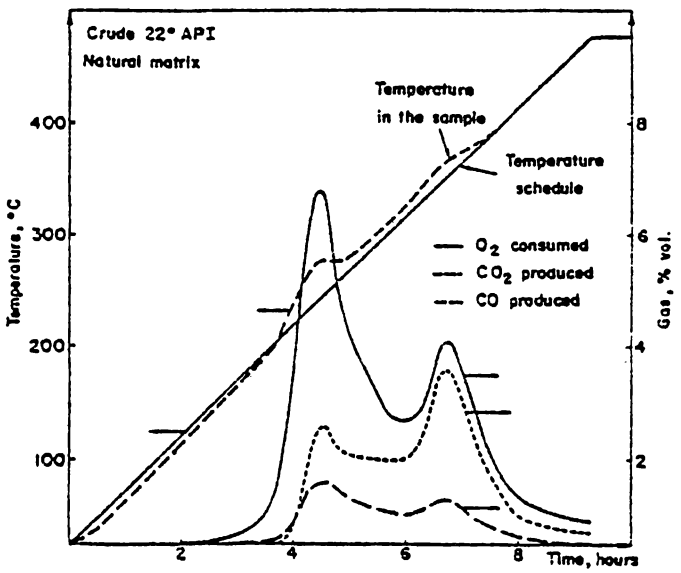

Figure 3- 2 DTA thermograms of the oxidation of a crude oil in a natural matrix containing clay (46)

between 0.5-1.0 He also found that the order of the reaction was dependent upon the crude oil but independent of the properties of the porous media. The result of his experiments indicated that the activation energy of the reaction was insensitive to the type of crude or porous media and was about 31,000 BTU/lb mole (17277 Cal/gm mole). He used crushed berea sand-stone as a porous media.

Guvenir[58] studied the effect of clay content on the dry forward combustion process of crude oil in porous media. He used Kaolinite type of clay and Iola crude oil. He made four combustion runs using different clay content varying from 0 to 15 percent by weight. He made one combustion run using amorphous silica powder, an inert material with relatively large surface area, to investigate whether clay had a catalytic effect on the process or the effect was due to its large surface area. Guvenier concluded that the surface area of the clay was the major contributor to the fuel deposition. Figure 3-3 shows the effect of the clay content on fuel deposition. Fuel deposition increased as the clay content increased.

Fassihi et al[59] performed a similar experiment to Guvenir's[58] with different crude oil. Fassihi observed that the presence of clay had an effect on the frontal behavoir of the combustion zone in the porous media. Two of their runs had almost the same initial conditions except that one had clay. It was found that the average front temperature of the combustion zone for the run without clay was lower than the one with clay. Also, oxygen utilization was improved for the run with clay and that a considerable amount of coke was left unburned.

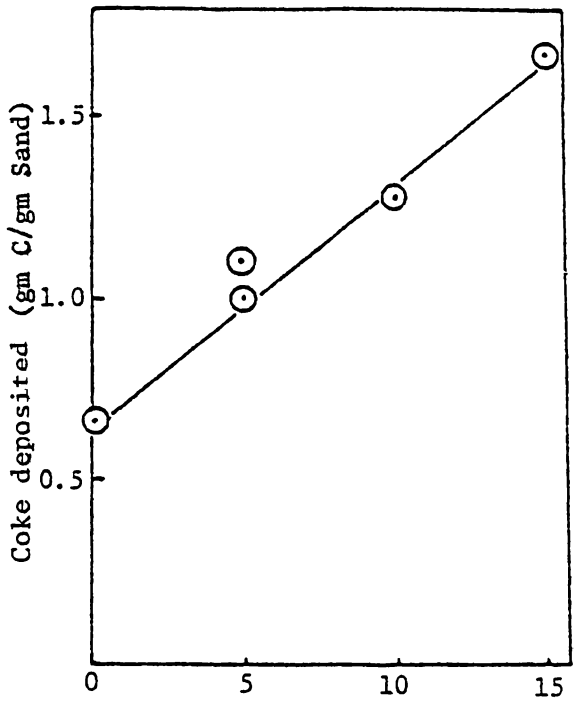

Figure 3-3 Fuel deposition vs. clay content of sand (58)

The literature shows that clay has an effect on the burning of crude oil, but there is no mention whether the effect is due to the catalytic nature of clay or due to the large surface area that clay possesses.

CHAPTER 4

Statement Of the Problem

According to the reported studies, the kinetics of coke formation and combustion, and low temperature oxidation reactions govern the in-situ combustion process. Much information is available in the literature on the hydrodynamic and thermal aspects of the in-situ combustion process. However, the reaction kinetics involved in the process remains the least investigated aspect of the in-situ combustion process. Only limited and inconclusive data are available in the literature on the kinetics of the process.

The idea of this study came from the study made by Guvenier.[58] Going through Guvenier's study, it was felt that further investigation was needed to study the effect of grain materials on thermo-oxidative behavuior of crude oil. The purpose of the present study was to see if clay catalytic effect could further be proven by obtaining kinetic parameters such as activation energy. It was also aimed to see if clay effects were due to its catalytic nature or to its large surface area. Thermogravimetric analysis (TGA) and differential scanning calorimetry (DSC) were used for the purpose of this study.

CHAPTER 5

Description of the apparatus

The apparatus used for the purpose of this study is DuPont 951 thermogravimetric analyzer (TGA) and DuPont 910 differential scanning calorimeter (DSC) modules in connect with DuPont R-90 thermal analyzer.

5-1 DuPont 951 thermogravimetric analyzer (TGA)

The 951 thermogravimetric analyzer in connect with the R-90 thermal analyzer and the X-Y plotter can record the amount and the rate of weight loss of materials either as a function of increasing temperature, or isothermally as a function of time.

Figure 5-1 presents the DuPont 951 TGA module and Table 5-1 presents specification of the same module. The TGA module consists of three major parts:

1- Furnace assembly

2- Balance assembly

3- Cabinet assembly

5-1-1 Furnance assembly

The furnace is controlled by the R-90 programming unit. The furnace can supply a constant temperature rise (1,5,10,20^{o}C/min) from ambient temperature up to 999^{o}C. Also, the furnace can be maintained at any temperature for any required time.

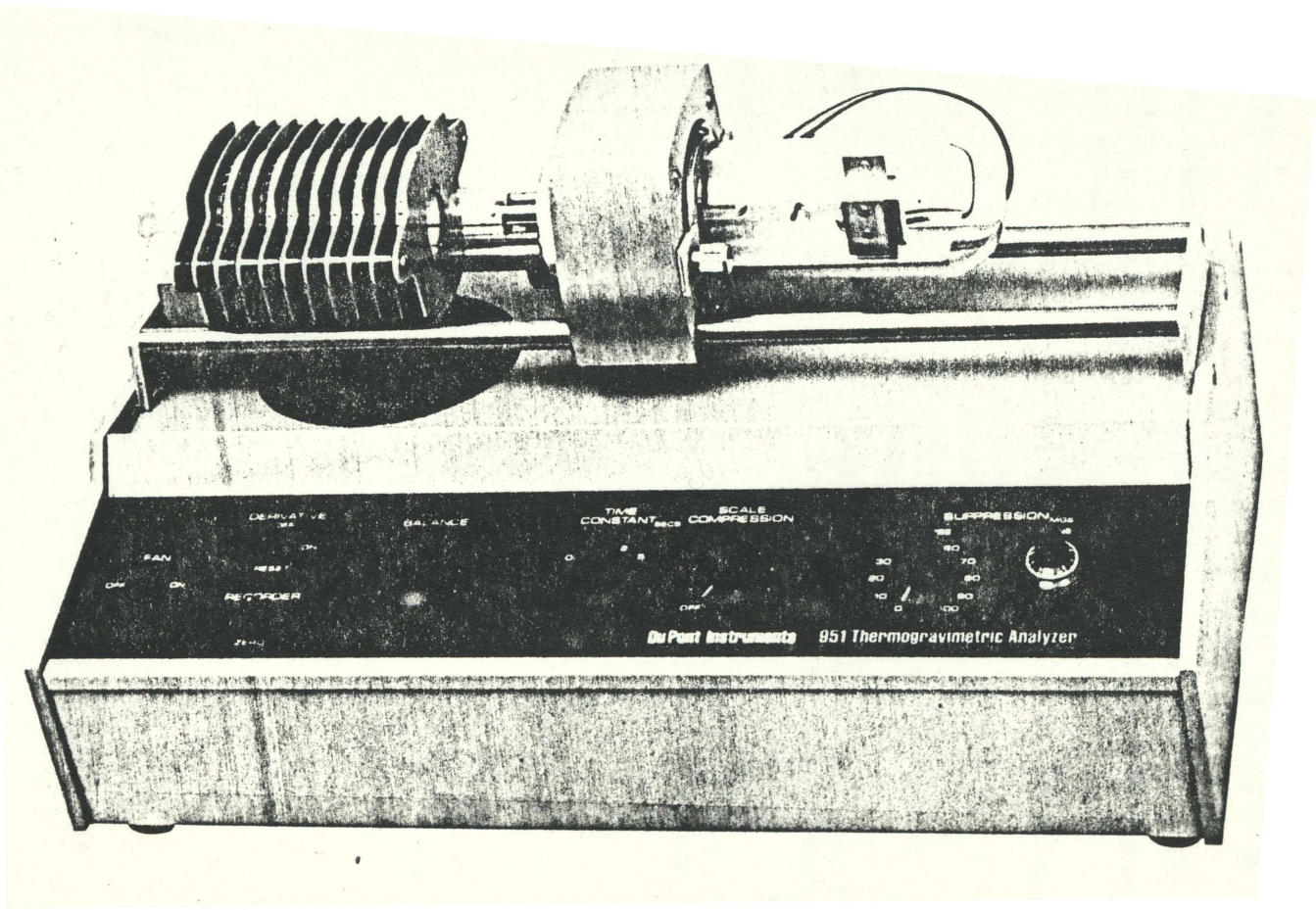

Figure 5-1 DuPont 951 thermogravimetric analyzer (62)

Table 5-1

DuPont 951 TGA Specifications (62)

Capacity:	1000 mg (including boat).
Mass ranges:	1, 2, 5, 10, 20, 50 and 100 mg full scale (5 in.).
Temperature range:	To 1200°C.
Suppression:	100.00 mg (stepped and continuously variable)
Suppression accuracy:	± 0.02 mg.
Sensitivity	0.2 percent of full scale (0.002 mg ultimate)
Precision	± 0.2 percent of full scale (± 0.002 mg ultimate).
Accuracy:	± 0.2 percent of full scale (± 0.002 mg ultimate).
Noise band	0.008 mg (zero time constant); 0.002 mg (1-sec time constant). Unaffected below gas flow rates of 2.5 1/min.
Time constant:	0, 1, 2, 5, 10 and 20 sec.
X-axis time base:	0.5 percent linearity; variable. 1 to 200 min. full scale.
Dimensions and weight	9 x 12 x 19 in.; 20 lb.

5-1-2 Balance assembly

The balance mechanism contains a null-balance, taut band electric meter movement with an optically actuated servoloop. The sample is placed in a container which is suspended directly on the balance beam. About 1mm aside of the sample tray, there is a thermocouple to measure the temperature of the sample. The sample chamber enclosed using a quartz furnace tube. The balance sensitivity is reported to be 2μg.

Purge gas is admitted through a hose fitting on the rear of the balance housing and exits through the opening in the furnace tube.

5-1-3 Cabinet assembly

The cabinet assembly houses the balance control and associated electronic circuits. The cabinet has a fan to cool the furnace rapidly, if needed. At the cabinet assembly there are four bottoms for manual control.

5-2 DuPont 910 differential scanning calorimeter (DSC)

The differential scanning calorimeter module in connect with the R-90 thermal analyzer and the X-Y plotter records the heat flow (dh/dt) in mili-cals, as a function of temperature or time.

Figure 5-2 presents the DuPont 910 DSC module and Table 5-2 presents the specifications of the same module.

The DSC apparatus consists of

1- The cell base module

2- The DSC cell.

5-2-1 Cell base module

The cell base module receives its signal from the R-90 programming unit. When the DSC cell is installed on the top of the cell base module, an electrical connection is formed which provides transmission of the R-90 signals to the cell and allows the transmission of the cell base thermocouples signals to the cell base. The cell base has buttons for manual control.

5-2-2 DSC cell

It consists of a constantan thermoelectric disc as a primary heat transfer element. There are two raised portions in the disc, one for the reference pan and the other for the sample pan. Heat is transferred from the two heaters under each raised portion of the constantan disc to both the sample pan and the reference pan. Under each raised portion of the constantan disc, there is a platinum resistance thermometer. Through comparing the signal from the platinum resistance thermometer

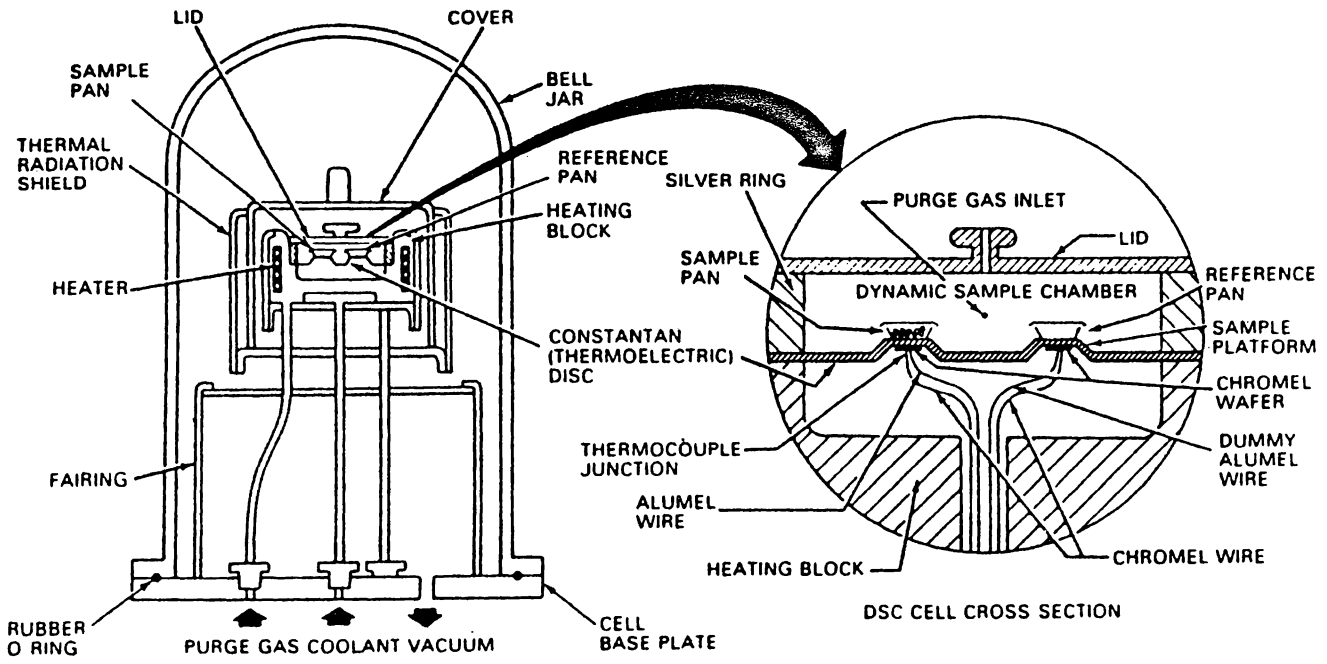

Figure 5-2 DuPont 910 differential scanning calorimeter (cell cross section) (62)

Table 5-2

DuPont 910 DSC Specifications (62)

Temperature range:	Room temperature to 660°C. Cooling Accessory provides quench cooling to -180°C and programmed colling to -120°C.
Cooling rate:	10°C/minute to -110°C.
Sample size:	0.5 to 100 mg.
Sample volume:	0.05 ml.
Sample pans:	Aluminum; open or hermetically sealed to 3 internal atmospheres.
Atmosphere:	Atmospheric to 2 Torr; preheated dynamic gas purge (in excess of 100 ml/min.).
Cell volume:	2 ml.
Temperature repeatability:	$\pm$ 1°C.
Differential Thermocouples:	Chromel-Constantan.
Sample Thermocouple:	Chromel-Alumel.
Control Thermocouple:	Platinel II.
Calorimetric Sensitivity:	.05 to 50 (mcal/sec.)/in.
Calorimetric Precision:	$\pm$ 1% (based on metal samples).

under the sample tray with that of the reference tray, a continuous and automatic adjustment of heater power (energy per unit time) will be provided to keep the sample holder temperature identical to that of the reference holder, provides a varying electrical signals, opposite but equivalent to the varying thermal behavior of the sample, which can be recorded by the X-Y plotter as a function of time or temperature.

Purge gas enters the cell through a hose fitting in the cell plate. The air is preheated to disc temperature by circulation before entering the sample chamber through the purge gas inlet.

5-3 DuPont R-90 thermal analyzer

The R-90 thermal analyzer is a programming unit. Through programming this unit isothermal control and four linear heating rates (1, 5, 10, and 20^{o}C/min) for the DuPont 951 thermogravimetric analyzer (TGA) or the DuPont 910 Differential Scanning Colorimeter (DSC) can be achieved. The R-90 also stores, protects, and recalls up to nine programs which can be applied sequentially. For more details about the units see the DuPont manual.

CHAPTER 6

EXPERIMENTAL PROCEDURES AND STEPS TAKEN TO REACH FINAL RESULTS

This chapter deals with the experimental procedures taken during this study and steps taken to reach the final results. Factors affecting the thermogravimetric technique curves and the choice of the best parameters are presented.

Approximately 100 runs were made using the TGA module. About 40 additional runs were made using the DSC module. The first 30 runs of the TGA and the first 5 runs of the DSC were exploratory runs to examine the capability of the equipment and results are not reported in this study.

6-1 TGA RUNS

Five different mixtures were used in the first 30 TGA runs, these mixtures were prepared using

1- Crude oil from Iola field, Allen county, Kansas, with ^{o}API gravity of 19.3 and viscosity of 530 cps at 25^{o}C.

2- Silica sand of average size, 35 mesh, from Wedron Silica Div., Pebble Beach Corp., Wedron, Ill.

3- Silica powder (amorphous silica IMSIL A-10) from Illinois Mineral Co., which has a surface area comparable to kaolinite surface area. (1.4 m^2/gm)

4- Clay (kaolinite type), from Good Earth Clays, Inc., Kansas City, Mo. (2-20 m^2/gm - surface area)

The choice of the mixtures used in the first 30 runs of the TGA came from the previous research.[58] Water was used in addition to the

above five components. The mixtures were prepared in a small beaker using a top loader balance (Mettler PN2216, Mettler Instrument Corporation, New Jersey) to weigh components of each mixture. The mixtures were stirred using a glass rod until the oil was well dispersed in the sand. The thermograms obtained using these mixtures were difficult to analyze because the water and oil weight losses occured at the same temperature range. Since the aim of this study was to investigate the thermo-oxidative behavior of burning crude oil on different grain materials and to study the catalytic effects of clay on the process, it was decided to study the mixtures without water. Eliminating water removes steam distillation effects on crude oil as well as the effects of any water minerals which may act as a catalyst.

During the 30 exploratory runs of the TGA, different values of heating rates, final temperatures, gas flow rates, and sample weight were tried. Also, the parameters of the X-Y plotter were changed to determine their effects on the produced curves and choose the suitable parameters which would allow the thermograms to remain in the limits of the graph papers. The final conditions chosen are shown in Table 6-1.

The choice of a 40 mg sample was to assure that the sample obtained from any mixture was representative of the mixture itself. It should be noted here that sample mass can affect the TG and DTG curves in three ways[22]:

1- The extent to which endothermic or exothermic reactions of the sample will cause the sample temperature to deviate from the linear temperature change (the larger the sample mass, the greater the deviation).

Table 6-1 Parameter values chosen for producing thermal curves.

Sample weight	40mg
Air or nitrogen flow rate	130cc/min
Intial temperature	25°C
Final temperature	600-650°C
Heating rate	5°C/min
Pressure	1 atm

Table 6-2 Mixtures prepared for the TGA and DSC runs.

Mixture #	Sand wt%	Clay wt%	Silica powder wt%	Ground sand wt%	Oil wt%
6	0	80	0	0	20
7	80	0	0	0	20
8	0	0	80	0	20
9	0	0	0	80	20
10	40	0	40	0	20
11	40	40	0	0	20
12	50	50	0	0	0
13	65	15	0	0	20
14	70	10	0	0	20

2- The degree of diffusion of the product gas through the void space around the solid particles (under static conditions, the atmosphere immediately surrounding the reacting particles will be somewhat governed by the bulk of the sample).

3- The existence of large thermal gradients through the sample, particularly if it has a low thermal conductivity.

Air or nitrogen from commercial cylinders were the gases used. Gas flow rate of 130 cc/min through the sample chamber was chosen to assure that the sample was always in the fresh gas atmosphere and to minimize the effect of external diffusion. Thermal decomposition would cause the atmosphere immediately surrounding the sample to be continuously changing. If the sample evolves a gaseous product as the temperature increases, the gas concentration surrounding the sample would increase. This will affect the rate of the reaction An inert gas such as nitrogen may be applied to the sample to remove the gaseous decomposition products of the cracking reaction, and to prevent the burning reaction from occuring.

Starting temperature was chosen a couple of degrees above the room temperature, i.e., $25^{o}C$. The $600^{o}C$-$650^{o}C$ final temperature was chosen because the oil weight loss was completed around $550^{o}C$-$600^{o}C$.

The choice of $5^{o}C$/min was selected after trying other heating rates to assure the greatest separation of different types of reactions. It is known that the slower the heating rate, the greater the degree of decompostion, and thus it follows that the shape of the thermogravimetric curves can be profoundly influenced by the heating rate[31].

The choice of operating at atmospheric pressure was due to the difficulty of pressurizing the TGA module.[26]

The air flow rate was measured using a rotameter. The rotameter was calibrated using a gas burette. The calibration curve is shown in Appendix C.

After these exploratory runs, it was decided to change the compostion of the mixtures. The composition for study were chosen and listed in Table 6-2 (mixtures 6-8). These mixtures were prepared in the same manner as before. The R-90 programmer parameters of Table 6-1 were kept constant during all TGA runs. Also, at this stage it was decided to have runs using clay, amorphous silica powder and oil by themselves to determine their behavior upon burning. Mixtures 6, 7, and 8 were burned in the TGA module in air atmosphere as well as in nitrogen atmosphere. It was very difficult to keep the initial sample weight at 40 mg so, the initial sample weight varied between 38-42 mg.

To possibly distinguish between surface area effects and catalytic effects, attempts were made to change the surface area by grinding the sand using mortar and pestle to increase its surface area or mixing the silica powder and clay with sand. New mixtures were prepared. The compositions of these mixtures are also shown in Table 6-2 (mixtures 9, 10, 11, and 12). These mixtures were burned using the TGA module in air atmosphere and all parameters of Table 6-1 were kept constant. Only air was used with these four mixtures. At this point the three thermograms were not the same (thermograms of mixtures 9, 10 and 11). There was an obvious difference between the shape of the thermogram of mixture 11 (40% clay - 40% sand - 20% oil) and the thermograms of both mixtures 9

(80% grind sand - 20% oil) and 10 (40% fine silica powder - 40% sand - 20% oil). According to these results it was decided to prepare new mixtures with lower amounts of clay. The composition of the new mixtures are also shown in Table 6-2 (mixtures 13 and 14). Runs made using these mixtures were unsuccessful due to the uncertainty of obtaining a sample of 40 mg having the same composition as the mixture, because clay weight fraction was relatively too small. Therefore, reproducibilities of the thermograms were very poor. These runs will not be discussed.

The last runs were made with burned clay. Clay was burned in an oven at 650°C to reach a constant weight. One run using burned clay was made. Figure 7-12 presents the results of this run. The curves showed no weight loss with temperature. A mixture was prepared in the same manner as before with 80% burned clay and 20% oil by weight. Two runs were made using this mixture. The thermograms obtained were similar to the 80% fine silica - 20% oil (mixture 8) thermogram.

To illustrate the clay's catalytic effects, it was decided to apply Arrhenius type kinetic model and ratio method to obtain kinetic parameters. Also, it was decided to use the DSC module to determine heat values of oil in each mixture and determine the effects of matrix content.

6-2 DSC runs

First the DSC was calibrated. To calibrate the DSC, three runs were made. For the first run, indium was used. For the second run zinc was used, and antimony was used for the third run. The same procedure described in DuPont's DSC handout was followed. The calibration curve

is shown in Appendix C.

The DSC module and the X-Y plotter were connected to the R-90 programmer unit. Parameters in Table 6-1 were kept constant, except for the sample weights which were around 13 mg. Samples were weighted using an analytical balance (Mettler H10, Mettler instrument Corporation, New Jersey). The curves obtained from the DSC study were analyzed using the appropriate equation (see Appendix B). The area under each peak was measured using a planimeter.

The DSC module has two sample trays, one acting as a refererence and the other as sample tray. For all mixtures which did not include clay, the reference tray was empty. For mixtures containing clay, the reference tray was filled with the same amount of clay in the mixture to offset the clay endothermic dehydration effects. Two runs were made to establish that the above prcedure successfully offset the clay effects. The first run was made using clay in the sample tray while the reference tray was empty. The result of this run is shown in figure 6-1. The results showed an endothermic peak between 400-500^{o}C which was expected. Another run was made using equal amounts of clay in both the reference pan and the sample pan. The result of this run, which is a straight line, is shown in Figure 6-2.

For each of the mentioned mixtures, at least 5 TGA runs and 3 DSC runs were performed. The reproducibility of the obtained thermograms was successful. A description of the obtained thermograms will be presented in the next chapter.

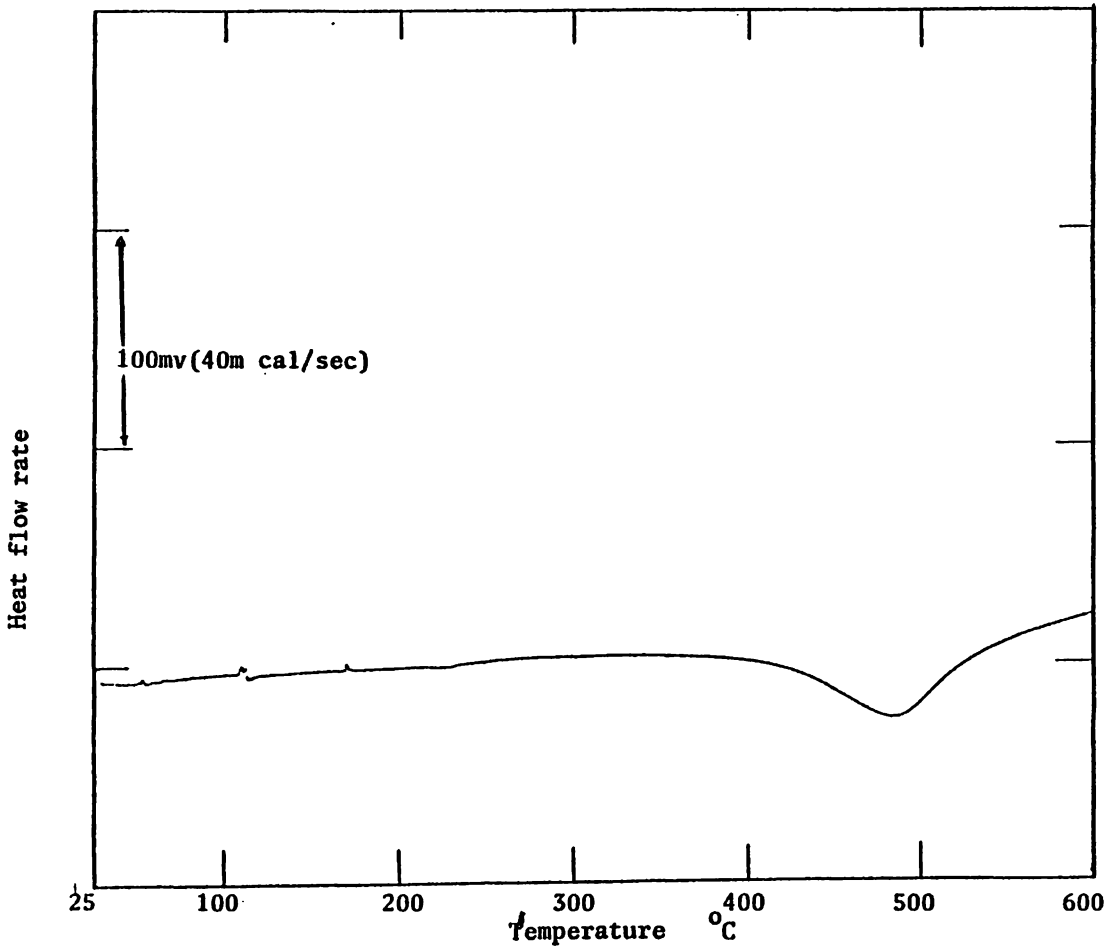

Figure 6-1 DSC thermogram of clay in the sample pan and empty reference pan in the presence of air flow.

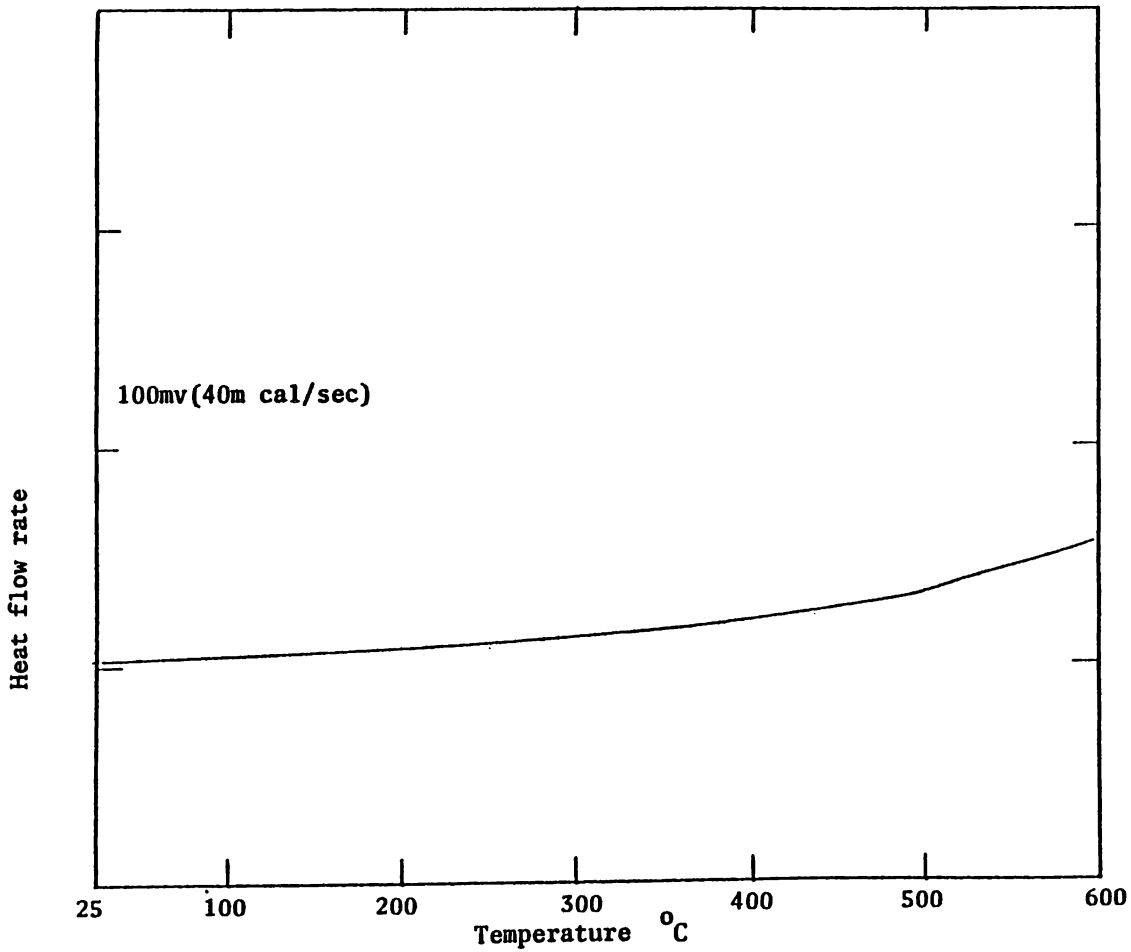

Figure 6-2 DSC thermogram of clay, using equal amounts in both the reference and sample pans, in the presence of air flow.

CHAPTER 7

Description of the Produced Thermograms

The TGA/DSC thermograms obtained during this study will be presented and discussed in this chapter. At this point our only concern was trying to compare the obtained thermograms, and to identify reactions taking place at each range of temperature (i.e. DTG peak). For this reason the effect of purging gas, grain materials, grain surface area, and heating rate on the produced thermograms was studied.

7-1 Effect of purging gas on TGA thermograms

Figures 7-1 and 7-2 illustrate the effect of purging gas on the crude oil thermograms. Figure 7-1 presents the TG and the DTG curves of heating crude oil in a nitrogen atmosphere. The weight of the sample used was 40.84 mg. The TG curve is smooth up to 350^{o}C. The DTG curve corresponds to this portion of the TG curve, with one distinct peak. The run was done in a nitrogen atmosphere, so there is no oxidation taking place. Therefore, in this temperature range, distillation is dominating. The DTG curve between 350^{o}C and 450^{o}C has a small hump which indicates that there is an additinal reaction taking place in this temperature range. This reaction could be a cracking reaction, since the molecules of oil will crack in this range of temperature in the absence of oxygen. A small residue of about 6% remained in the pan even after the temperature reached 650^{o}C.

Figure 7-2 presents the TG and the DTG curves of the heating of crude oil in an air atmosphere. The sample weight was 36.94 mg.

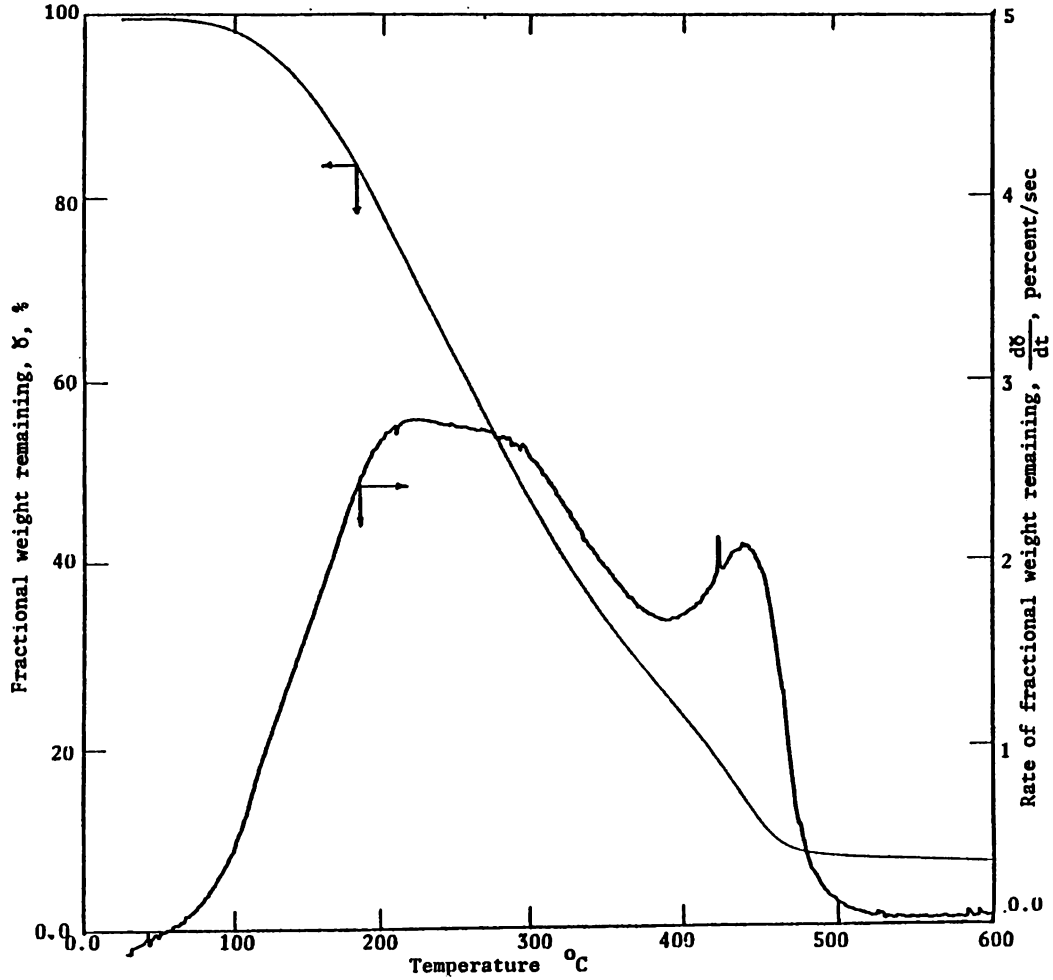

Figure 7-1 TGA thermogram of crude oil distillation in the presence of nitrogen flow.

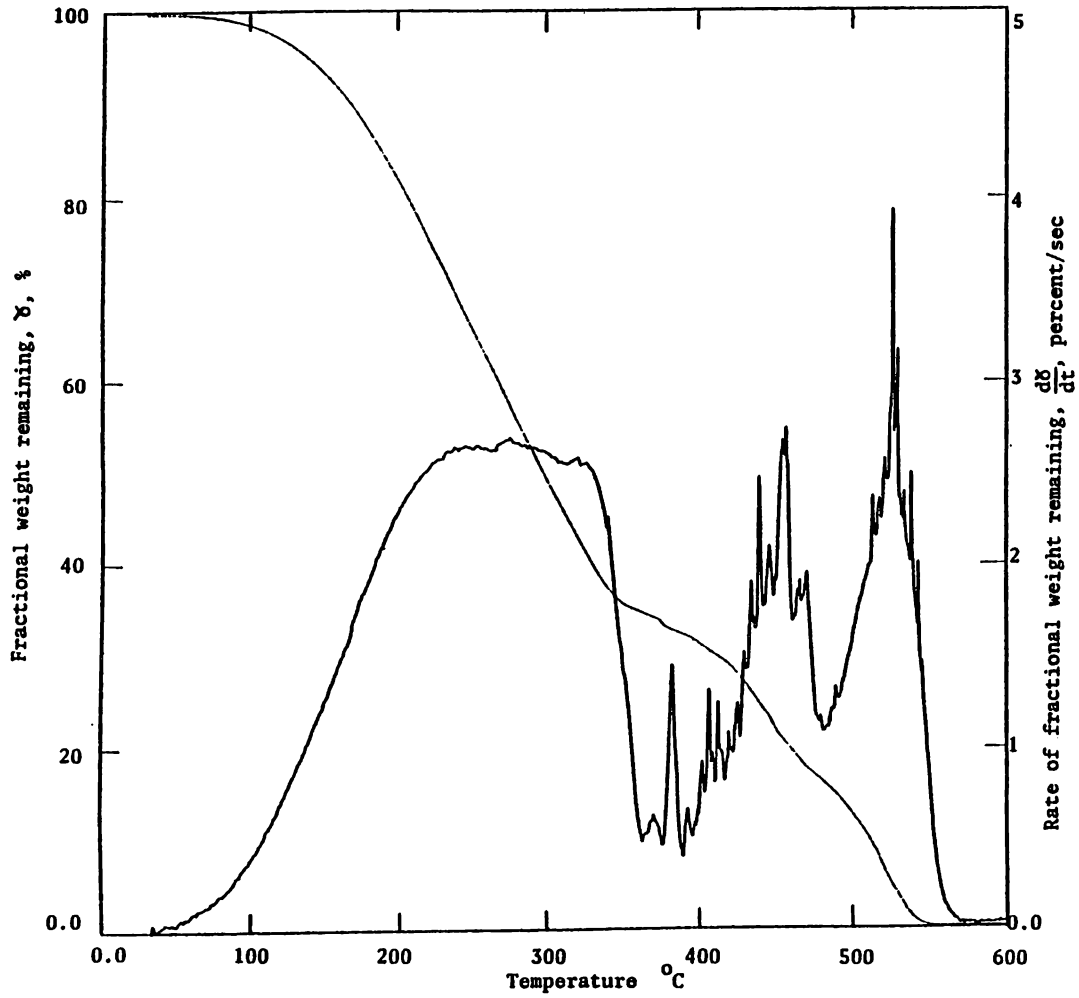

Figure 7-2: TGA thermogram of crude oil combustion in the presence of air flow.

It is noted that up to 327°C, the TG curve has a smooth shape. This portion of the TG curve corresponds to one distinct peak in the DTG curve. Comparing this region with the same region in Figure 7-1, one can say that at this peak distillation dominates. Between 350°C and 550°C one can distinguish two peaks on the DTG curve. One peak occurs between 350°C and 475°C while the other peak occurs between 475°C and 550°C. Both peaks correspond to a small deviation in the TG curve after the smooth portion of the curve. In these two peaks, burning and cracking are dominant. The deviation in the TG curve means a weight gain which may be due to the oxygen absorption. The results of J. Bae[47] for 20 °API crude oil presented in Figure 2-3 (Chapter 2) indicates the same kind of weight gain. He classified this type of crude as type L. The combustion was completed at 550°C and no residue was observed in the pan.

The first peak will always be called the distillation peak while the second and third peaks will always be called the craking and burning peaks. To calculate the amount of oil undergoing cracking, burning or distillation in each peak, the exhaust gases have to be analyzed and the amount of carbon monoxide, carbon dioxide, oxygen, and light hydrocarbons should be calculated. Due to the lack of gas analysis, it was not possible to calculate that, so this point was dropped.

7-2 Effect of Grain Materials on TGA Thermograms

The results of mixtures 6, 7, and 8 will be presented here to show the effects of grain materials on the TGA thermograms. Figure 7-3 presents the TG and the DTG curves obtained from heating of 40.68 mg of

mixture 7 (80% sand - 20% oil) in a nitrogen atmosphere. The DTG curve shows similarity with the curves from Figure 7-1 (100% crude oil). The same description of Figure 7-1 is applied here.

Figure 7-4 presents the TG and the DTG curves obtained from burning 41.6 mg of mixture 7 (80% sand - 20% oil) in an air atmoshpere. The TG and DTG curves are similar to the curves of Figure 7-2 (100% crude oil - air atmosphere). The peaks occured in almost the same region of temperature. The description of Figure 7-2 is applied to Figure 7-4.

Figure 7-5 presents the TG and DTG curves from heating of 40.68 mg of mixture 8 (80% fine silica - 20% oil) in a nitrogen atmosphere. Figure 7-1 (100% crude oil) thermograms are similar to those of Figure 7-5 and the same discussion is also applied here.

Figure 7-6 presents the TG and DTG curves of heating of 39.82 mg of mixture 8 (80% fine silica - 20% oil) in an air atmosphere. The TG curve has a smooth curve up to 275^{o}C which corresponds to the smooth portion of the first peak on the DTG curve. Then, a hump in the DTG curve occurs (second peak) which means that there was a different reaction taking place in this temperature range (275^{o}C - 360^{o}C). These reactions may be the low temperature oxidation reactions (LTO) which occur efficiently on the large surface area of the silica powder, or this hump may be due to cracking reactions and some burning, or both.

The DTG curve between (375^{o}C - 550^{o}C) has only one distinct peak which is different from Figure 7-2 (100% crude oil) and Figure 7-4 (80% sand - 20% oil), where two peaks occured. In this peak cracking and burning were dominating. Up to this point different behavior was observed between the burning of crude oil in the presence of sand grain

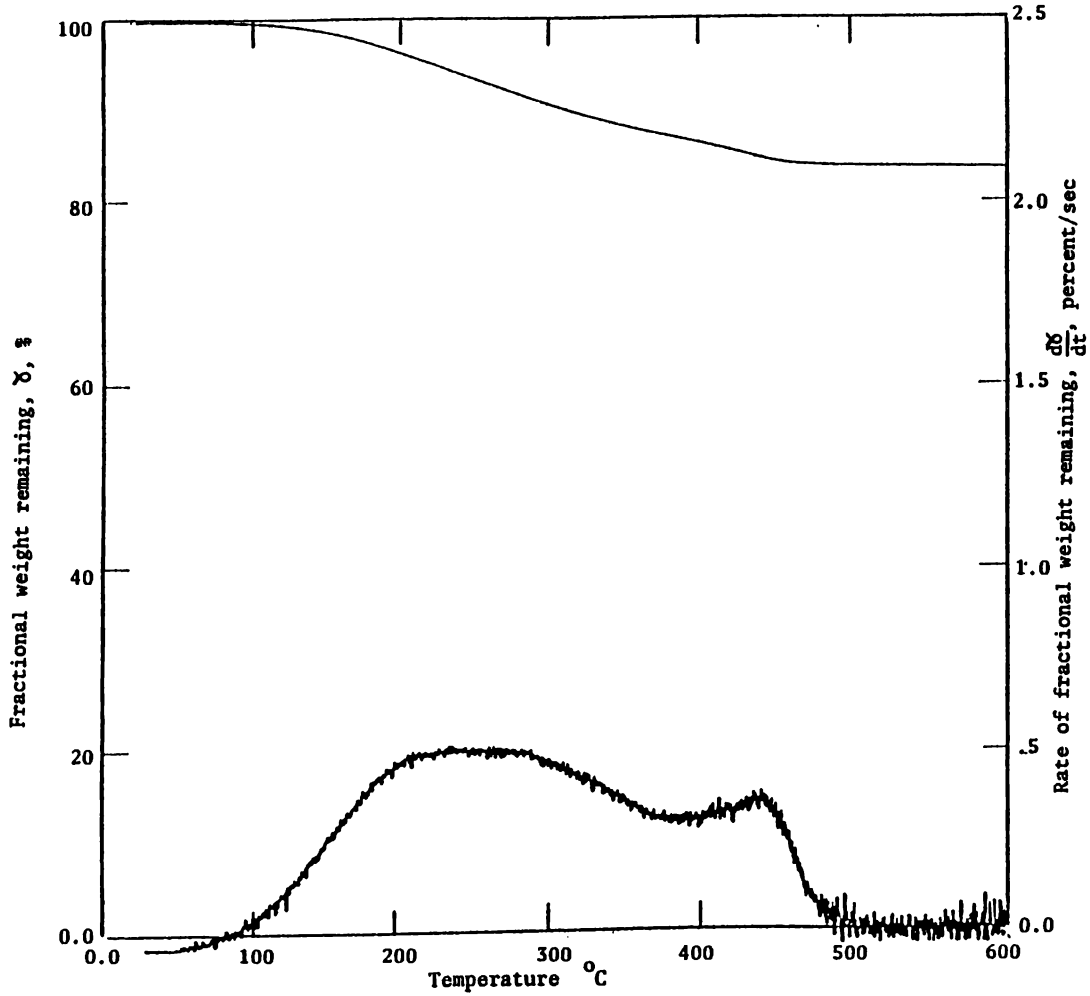

Figure 7-3 TGA thermograms of mixture 7 (80%sand-20%oil) in the presence of nitrogen flow.

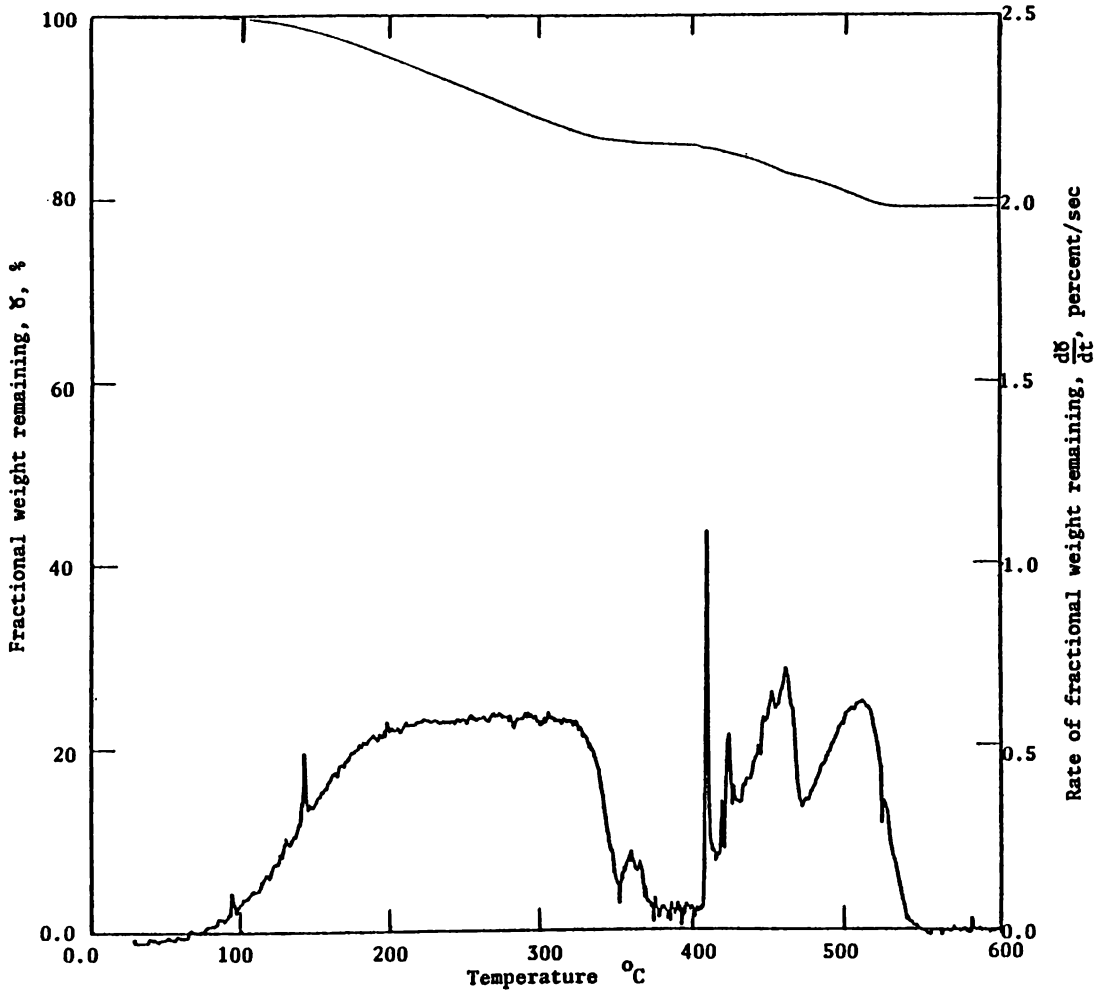

Figure 7-4 TGA thermogram for mixture 7 (80%sand-20%oil) in the presence of air flow.

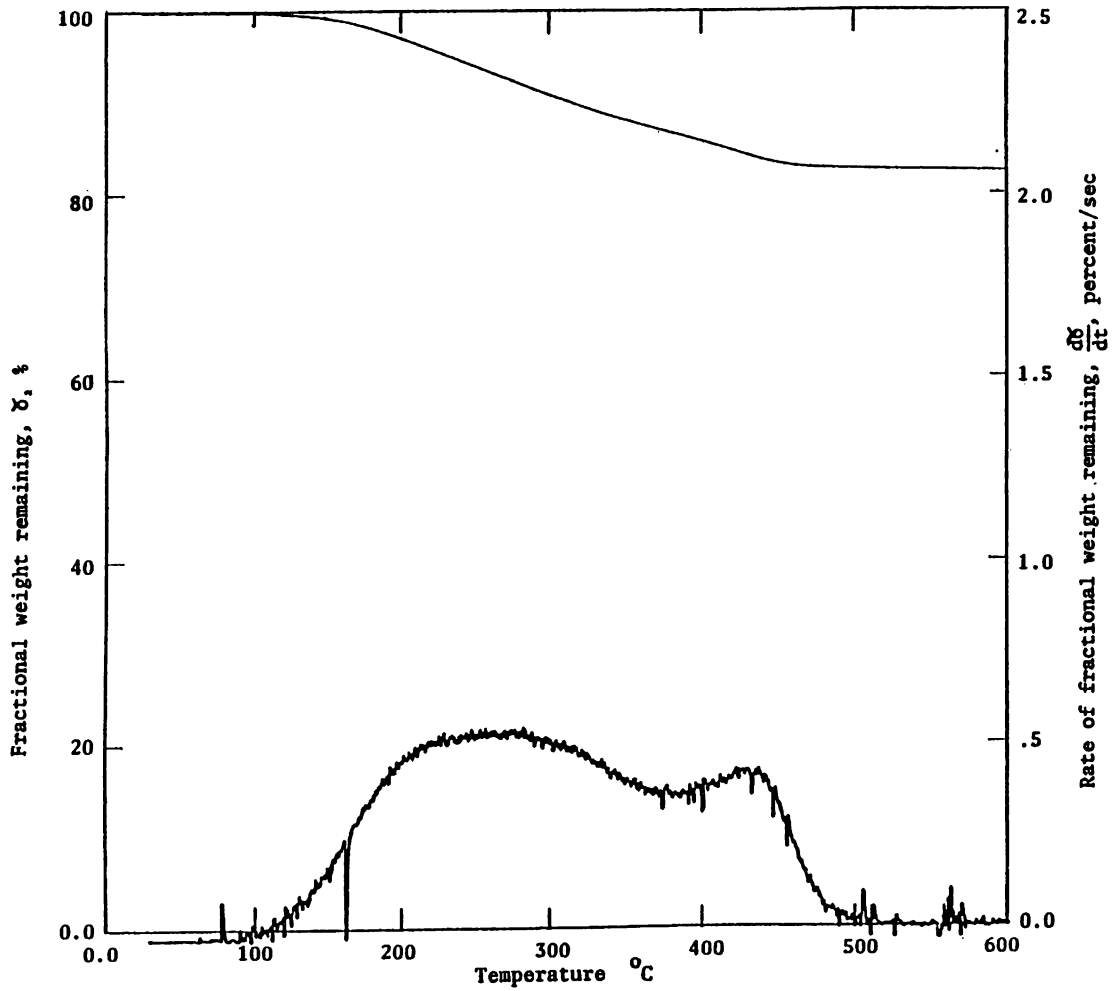

Figure 7-5 TGA thermogram for mixture 8 (80%silica powder-20%oil) in the presence of nitrogen flow.

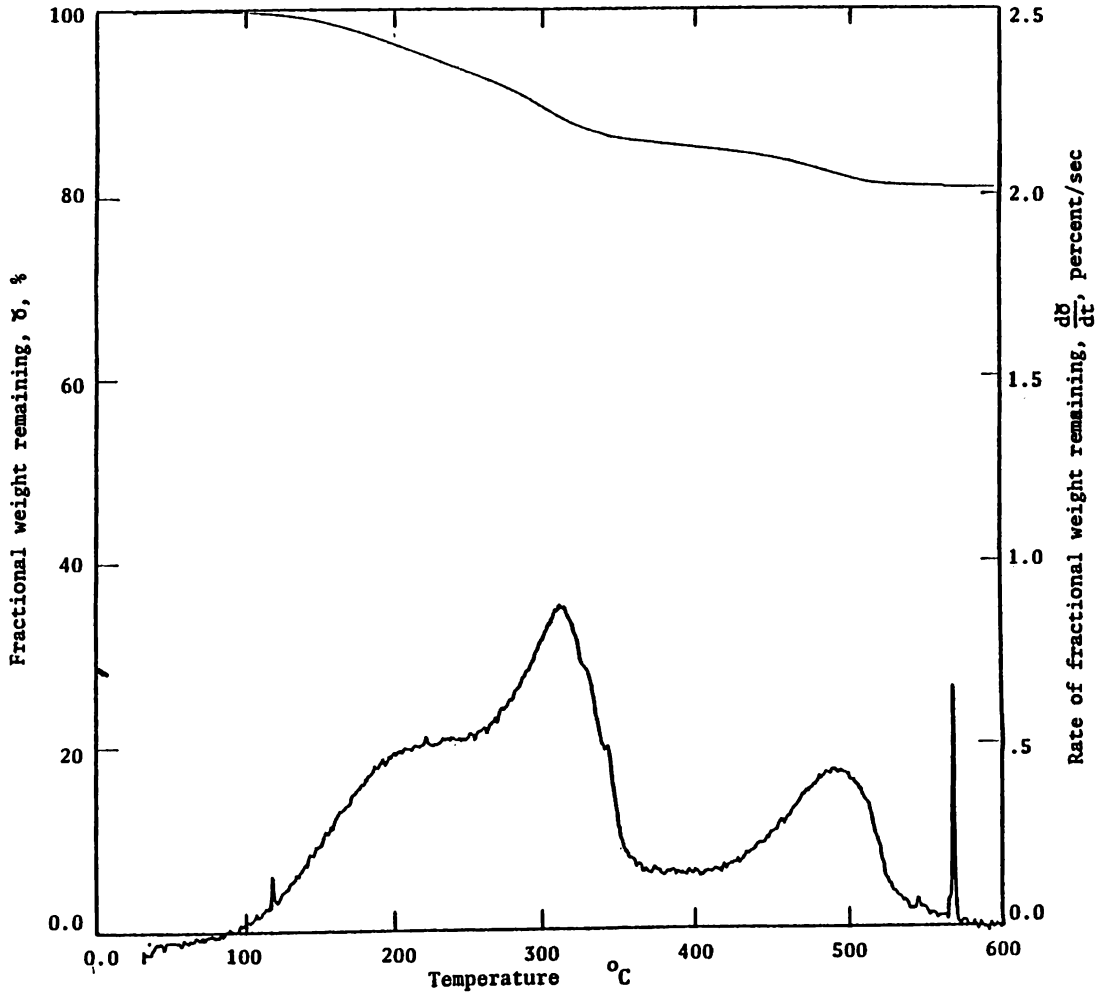

Figure 7-6 TGA thermogram for mixture 8 (80%silica powder-20%oil) in the presence of air flow.

and that in the presence of fine silica powder.

Figure 7-7 presents the TG and the DTG curves from heating of 41.23 mg of silica powder in air atmosphere. The curves showed no weight loss with temperature.

Figure 7-8 presents the results obtained from heating of 39.51 mg of sample 6 (80% clay - 20% oil) in nitrogen atmosphere using the TGA module. The results were similar to that of Figures 7-1, 7-3, and 7-5 except that the TG curves showed a larger weight loss than previously observed. It was believed that this weight loss was due to the presence of clay. To prove this point, a run was made with 35 mg of clay in nitrogen atmosphere using the TGA module. The resulting curves are shown in Figure 7-9. Clay showed a weight loss with temperature. This weight loss is attributed to the dehydration of clay. Correction due to the clay weight loss with temperature was performed by subtracting the reading of the TG and DTG curves of Figure 7-9 and the readings of the TG and DTG curves of Figure 7-8. The differences in the TG readings represent the oil weight loss while the differences in the DTG readings represent the rate of oil loss with respect to temperature.

Figure 7-10 shows the TG and the DTG curves from heating 39.82 mg of sample 6 (80% clay - 20% oil) in air atmosphere. The results obtained here were similar to Figure 7-6 (80% fine silica - 20% oil), so the same descriptions of these curves can be applied. One difference was the large peak area (peak 3) of (80% clay - 20% oil) compared with peak area of sample 8 (80% fine silica - 20% oil), this is due to the clay weight loss in this range of temperature (375^{o}C - 550^{o}C) as seen in Figure 7-11. Figure 7-11 shows the TG and DTG curves from heating of

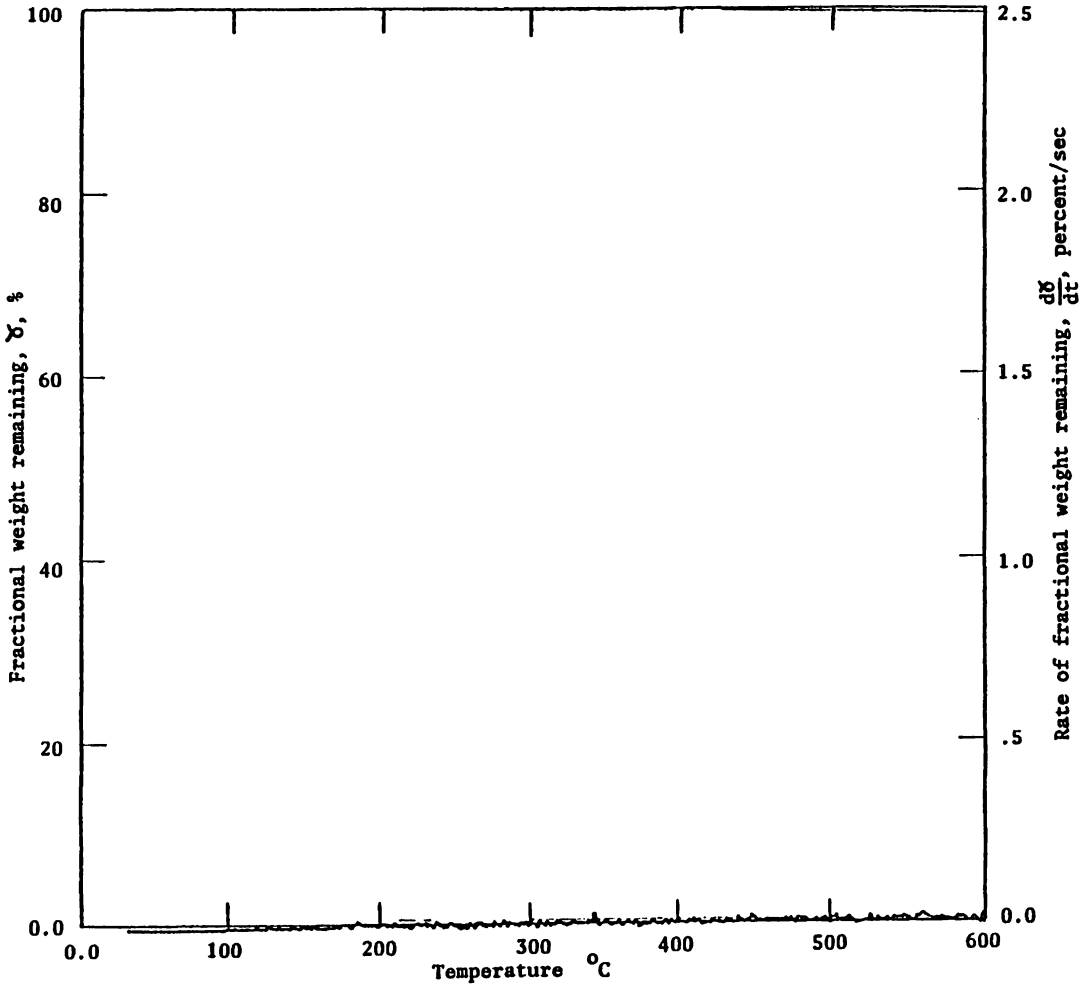

Figure 7-7 TGA thermogram for silica powder in the presence of air flow.

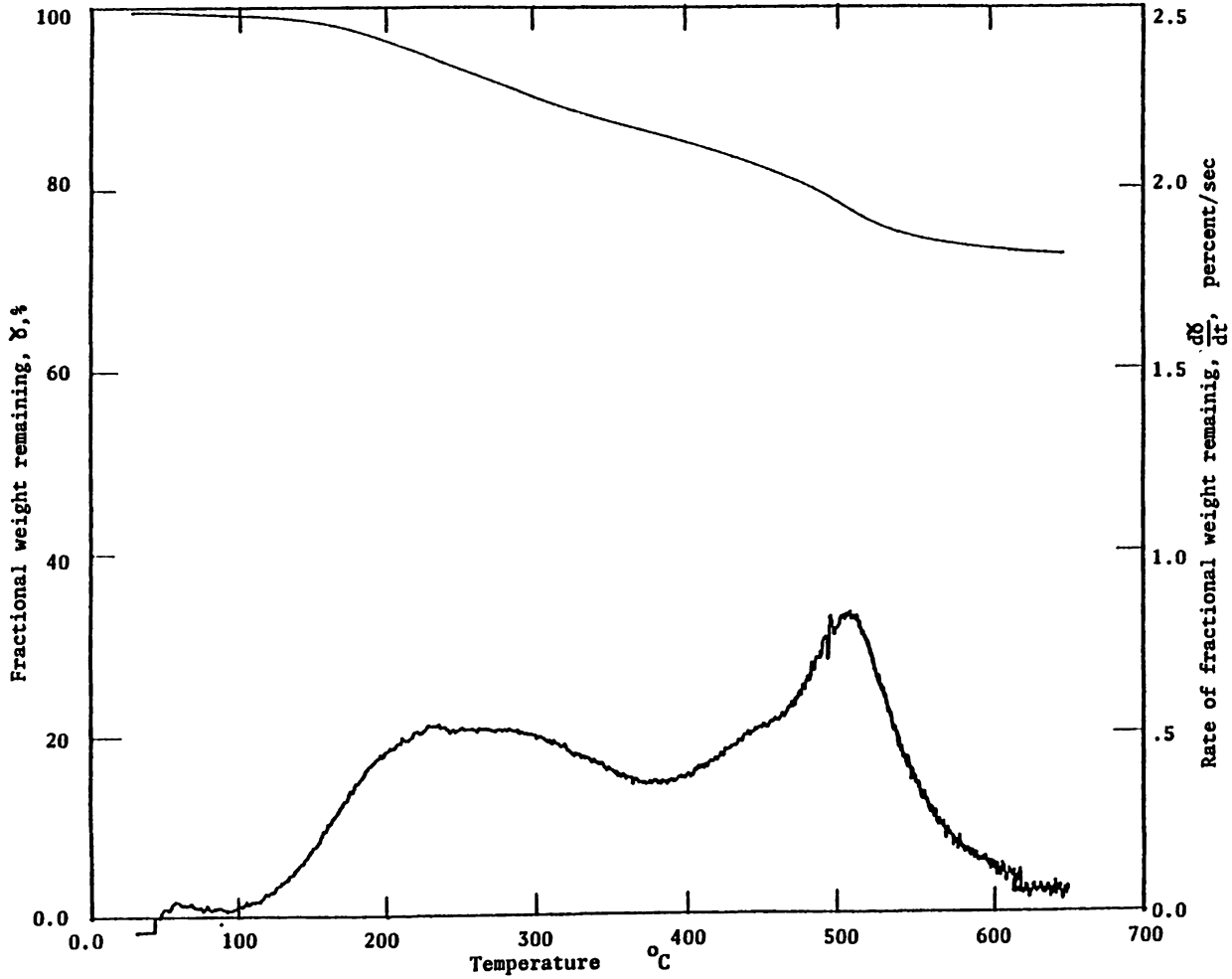

Figure 7-8 TGA thermogram for mixture 6 (80%clay-20%oil) in the presence of nitrogen flow.

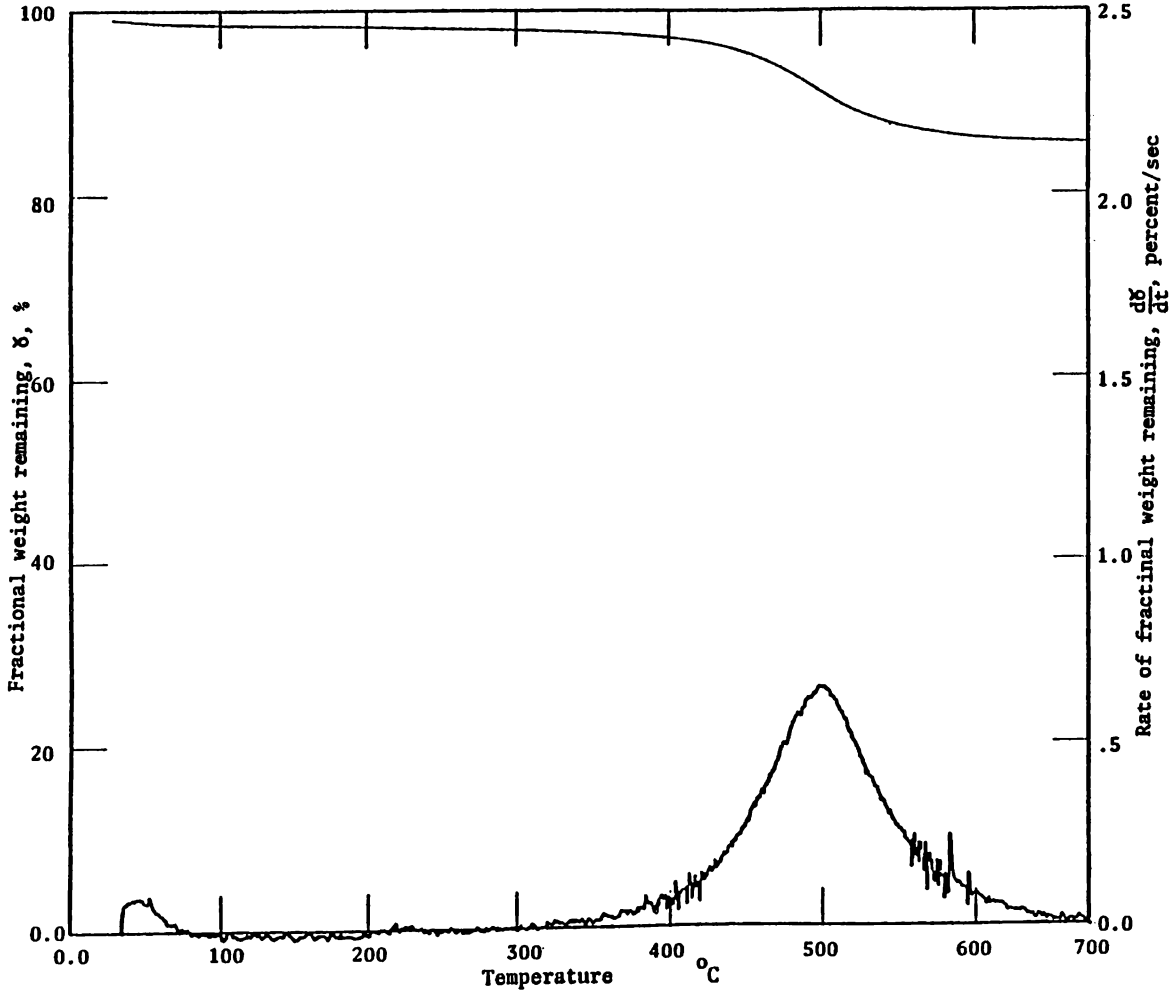

Figure 7-9 TGA thermogram of 100% clay in the presence of nitrogen flow.

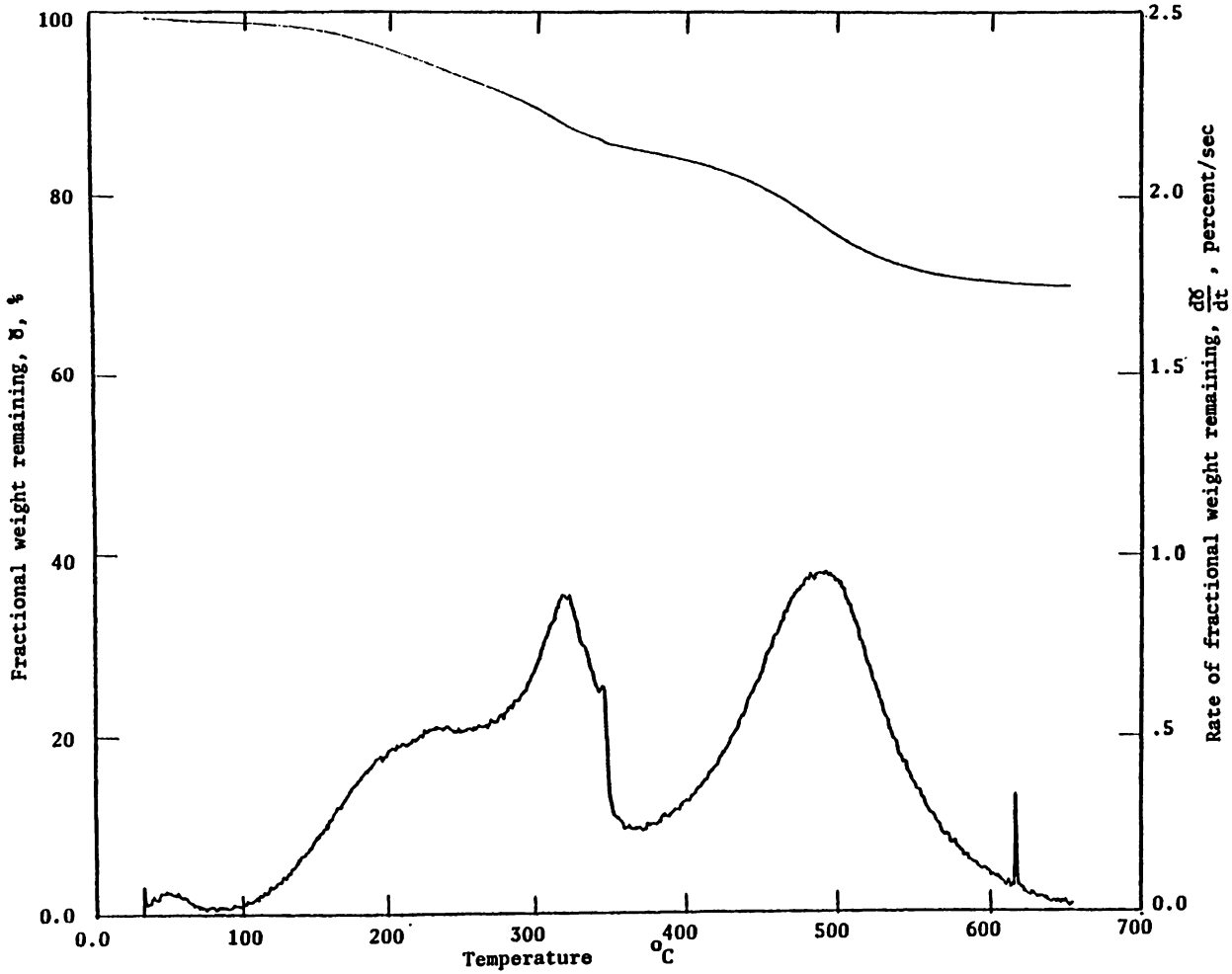

Figure 7-10 TGA thermogram for mixture 6 (80%clay-20%oil) in the presence of air flow.

39.7 mg of clay in an air atmosphere.

Figure 7-12 shows the results of heating of 39.4 mg of burned clay in air atmosphere using the TGA module. The curves indicate no weight loss with temperature. Burned clay was obtained by keeping the clay in an electrical oven at temperature of 600°C for about 5-6 hrs.

Figure 7-13 shows the TG and the DTG curves obtained from heating 40.97 mg of mixture of 80% burned clay - 20% oil in air atmosphere. The resulting curves were similar to the curves of figure 7-6 (80% fine silica powder - 20 % oil).

Derivative thermograms of crude oil heated in air in the presence of different grain materials are compared in Figure 7-14. The shape of the thermograms of the crude oil combustion in the presence of sand closely resemble that of crude oil alone given in Figure 7-2 with the same major reactions in approximately the same temperature range. However, their shapes are significantly different from those of silica powder, clay and burned clay.

7-3 Effect of grain surface area on TGA thermograms

In this section the results obtained from mixtures 9, 10, and 11 will be discussed. Figure 7-15 shows the results of heating 39.68 mg of mixture 9 (80% ground sand - 20% oil) in an air atmosphere. The TG curve as well as the DTG curves did not show much difference from Figure 7-4 (80% sand - 20% oil), i.e., the grain sand did not have any effects on crude oil burning.

Figure 7-16 shows the results of heating of 40.32 mg. of mixture 10 (40% fine silica - 40% sand - 20% oil) in an air atmosphere. The TG

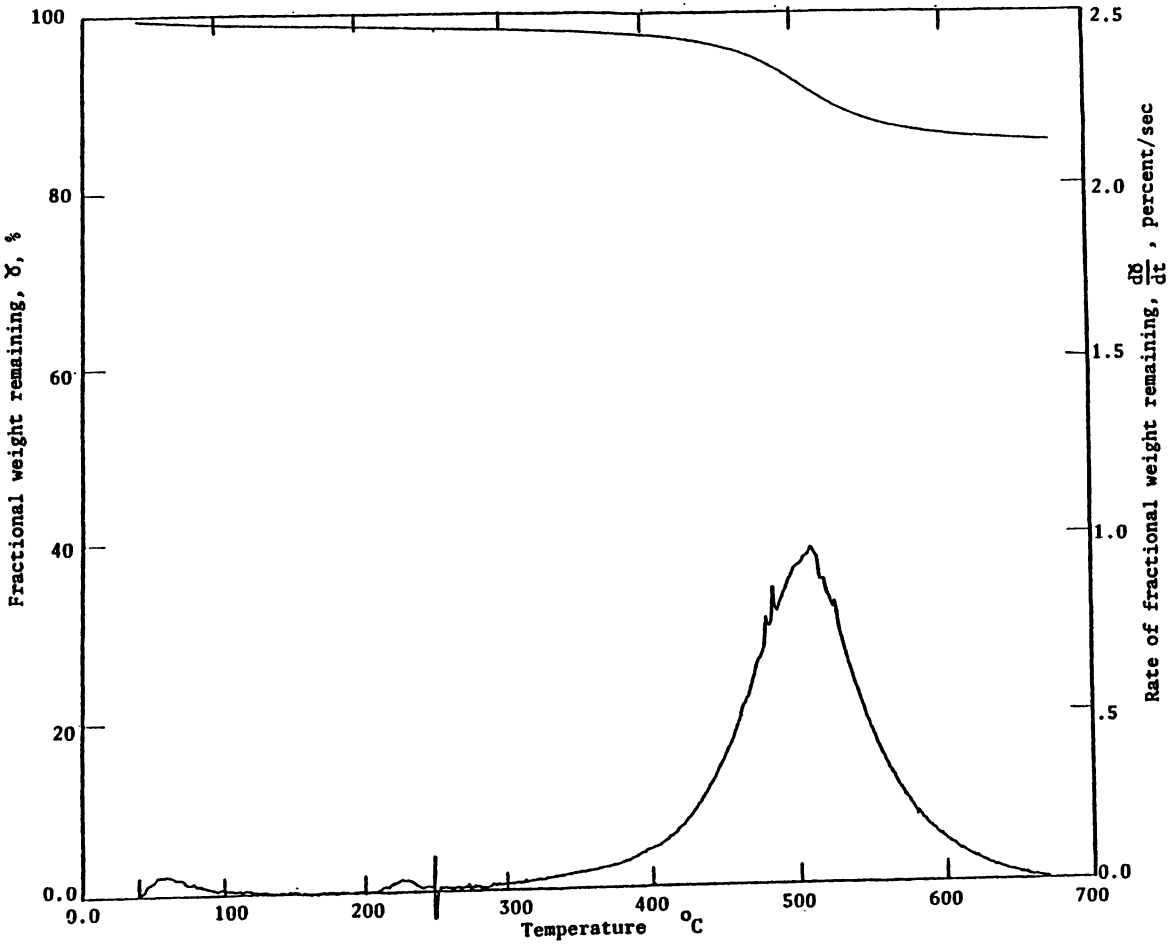

Figure 7-11 : TGA thermogram of 100% clay in the presence of air flow.

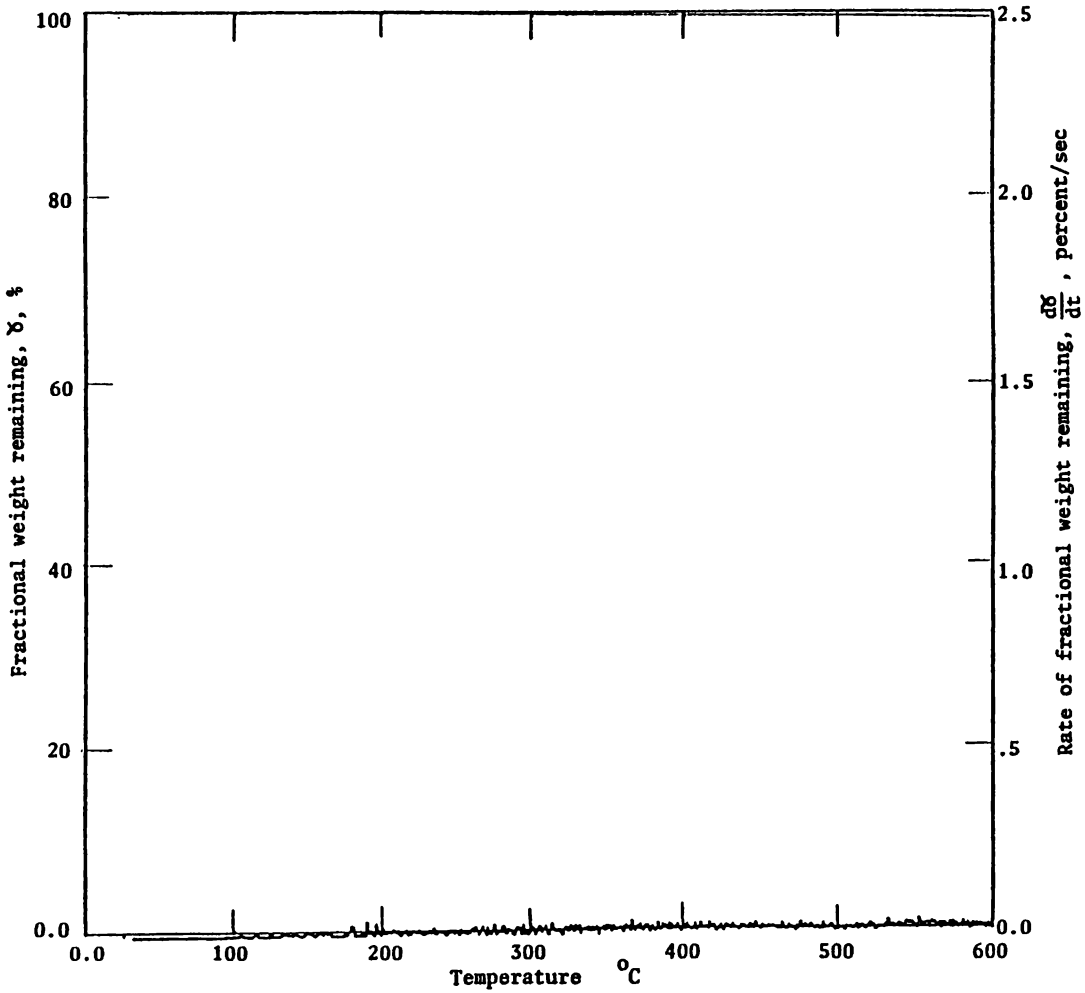

Figure 7-12 TGA thermogram of 100% burned clay in the presence of air flow.

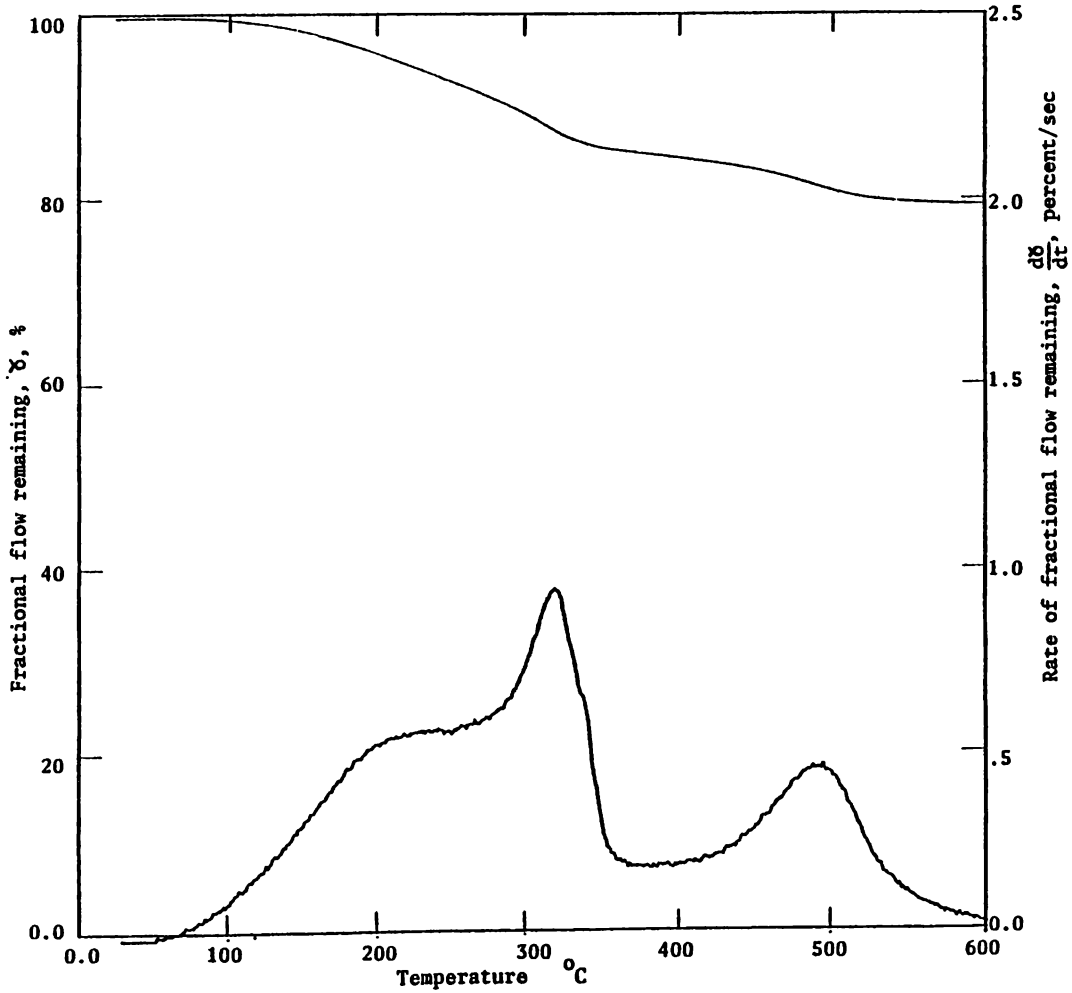

Figure 7-13 TGA thermogram of 80%burned clay- 20%oil in the presence of air flow.

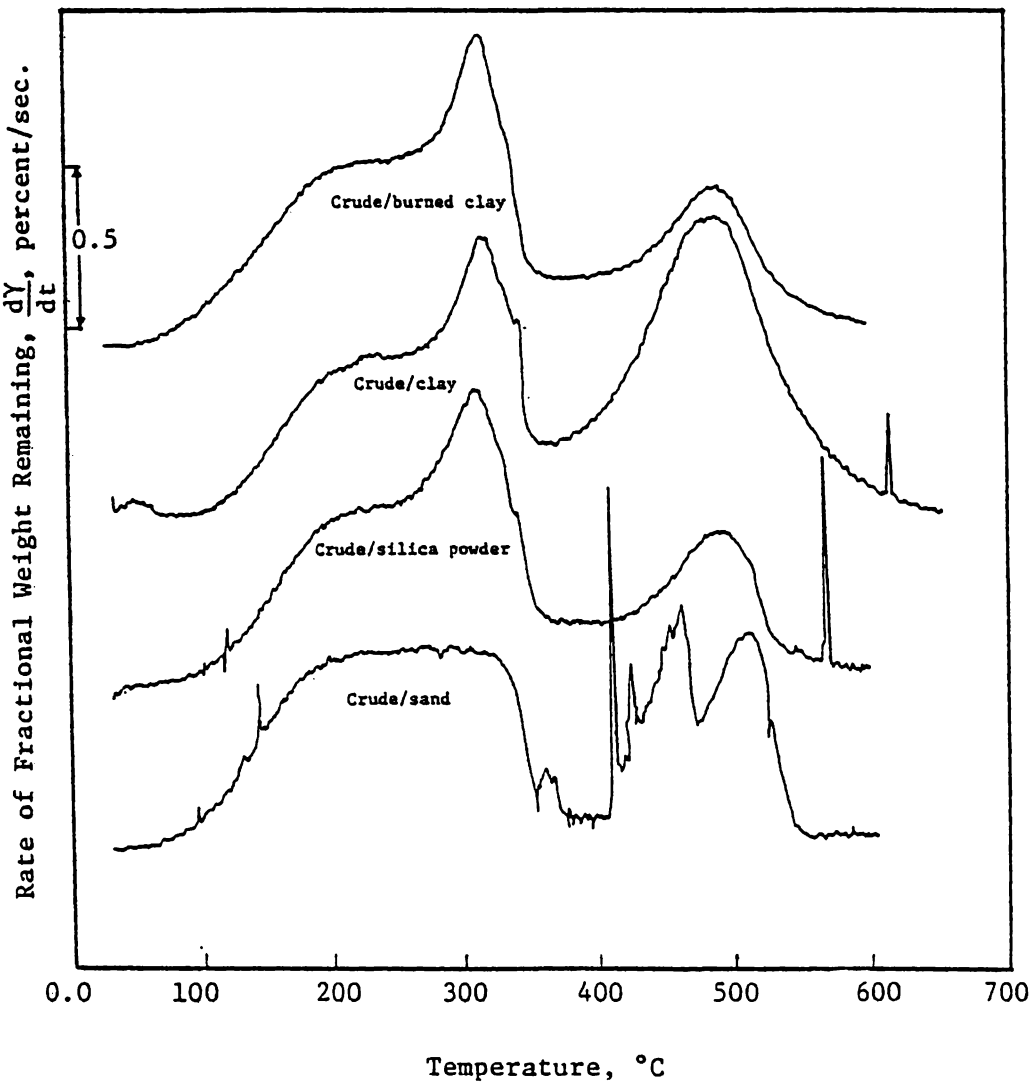

Figure 7-14 Effect of grain materials on TGA derivative thermograms from crude oil combustion

and the DTG curves were similar to the one obtained by heating mixture 7 (80% sand - 20% oil). It was apparent that fine silica had no effect on oil burning if it is used in relatively small amounts.

Figure 7-17 shows the results from heating of 41.66 mg of mixture 11 (40% clay - 40% sand - 20% oil) in air atmosphere. The TG and the DTG curves have the same shape as that from mixture 6 (80% clay - 20% oil). To see the clay effects on the produced curves a run was made using mixture 12 (50% sand - 50% clay). These curves are shown in Figure 7-18. The results showed a weight loss of clay between 375° - 550°C. These curves were used to correct the readings obtained from curves of mixture 11 (40% clay - 40% sand - 20% oil).

The DTG curves of mixture 9 (80% ground sand - 20% oil), mixture 10 (40% silica powder - 40% sand - 20% oil), and mixture 11 (40% clay - 40% sand - 20% oil) are compared with each other in Figure 7-19.

Practically no effect of grinding sand was observed. But, although the weight fractions of clay and silica powder in the mixture were reduced to the same amount, the clay effect on the DTG curve was more pronounced than that of silica powder.

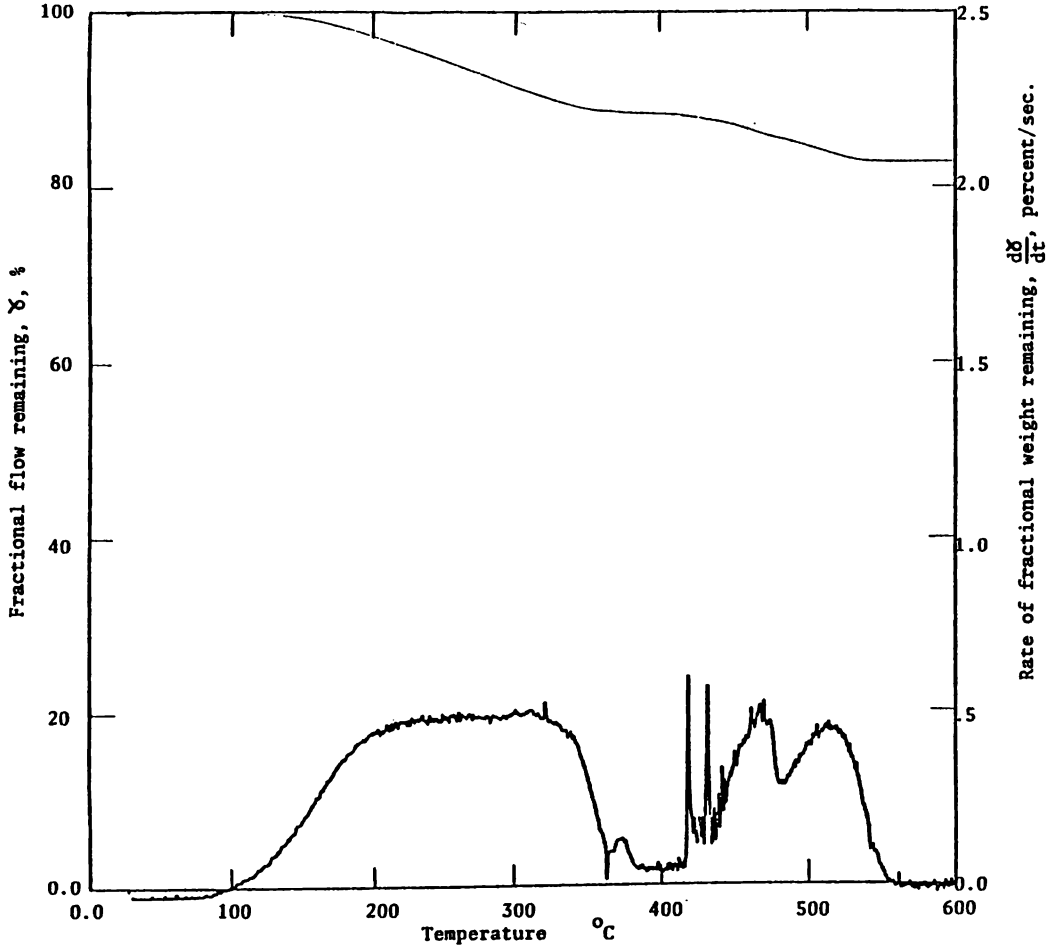

Figure 7-15 : TGA themogram for 80% ground sand-20% oil in the presence of air flow.

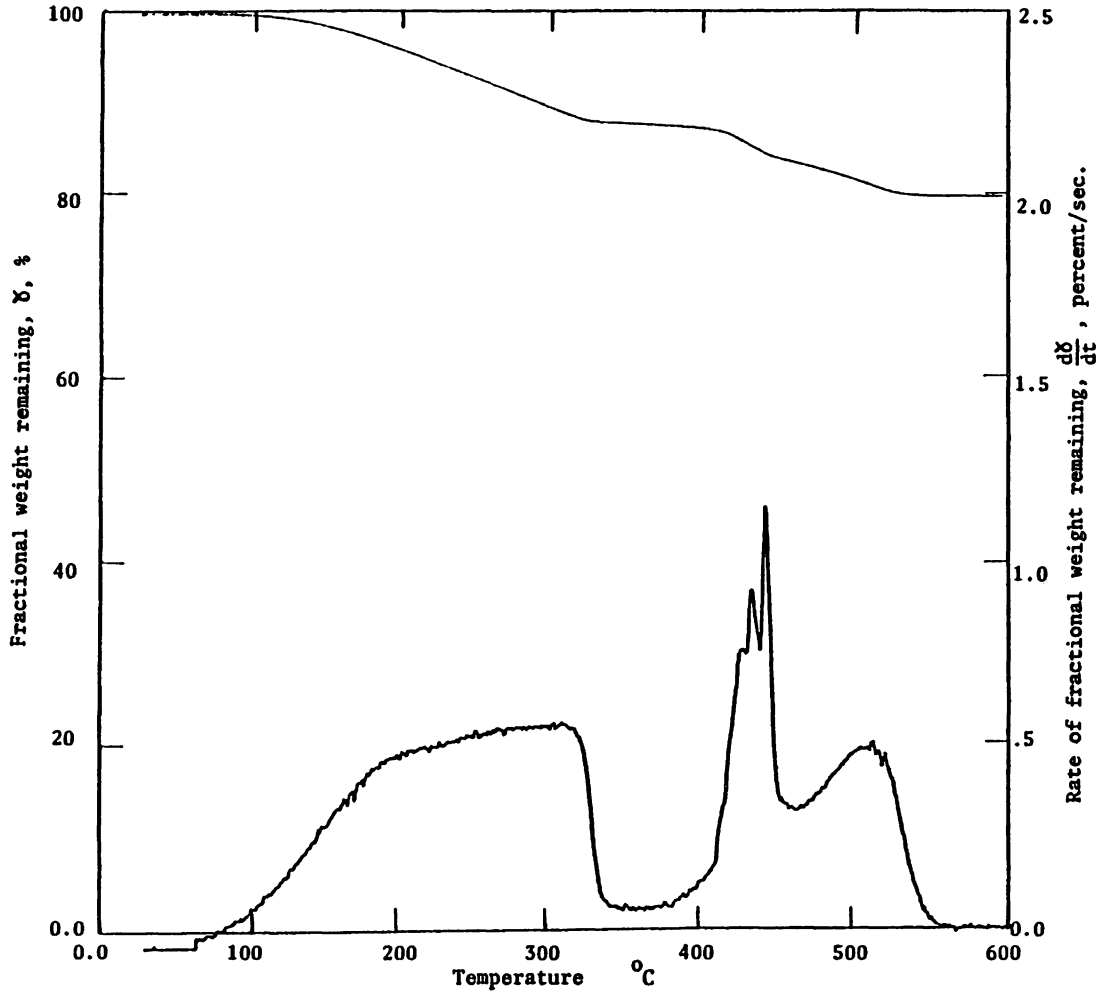

Figure 7-16 TGA thermogram of mixture 10 (40%silica powder-40%sand -20%oil) in the presence of air flow.

Figure 7-17 : TGA thermogram for mixture 11 (40%clay-40%sand-20%oil) in the presence of air flow.

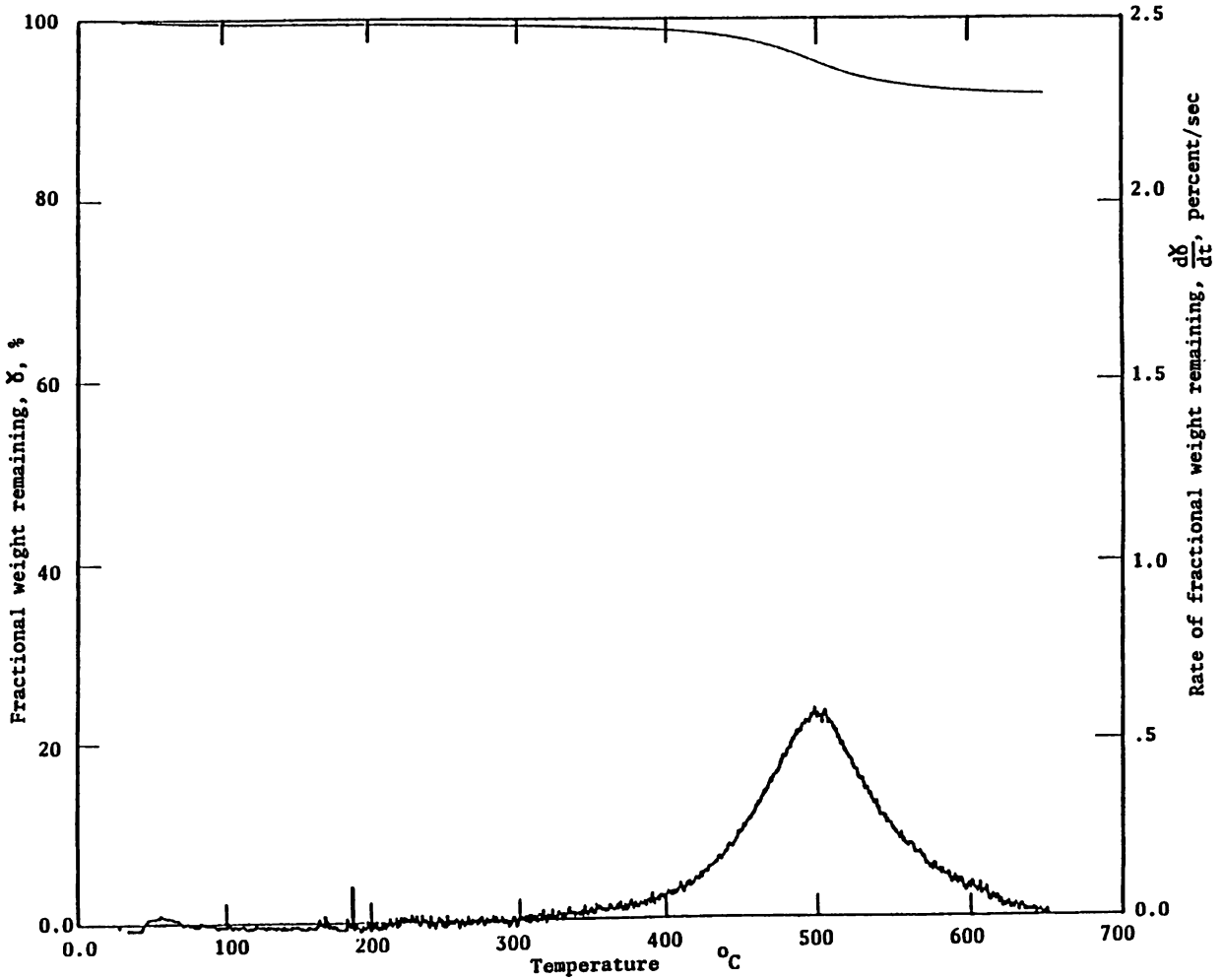

Figure 7-18 TGA thermogram of mixture 12 (50%clay-50%sand) in the presence of air flow.

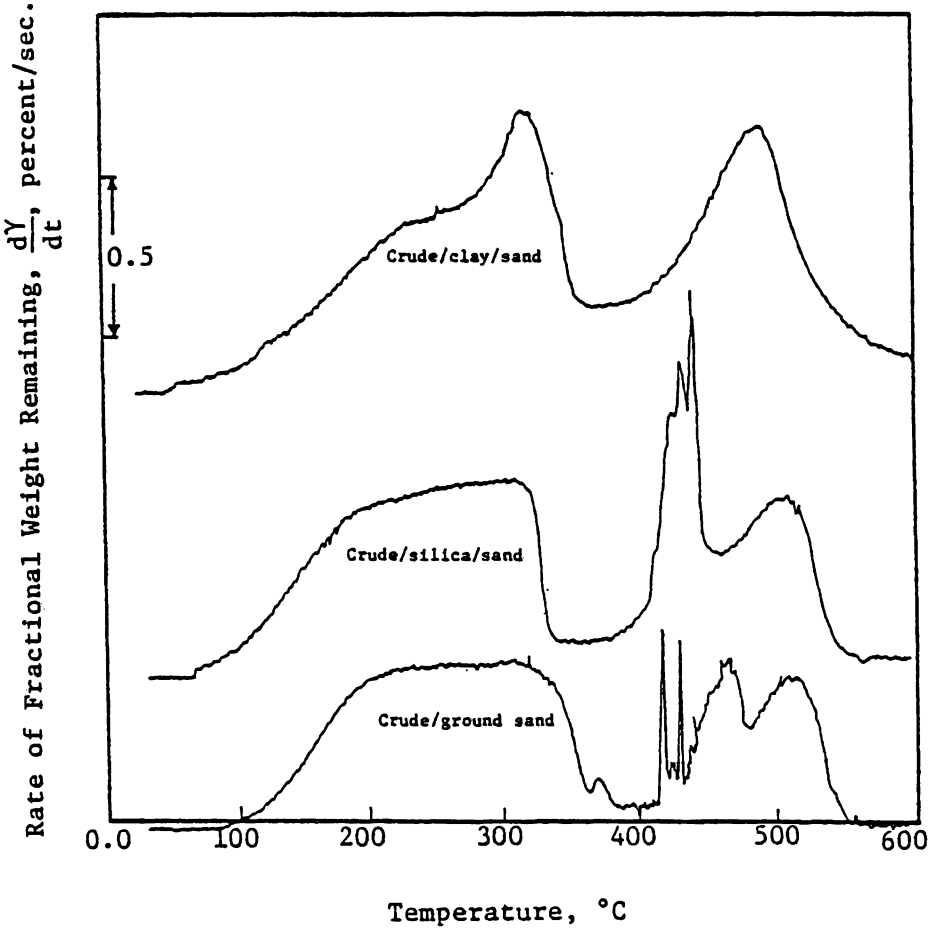

Figure 7-19 Effect of surface area on TGA derivati thermograms from crude oil combustion.

7-4 Effect of heating rate on the TGA thermograms

To assure that the choice of $5^{o}C$/min is a good choice, 3 runs were made using crude oil by itself. One run was made with heating rate of $1^{o}C$/min. The second run was made with heating rate of $5^{o}C$/min while the third run was made using a heating rate of $10^{o}C$/min. Figures 7-2, 7-20, 7-21 present the results of the three runs respectively. The same general trend of reaction mechanism was noted for the 3 thermograms. Later in Chapter 8 it will be shown that the kinetic parameters for both $1^{o}C$/min and $5^{o}C$/min are almost the same while they were different for $10^{o}C$/min. So, it was suspected that the heating rate in the last case was so fast that the reaction did not have enough time to be completed.

7-5 DSC thermograms

The DSC runs were performed to obtain the heat value of the combustion process and to investigate the effects of grain materials. Figure 7-22 presents the DSC curve obtained from heating 15.3 mg of crude oil in an air atmosphere. The curve has three distinct regions. The first region is between $25^{o}C$ and $350^{o}C$, the second region is between $350^{o}C$ - $450^{o}C$, and the third region is between $450^{o}C$ - $550^{o}C$. In the first region, distillation is dominating, which is endothermic. Also there is some burning of crude oil occuring and low temperature oxidation reactions are taking place. It was believed that the straight line obtained at the beginning of this region, no heat generation, is due to the low sensetivity of the DSC which could not detect this small heat amounts.

Between $225^{o}C$ and $350^{o}C$ there is one distinct exothermic peak, i.e., there was heat generated in this range, but still some distilla-

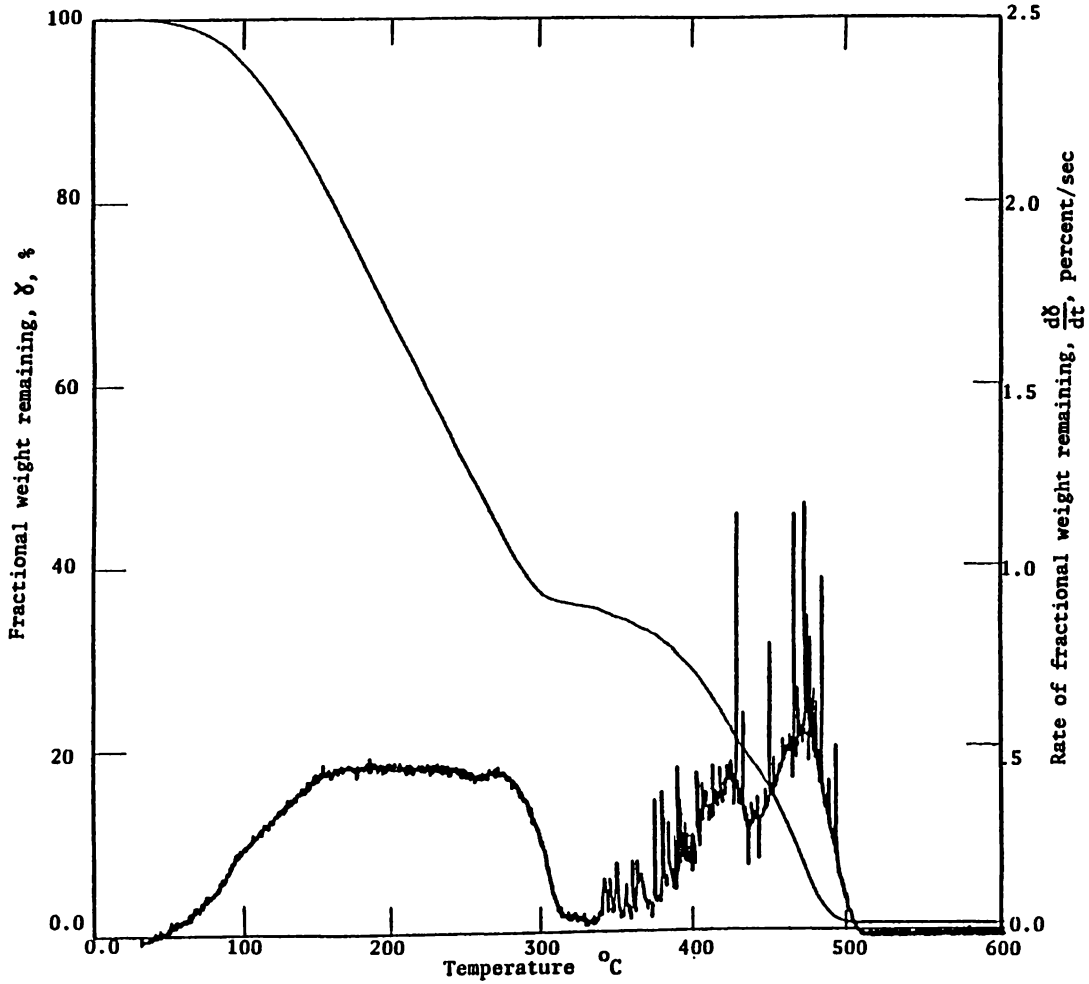

Figure 7-20: TGA thermogram of crude oil combustion in the presence of air flow using heating rate of 1 °C/min.

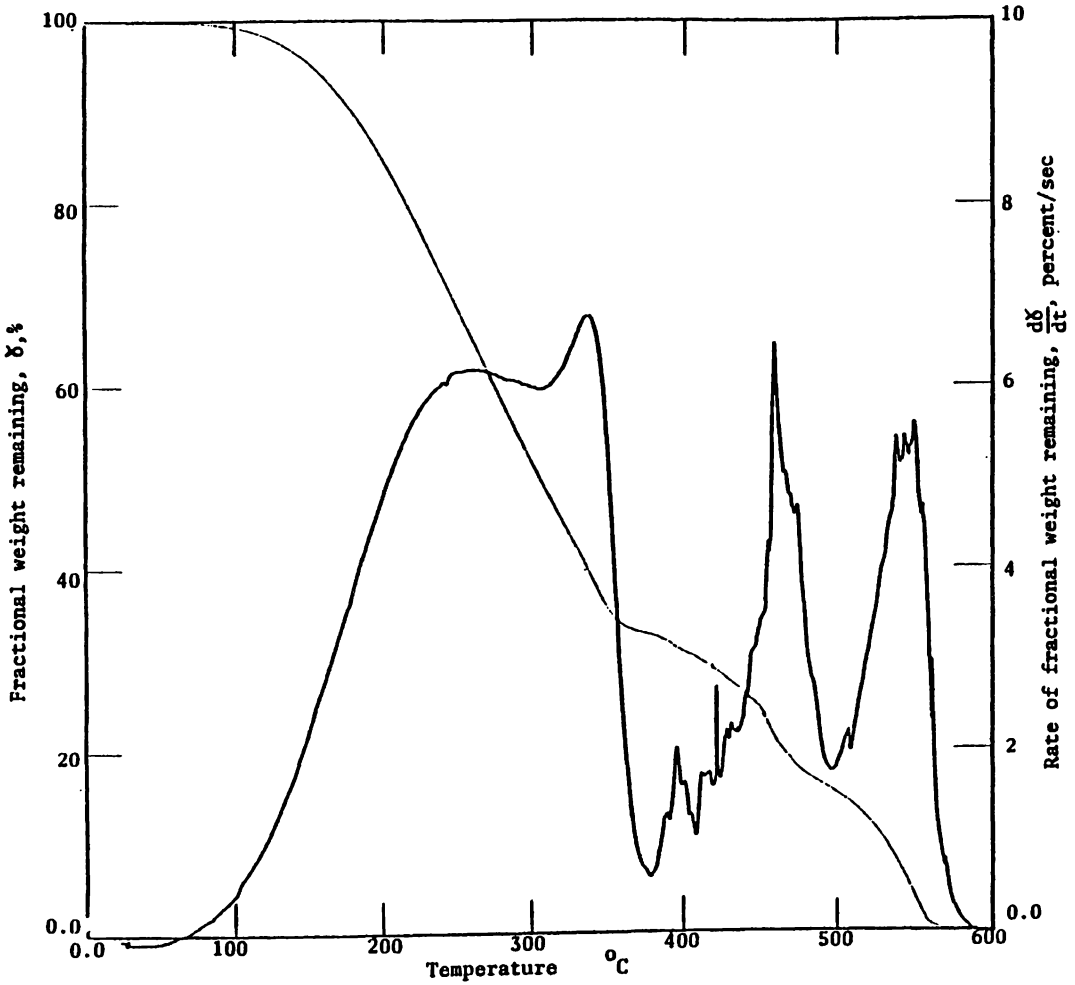

Figure 7-21 TGA thermogram of crude oil combustion in the presence of air flow using a heating rate of 10°C/min.

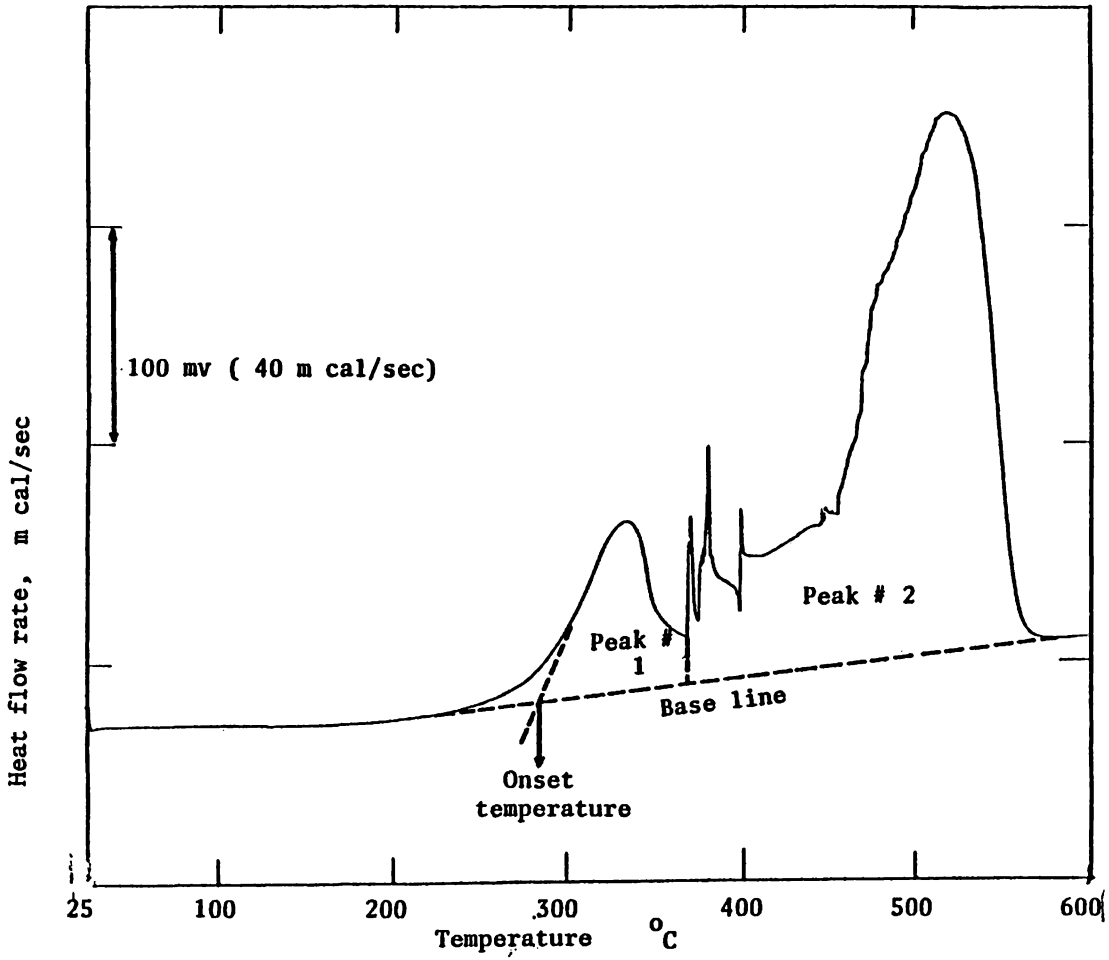

Figure 7-22 DSC thermogram of oil combustion in the presence of air flow.

tion occurs. It was believed that this heat generated was due to burning of crude oil or low termperature oxidation reactions which are exothermic reactions,[57] or both. In the second peak (second and third region) there is cracking and burning taking place. The exothermic peak indicates that the amount of heat produced by burning is greater than that required for cracking. This peak can be seen as two peaks, one between 350°C - 450°C and the other between 450°C - 550°C.

The amount of heat generated in the three regions was smaller than the reported crude oil heat of combustion value, This is due to the distillation of lighter hydrocarbons which are not producing heat, but will be included in the weight loss curve.

Figure 7-23 presents the result obtained from heating of 27.2 mg of mixture 7 (80% sand - 20% oil). This curve is similar to the curve of Figure 7-22 (100% crude oil), i.e., same peaks occured in approximately the same temperature range, so the same description of Figure 7-22 is applied here. It was obvious that sand had no effect on crude oil burning from the similarity of both results.

Figure 7-24 presents the results obtained from heating of 14.4 mg of mixture 8. The resulting curve shows two distinct exothermic peaks, one between 225°C - 400°C and the other between 400°C - 550°C. The straight line up to 225°C is due to lack of any detectable exothermic or endothermic reactions. The exothermic peak between (225°C - 400°C) may be due to low temperature oxidation reactions or burning of crude oil, or both. The second exothermic peak between (400°C - 550°C) is due to the burning of crude oil. This figure should be compared to Figures 7-22 and 7-23 to see the difference. In Figures 7-22 and 7-23 three

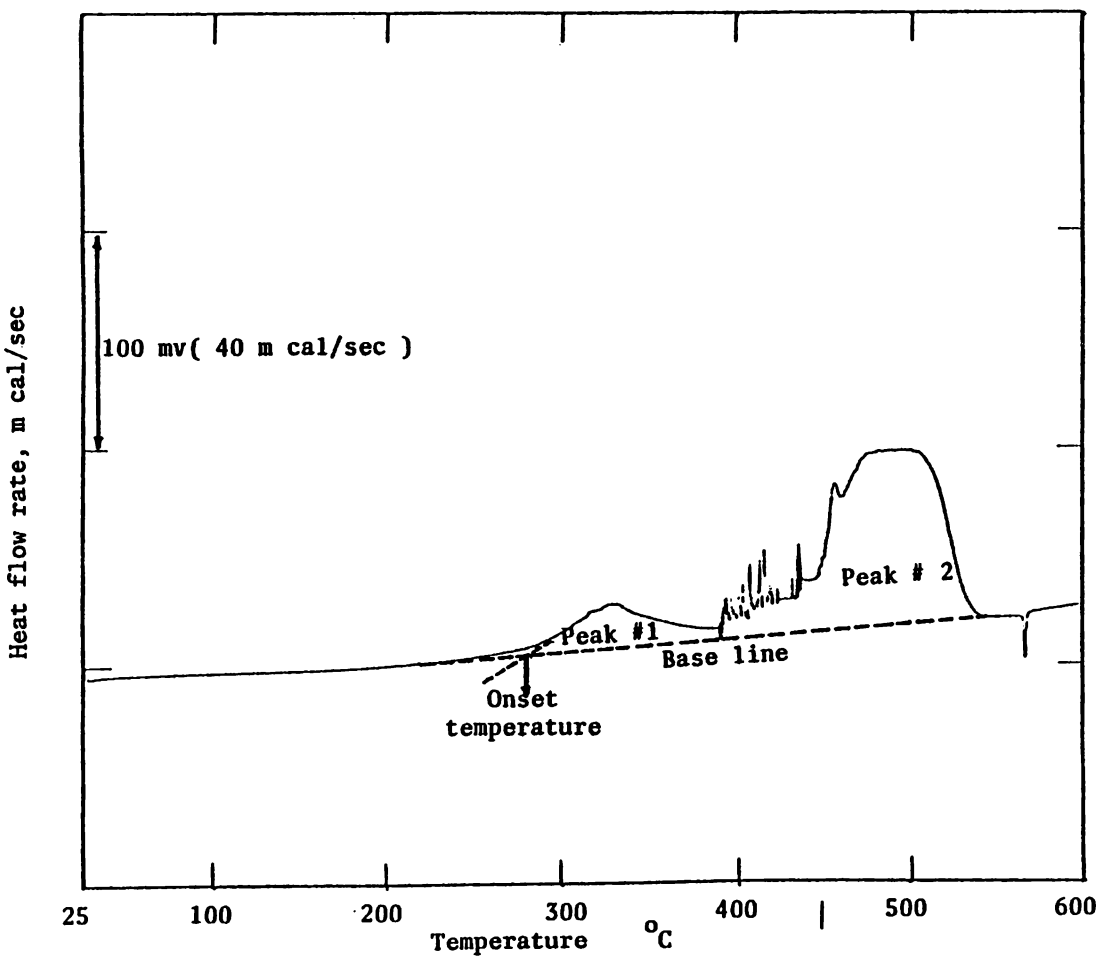

Figure 7-23 DSC thermogram of mixture 7 (80%sand-20%oil) in the presence of air flow.

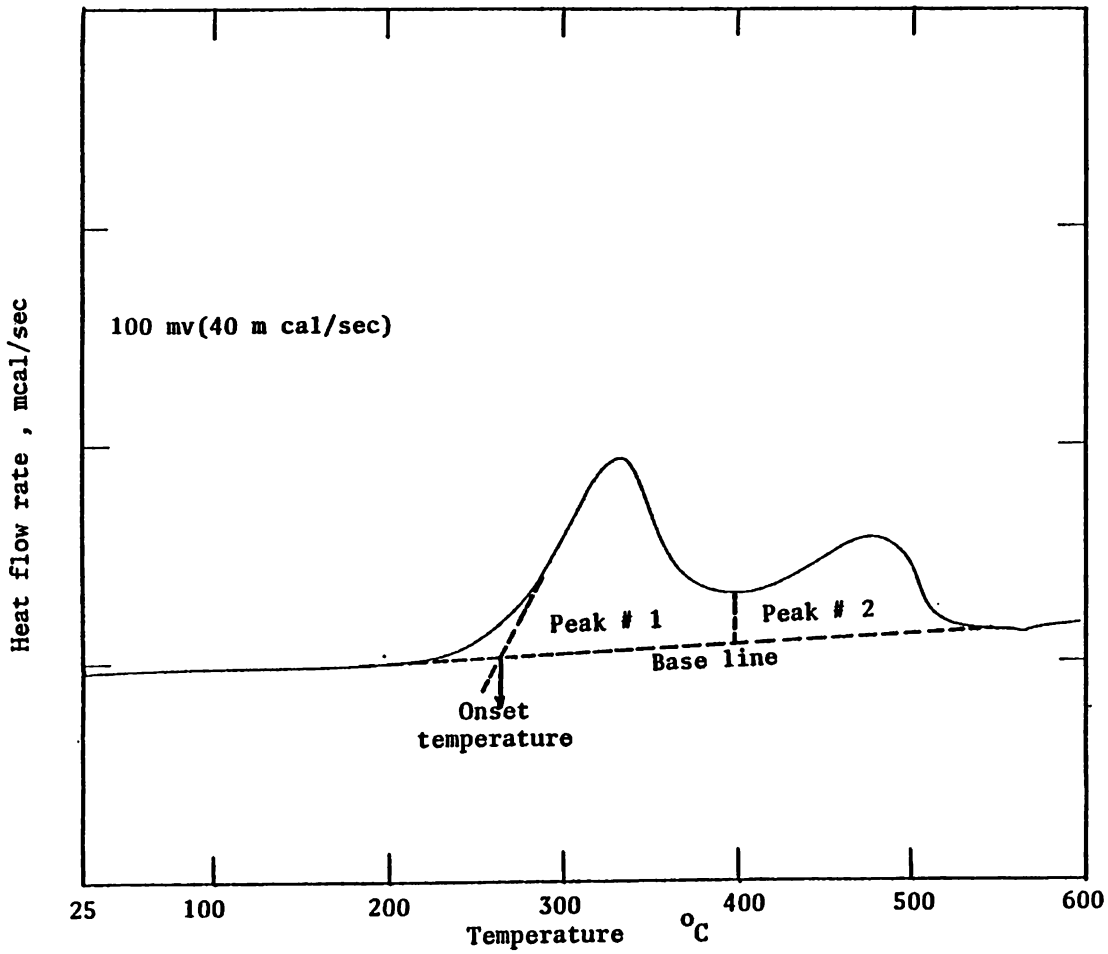

Figure 7-24 DSC thermogram of mixture 8 (80%silica powder-20%oil) in the presence of air flow.

distinct peaks occured (considering last peak consists of two peaks), while in Figure 7-24 only two distinct peaks were produced. This means that fine silica powder had an effect on crude oil burning.

Figure 7-25 presents the results obtained from heating of 15.5 mg of mixture 6 (80% clay - 20% oil). the reference tray was loaded with 11.5 mg clay to offset its effect on the produced curve. The curve obtained was similar to Figure 7-24 (80% fine silica - 20% oil).

Figure 7-26 presents the curve produced from heating of 12.5 mg of sample 10 (40% fine silica - 40% sand - 20% oil). The resulting curve showed again two distinguished peaks. This Figure resambles Figure 7-23 (80% sand-20% oil) more closely than figure 7-24 (80% silica powder - 20% oil).

Figure 7-27 shows the results from burning 16.7 mg of mixture 11 (40% sand - 40% clay - 20% oil). The reference tray was loaded with 12.3 mg of mixture 12 (50% clay - 50% sand) to offset the clay effects on the produced curve. The resulting curve was similar to Figure 7-25 (80% clay - 20% oil).

Up to this point, it was clear that in all TGA thermograms three distinct regions, namely distillation and two combustion/cracking regions, were observed. Also, the addition of kaolinite clay or IMSIL silica powder (large amounts) changed the shape of the crude oil TGA and DSC thermograms significantly while sand and ground sand had no effect. A quantitative study was needed to interpret all the obtained thermograms and compare the generated results. Chapter 8 presents this quantitative study.

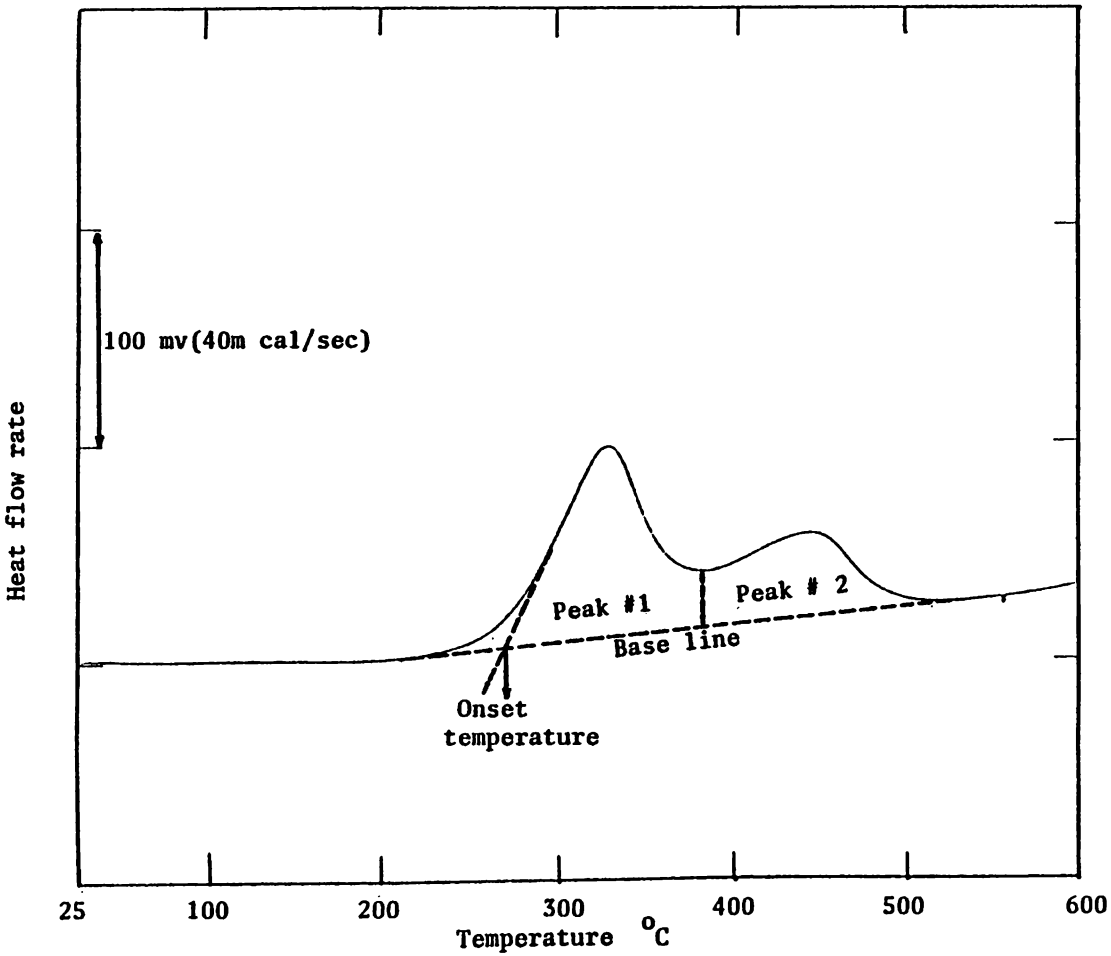

Figure 7-25 DSC thermogram of mixture 6 (80%clay-20%oil) in the presence of air flow,

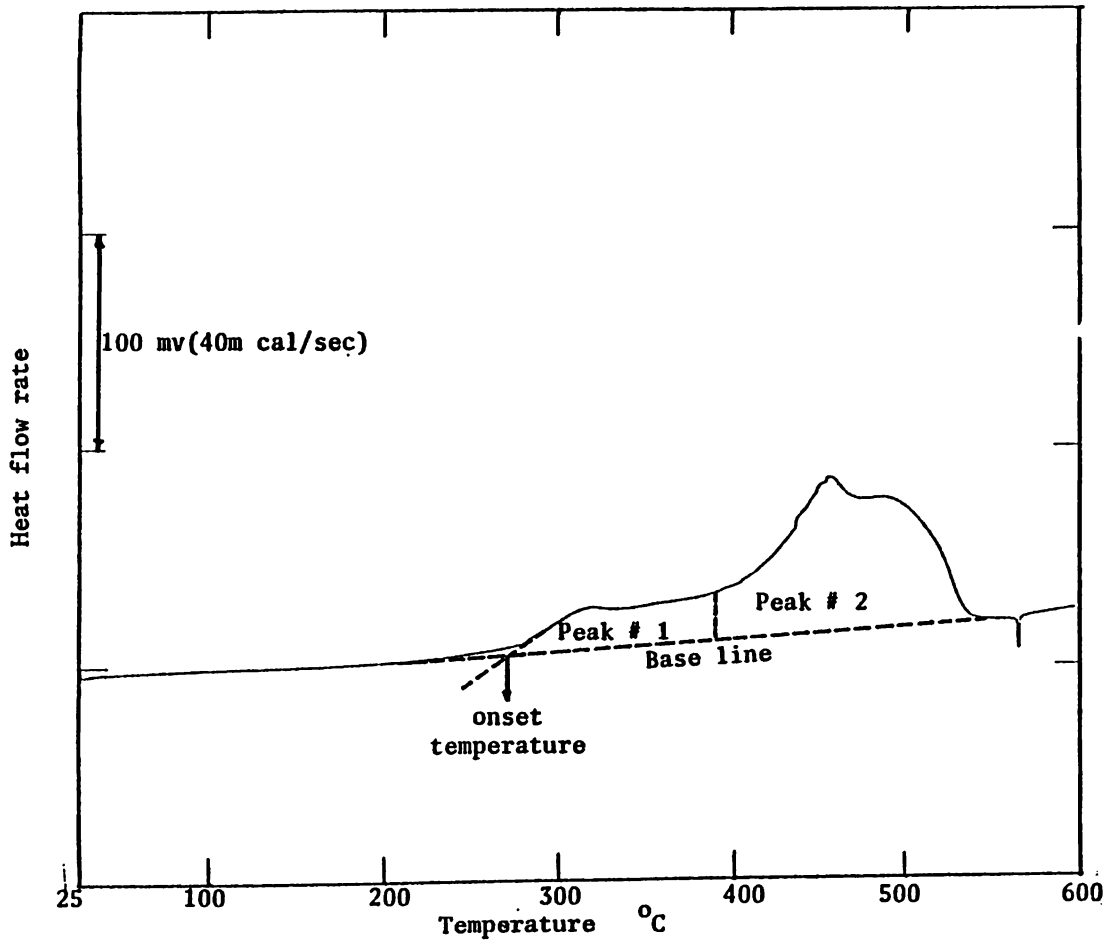

Figure 7-26 DSC thermogram of mixture 10 (40%silica powder-40%sand-20%oil) in the presence of air flow.

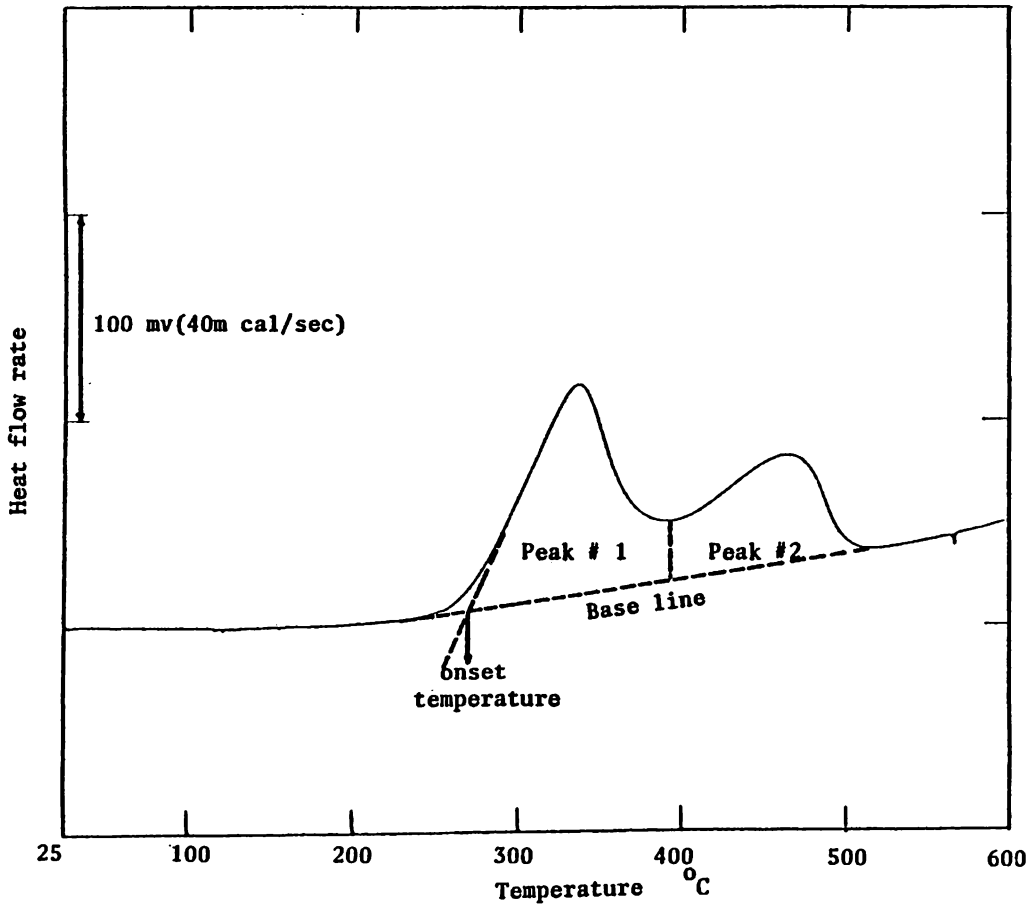

Figure 7-27 DSC thermogram of mixture 11 (40%clay-40%sand-20%oil) in the presence of air flow.

CHAPTER 8

Analysis of the Thermograms

This chapter presents the quantitative study of the thermograms obatined from both the TGA and the DSC. Mickelson and Einhorn[35] ratio method was applied to the TGA thermograms to generate kinetic data. Activation energy and reaction order estimated from this method were used to illustrate the possible catalytic effects of clay on the process.the DuPont suggested equations were used to calculate heat values from the DSC thermograms for the mixtures investigated. Sample calculation as well as the final results will be presented in this chapter.

8-1 Comparison of the crude oil weight loss in the presence of different matrix content

To determine the difference in weight loss between heating crude oil in the presence of different grain matrix, this procedure was taken:

A- For matrix which did not show any weight loss with temperature

This sample calculation can be applied to any matrix which does not show any weight loss with temperature such as fine silica powder, sand, or a mixture of both. Figure 8-1 presents a sample thermogram Length A represents the maximum weight loss, which corresponds to the total amount of oil in the sample. Length B presents the amount of oil loss at a given temperature, therefore, the percentage of the crude oil weight loss at point B is:

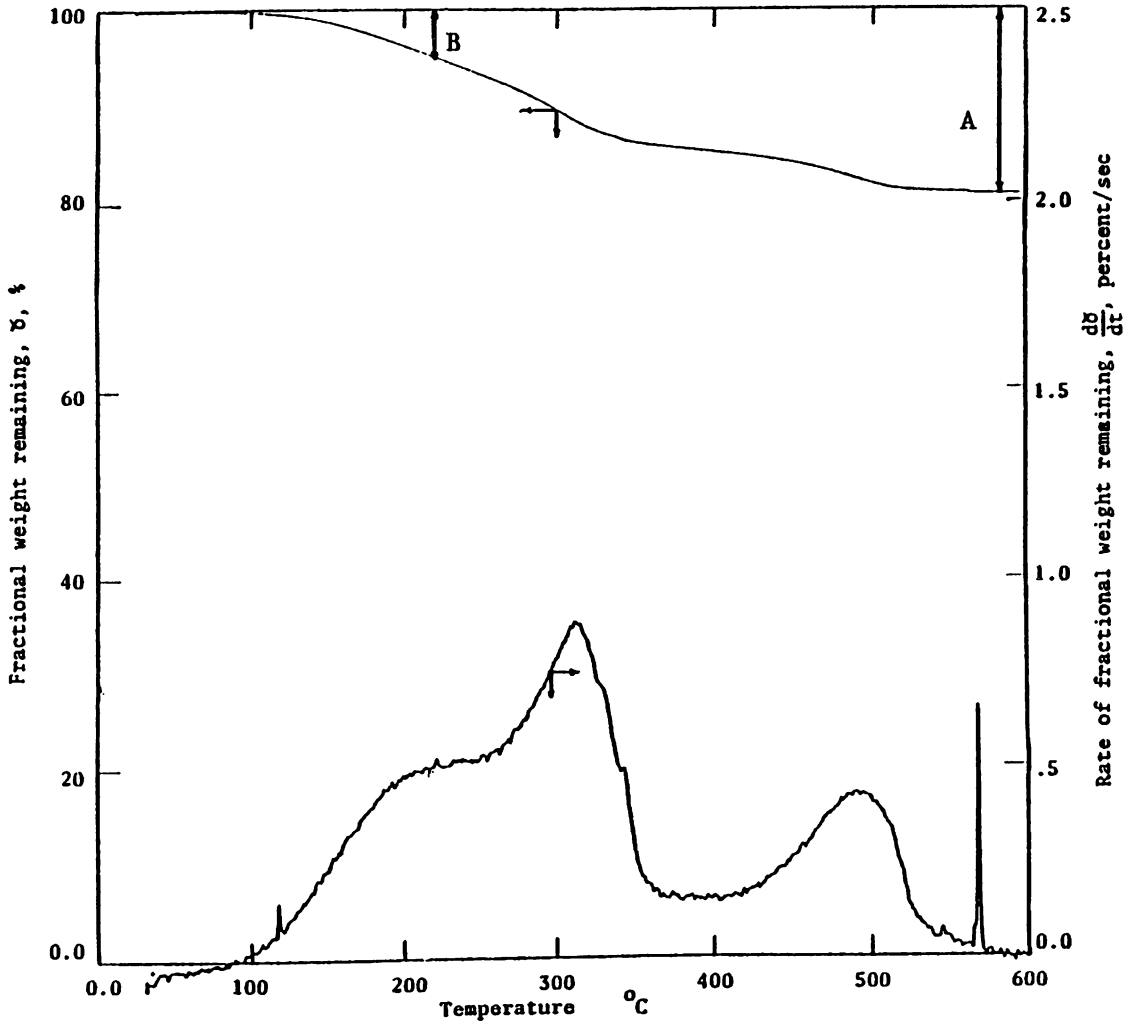

Figure 8-1 TG and DTG curves for heating of crude oil in the presence of matrix with no weight loss with temperature

$$\frac{B}{A} \times 100$$

These points are plotted along with the TG thermograms of Figures 7-1 or 7-2 in Figures 8-3 to 8-5.

B- For matrix which shows a weight loss with temperature

This sample calculation can be applied to any matrix which shows weight loss with temperature such as clay. The TG curve from heating of the matrix containing clay is overlapped on the TG curve from heating of the same matrix mixed with oil. Figure 8-2 presents a sample of the overlapped curves. In Figure 8-2 "A" represents the total amount of oil loss, while "B" represents the oil loss at a given temperature. The same procedure as in part A was undertaken to calculate the crude oil weight loss with temperature in the presence of clay.

Results in Figures 7-4, 7-6, and 7-10 (80% sand - 20% oil, 80% fine silica powder- 20% oil, and 80% clay - 20% oil) were converted into crude oil weight loss in order to distinguish the differences in weight loss between heating crude oil in the presence of sand, fine silica powder, clay matrix. Figure 8-3 presents these results. Data points from the 80% sand - 20% oil thermogram fall exactly on the 100% crude oil TG curve. The data points of the 80% fine silica powder - 20% oil thermogram also fell on the distillation portion of the 100% crude oil curve. However, a small effect did show up on the burning/cracking portion of the TG curve, i.e., deviation from the 100% oil curve to a higher weight loss. The points of the 80% clay - 20% oil thermogram

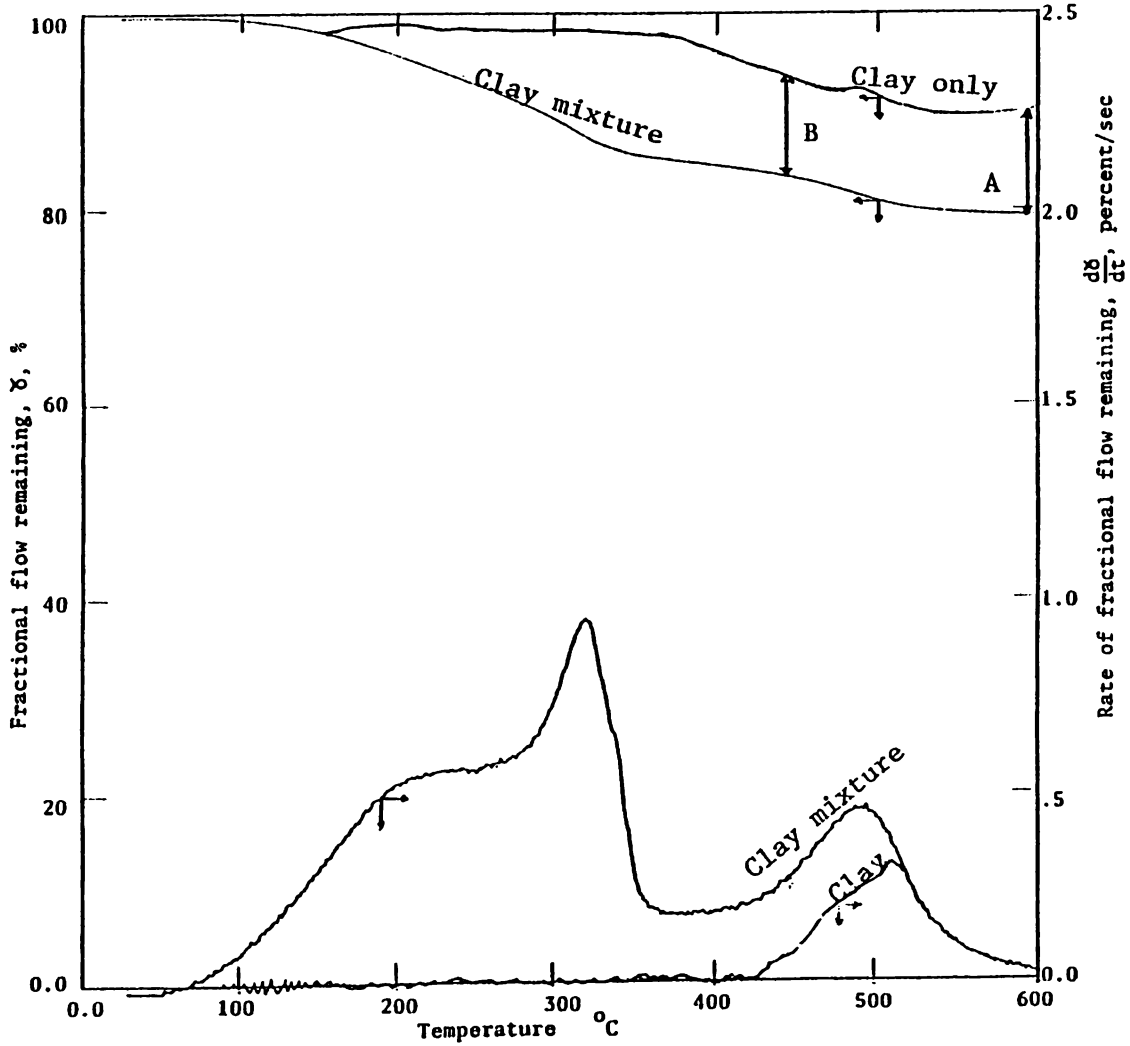

Figure 8-2 Overlapped TG and DTG thermograms for heating of clay and crude oil in the presence of clay

showed also no effects on the distillation portion of the TG curve of oil, but showed greater effects than the 80% fine silica powder - 20% oil thermogram on the burning cracking portion of the TG curve of oil, i.e., higher weight loss of oil in the presence of clay matrix.

In summary, sand has no effect on crude oil burning, while silica powder has some effect and clay has the most pronounced effect on crude oil weight loss.

To determine the effects of smaller surface area, Figure 7-17 (40% clay - 40% sand - 20% oil) and Figure 7-16 (40% fine silica powder - 40 % sand - 40% oil) were converted into oil weight loss and plotted in Figure 8-4. Data points from the 40% fine silica powder - 40% sand - 20% oil thermogram fell almost on the crude oil TG curve. The data points of the 40% clay - 40% sand - 20% oil thermogram showed no effects on the distillation portion of the oil curve and showed deviation from the crude oil curve in the cracking/burning region, i.e., higher weight loss than the crude oil curve.

To study the crude oil weight loss in a nitrogen atmosphere, Figures 7-3, 7-5, and 7-8 (80% sand - 20% oil , 80% clay - 20% oil, 80% fine silica - 20% oil) were converted into crude oil weight loss and plotted in Figure 8-5. To generate the data of the 80% clay - 20% oil thermogram, Figures 7-8 and 7-9 were overlapped and the reading was taken as the distance between both curves. The same procedure as that in the case of matrix showing weight loss with temperature was used.

In Figure 8-5 one can see the effect of clay on heating crude oil in a nitrogen atmosphere. These results showed that the weight loss of crude oil in the presence of clay and flowing nitrogen at a given tem-

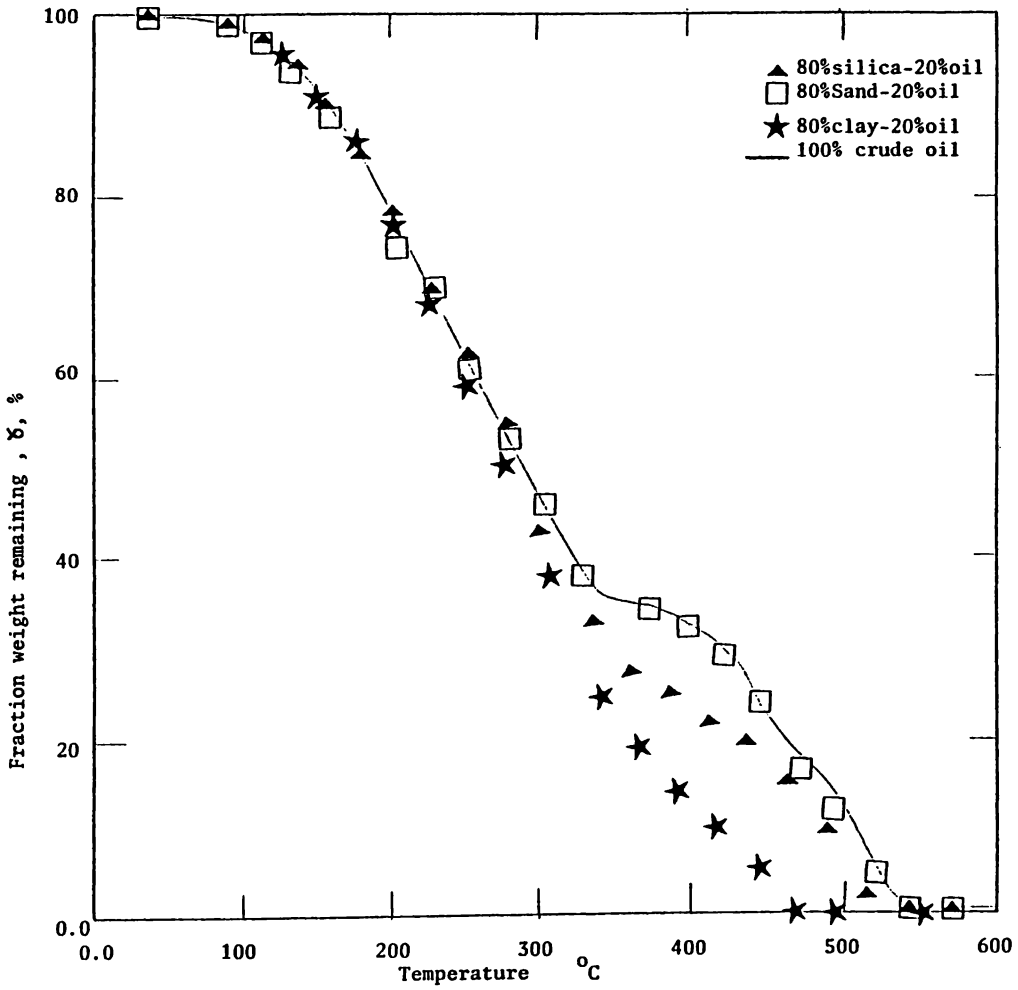

Figure 8-3 Weight loss comparison of crude oil burning in the presence of different grain materials.

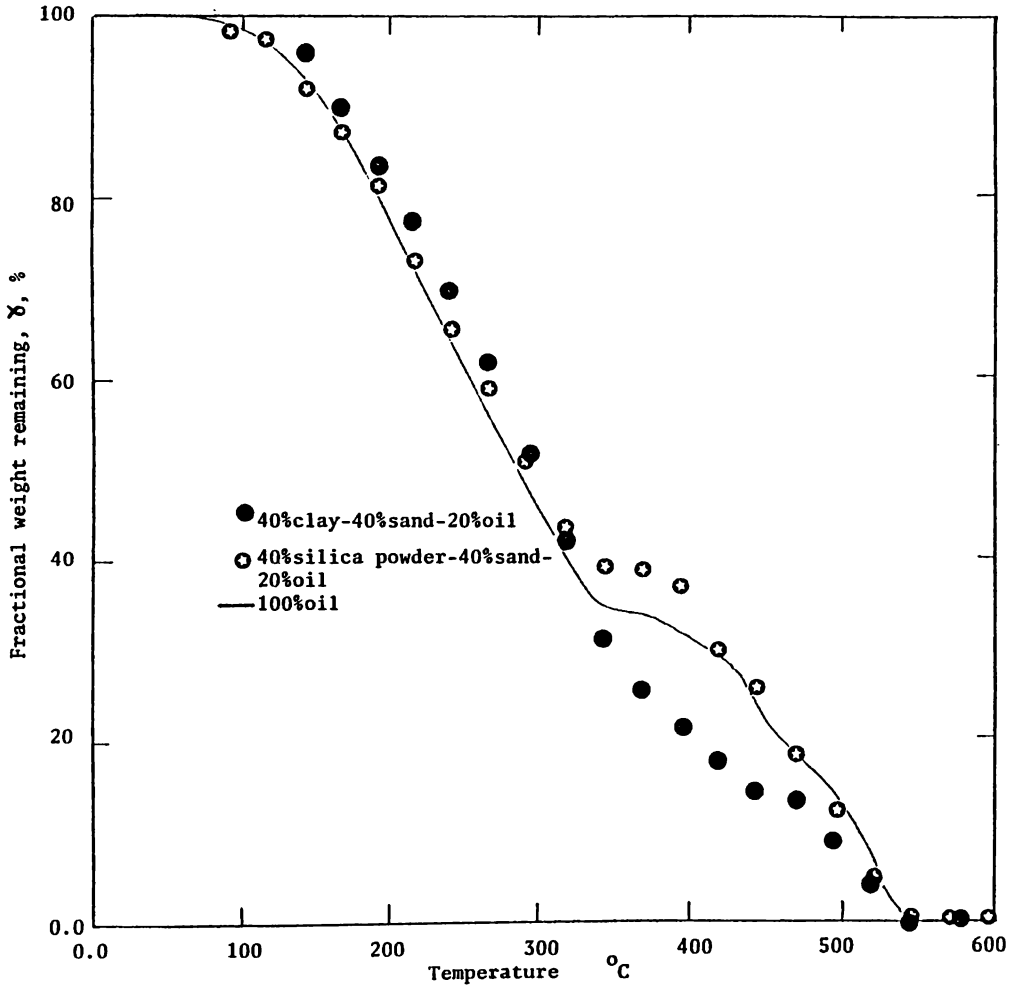

Figure 8-4 Weight loss comparison of crude oil combustion in the presence of different grain materials.

perature was much less than in its absence. This implies that crude oil is absorbed onto the clay surface and cannot be easily distilled by flowing nitrogen.

In comparing Figures 8-3 and 8-5 it is interesting to note that the clay effect is reversed, with respect to crude oil weight loss at a given temperature for flowing nitrogen, to that of flowing air. Also, from Figure 8-5, one can see that the crude oil weight loss in the presence of sand and silica powder seems to be somewhat smaller than in the presence of clay. This effect was expected for the silica powder and clay due to their large surface area. However, the change in weight loss behavior in the presence of sand was attributed to the uncertainty involved in sampling from the sand mixture in the beaker. In the case of clay and silica powder the oil absorbs onto the grain and the mixture is stable and uniform, while the sand tends to seperate from the oil and settles to the bottom of the beaker. Although before each run the content of the beaker was mixed thoroughly, oil content in the small sample taken (40 mg) could be less than the actual oil content saturation in the beaker. If the sample taken from the beaker was assumed to contain .4 mg less crude oil (which is quite possible in the case of sand-crude oil mixture) the data points of the sand in Figure 8-5 are lowered to the curve of crude oil weight loss.

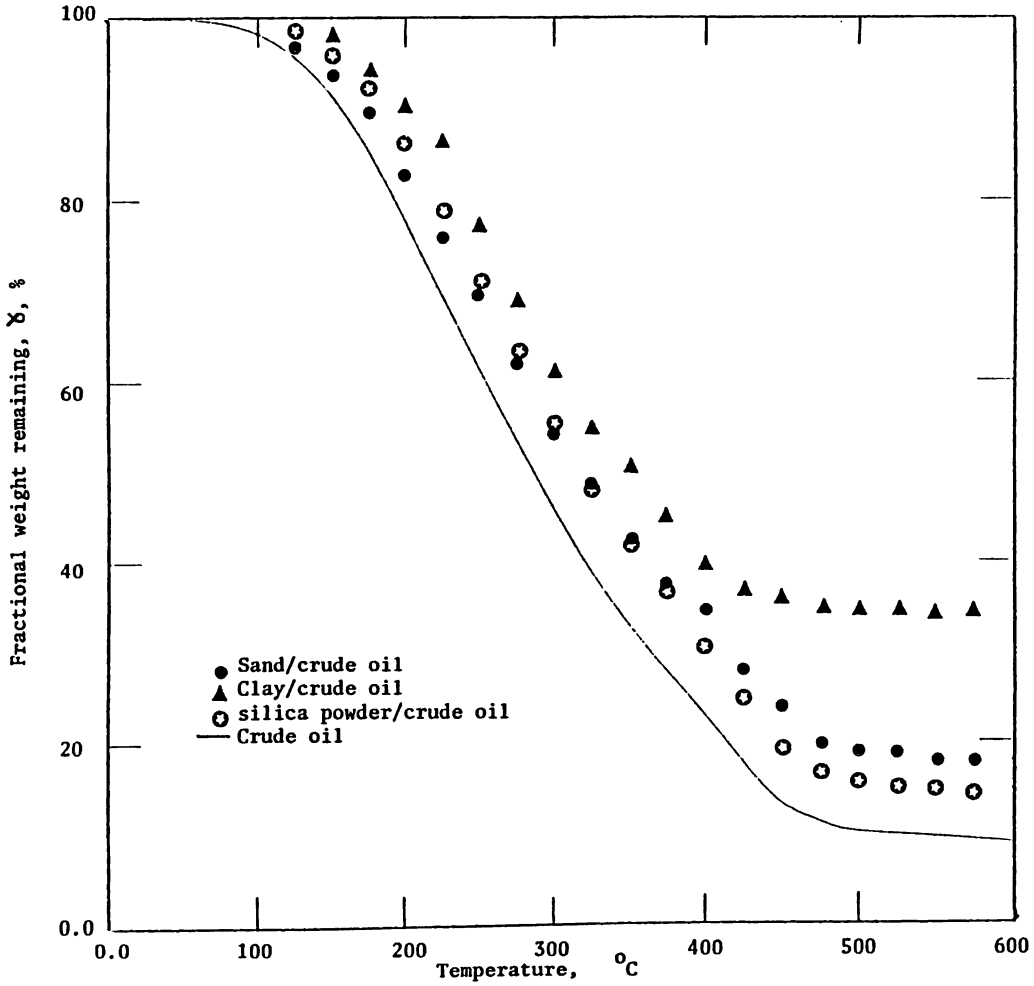

Figure 8-5: Weight loss comparison of crude oil distillation in the presence of different grain materials.

8-2 Kinetic analysis of the TGA thermograms

The Freeman and Carroll's[33] method was applied first because it has the advantage that most portions of the thermogram can be used in interpreting the kinetics of the decomposition reaction. The explanation of the model is given in Appendix A.

This method failed to give straight lines when plotting.

$$\frac{d\log(-d\gamma/dT)}{d\log\gamma} \quad \text{versus} \quad \frac{dT}{T^2\, d\log\gamma}$$

the main difficulty in getting a straight line was due to the uncertainity in computing two slopes. Not only must the slope $(-d\gamma/dT)$ be determined precisely, but also the derivatives of $\log(-d\gamma/dT)$ and $\log\gamma$ with respect to temperature T (or the slopes $d\log(-d\gamma/dT)/dT$ and $d\log\gamma/dT$) must be accurately determined. This method[33] was dropped and the ratio method[35] was used. The description of the ratio method is given in Appendix A.

The main equation of the ratio method is:

$$\log((-d\gamma/dt)_j/(-d\gamma/dt)_i) = \frac{E}{2.303\,R} \times \frac{T_j - T_i}{T_j\, T_i} - n \log(\gamma_i/\gamma_j)$$

so, by keeping (γ_i/γ_j) constant a plot of

$\log((-d\gamma/dt)_j/(-d\gamma/dt)_i)$ versus $\frac{T_j - T_i}{T_j\, T_i}$ would yield a straight line

From the slope of the straight line the activation energy, E, can be calculated and from the intersection with Y axis a value for the reaction order, n, can be determined.

The value of γ_i/γ_j is called the ratio. If kept constant, the selection of its value dictates how many points will be obtained from a particular section of the thermogram. Also, it should be noted that ratios quite near to unity require a very accurate knowledge of the temperature and the slope of the thermogram.

The values of $(d\gamma/dt)$ can be accurately determined from the DuPont 951 thermogravimetric analyzer which was used in this study. This system provides differential thermogravimetric data in addition to the weight loss thermogram.

Thermograms were analysed using ratio method. These include:

1- 100% crude oil in air atmosphere. (Figure 7-2)

2- 80% sand - 20% oil in air atmosphere. (Figure 7-4)

3- 80% fine silica - 20% oil in air atmosphere. (Figure 7-6)

4- 40% fine silica - 40% sand - 20% oil
in air atmosphere. (Figure 7-16)

5- 40% clay - 40% sand - 20% oil
in air atmosphere. (Figure 7-17)

6- 80% clay - 20% oil in air atmosphere. (Figure 7-11)

7- Last peak of 80% burned clay - 20% oil (Figure 7-13)
in air atmosphere.

It should be mentioned here that the reproducibilities of the thermograms were always successful, i.e., for the same mixture one can

distinguish the same peaks in the same temperature range from two different runs if the heating rate is kept constant, so it was decided to analyze only one thermogram for each mixture.

The 3 regions described in Chapter 7 were analyzed separately. Only the last peak of Figure 7-13 (80% burned clay - 20% oil) was analyzed since the rest of the thermogram was identical to Figures 7-11 and 7-6. A sample calculation for applying the ratio method to the produced TGA thermograms is given in Appendix E.

It is important to note that crude oil is composed of many components and a whole chain of different mechanisms is occuring during any chemical reaction. It is not intended to study or even detect these individual mechanisms. However, it is hoped to be able to group the major components with similar mechanisms (distillation - combustion/cracking) of a given crude oil by studing appropriate thermograms and produce some kind of average kinetic data for these groups, and finally, study the effect of clay on these kinetic parameters.

From the straight lines generated for each peak of the previously mentioned thermograms, the data of Table 8-1 was obtained. The Arrhenius type plots, for each produced peak of the thermograms, are shown in Appendix D, and the calculated points for each plot is given in the same appendix.

It should be noted that there are some points which deviate from the straight line. In Figure 8-6 (80% clay - 20% oil), the second peak straight line, points 1, 7, and 8 deviate from the straight line. These points are at the very end of the peak (points 7 and 8) or at the very

beginning of the peak (point 1). Points 1, 2, 3, 6, and 7 in Figure 8-7 present the position of γ_i while points 1', 2', 3', 6', and 7' present the position of γ_j.

From the results shown in Table 8-1, the order of the reaction of all distillation peaks obtained from Figures 7-2, 7-4, 7-6, 7-11, 7-16, and 7-17 was 2.2, and the activation energy for the same peaks was between 6000 - 6900 cal/gm mole. The matrix content did not have any effects on the distillation curves. Adonyi[49] reported a reaction order of zero for pure substances, 1 - 2.5 for benzene mixture, and .6 - 4 for cyclohexane mixture.

For Figures 7-6, 7-11 and 7-17 the results of the second peaks were similar. The reaction order was between 1.1 - 1.4 and the activation energy was between 14,800 - 18,000 cal/gm mole. It should be noted that the 40% clay thermogram (Figure 7-17) gave almost the same results as the 80% clay run (Figure 7-11). In these second peaks of the mentioned figures, it was believed that the low temperature oxidation reactions were taking place. Comparing the activation energy calculated in these peaks with that reported by Dabbous[48], one can see the similarity of the results. Dabbous reported an activation energy of 17223 cal/gm mole, for low temperature oxidation reactions occuring below 315°C, which agrees with these results.

For the second peaks of Figures 7-2, 7-4 and 7-16, 100% crude oil, 80% sand - 20% oil, and 40% fine silica powder - 40% sand - 20% oil respectively, the results were similar. The reaction order was in the range of 1.4 - 1.7 and the activation energy was between 41,000 - 46,000 cal/gm mole. Comparing these results with those of 80% silica powder-

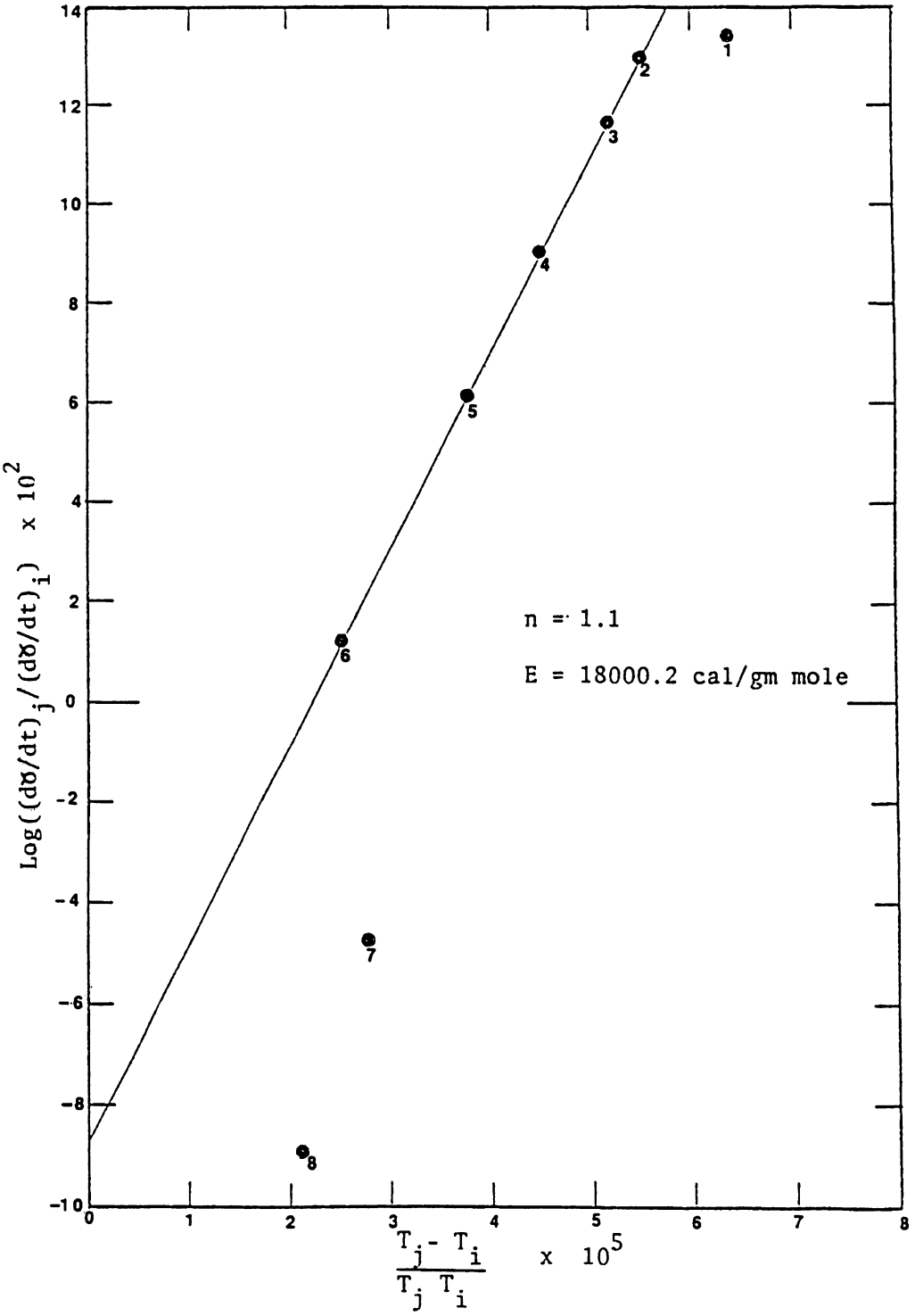

Figure 8-6 Straight line constructed using the Ratio method for peak #2 of figure 8-7 (80%clay-20%oil)

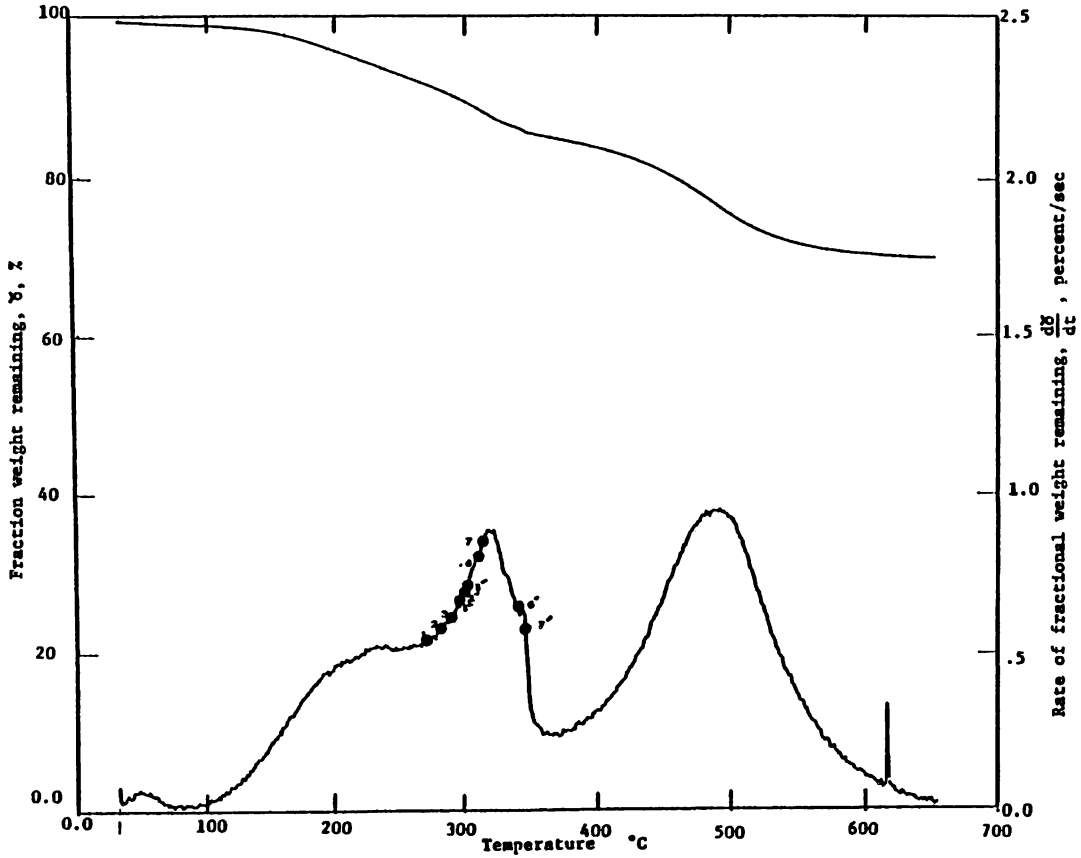

Figure 8-7 Position of α_i and α_j for mixture 6
(80% Clay - 20% oil)

Table 8-1: Kinetic Parameters generated from ratio method

Figure #	Sample Tested	Peak #1			Peak #2			Peak #3		
		Temp. Range	Act. energy cal/gm mole	Reaction Order	Temp. Range	Act. energy cal/gm mole	Reaction Order	Temp. Range	Act. energy cal/gm mole	Reaction Order
7-2	100% crude oil	25-350	6800	2.2	350-475	41184	1.7	475-550	45760	1.2
7-4	80% sand - 20% oil	25-350	6000	2.2	350-475	42329	1.4	475-550	47667	1.1
7-6	80% fine silica - 20% oil	25-275	6275	2.2	275-370	14872	1.4	375-575	38553	1.4
7-11	80% clay - 20% oil	25-275	6864	2.2	275-370	18000	1.1	370-550	18686	1.3
7-16	40% fine silica - 40% sand - 20% oil	25-350	6100	2.2	350-475	45761	1.7	475-550	47667	1.1
7-17	40% clay - 40% sand - 20% oil	25-275	6864	2.2	275-370	15863	1.1	370-550	18762	1.3
7-13	80% burned clay - 20% oil							370-550	24711	1.2

20% crude oil one can conclude that as the amount of silica powder is reduced its effect on the crude oil burning is lost.

For the third peaks of Figures 7-6, 7-11, and 7-17 a big difference in the calculated results were found. The third peaks of Figures 7-17 and 7-11 (clay runs) showed a reaction order of 1.3 and an activation energy of 18,700 - 19,000 cal/gm mole, while the 80% fine silica run (Figure 7-6) gave a reaction order of 1.4 and an activation energy of 38,553 cal/gm mole, which is almost double the activation energy obtained from the clay runs. This indicates, definitely, that clay had a catalytic effect on this region. Bousaid[56] reported that the activation energy of oil decreased from 14,782 cal/gm mole to about 11,114 cal/gm mole when 20% by weight clay was added to the sand matrix. The difference between this study and Bousaid's study was that Bousaid coked the oil-sand mixture by heating it to a high temperature in a nitrogen atmosphere before each run. Vossoughi[60] et al. found that the coked crude oil in a nitrogen atmosphere is quite different from that coked in an air atmosphere. So, it was expected to generate different values of activation energy than those reported by Bousaid.

For peak 3 of Figure 7-13 (80% burned clay - 20% oil), the results still showed the clay's catalytic effects. The order of the reaction was 1.2 and the activation energy was in the neighborhood of 25,000 cal/gm mole. The higher activation energy than that obtained in the clay runs (peak 3 of Figures 7-11 and 7-17) may have been due to the disruption or alteration of the structure of clay, which would make the clay partially lose its catalytic effects.

8-3 Analysis of the TGA runs of crude oil at different heating rates

Thermograms of Figures 7-20, 7-21, 7-2 were analyzed using the ratio method to see the effect of heating rate on the generated kinetic parameters.

Both heating rates of $1^{o}C$/min and $5^{o}C$/min produced almost the same results, while the heating rate of $10^{o}C$/min produced different results. The straight lines obtained for the three runs using the ratio method are seen in Figures 8-8, 8-9 and 8-10. Table 8-2 presents the kinetic data obtained at each heating rate. It is suspected that the heating rate in the case of $10^{o}C$/min is so fast that the reaction did not have enough time to be completed.

8-4 Analysis of the DSC curves

Differential scanning calorimetry runs were performed to obtain the heat value of crude oil burning and the effect of grain material on this value. The equation used to calculate the heat values is the formula suggested in the apparatus handout published by DuPont[62]. The formula is:

$$\Delta H = \frac{A}{m} (60\ B\ E\ \Delta q_s) \qquad (8\text{-}1)$$

Where

A = Peak area in cm^2

m = Sample mass in mg

B = Time base setting in min/cm

E = Cell calibration coeffecient at the temperature of the experiment in mW/mV

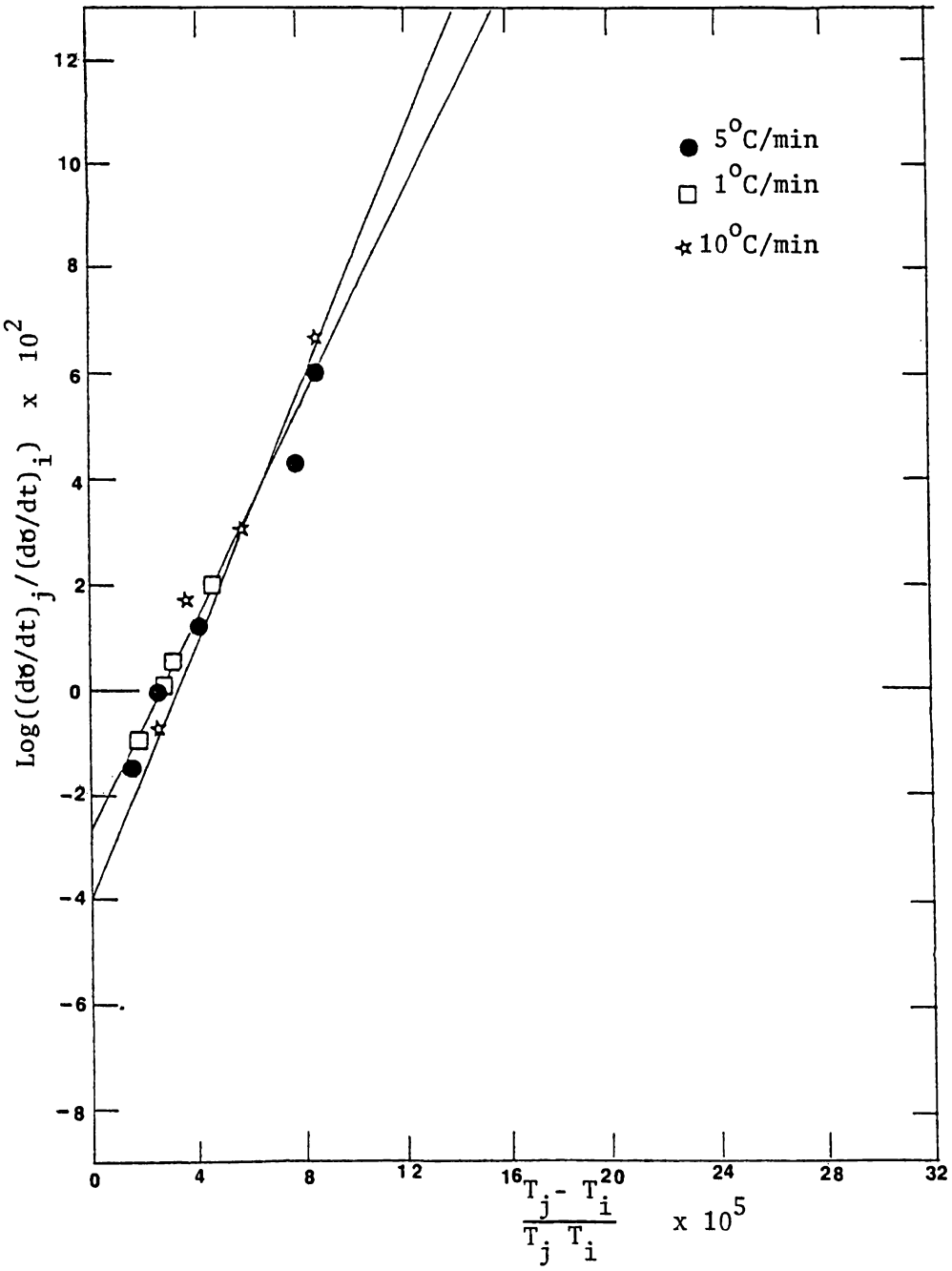

Figure 8-8 Straight lines obtained by ratio method for crude oil at different heating rates (peak 3)

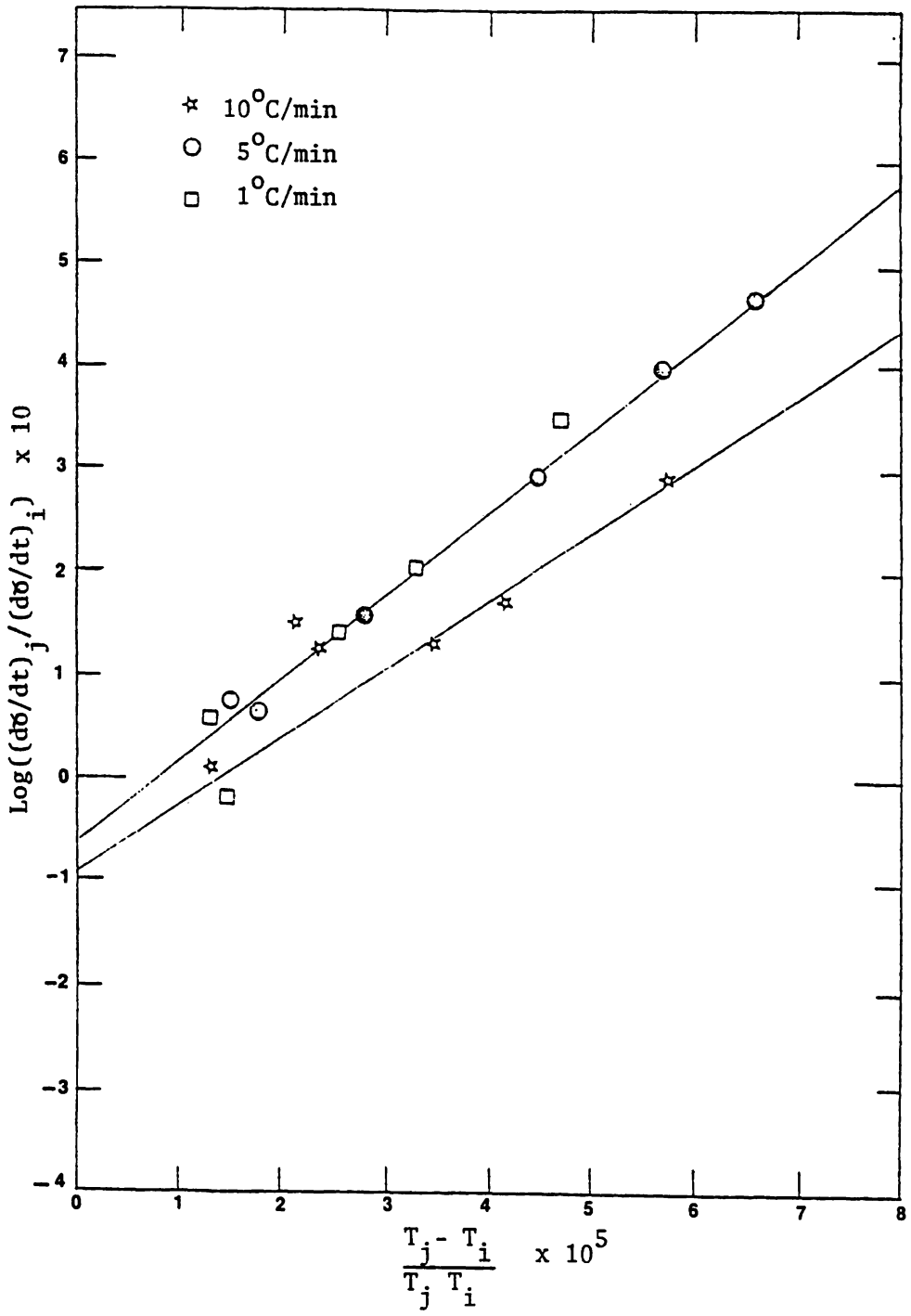

Figure 8-9 : Straight lines obtained by ratio method for crude oil at different heating rates (peak 2)

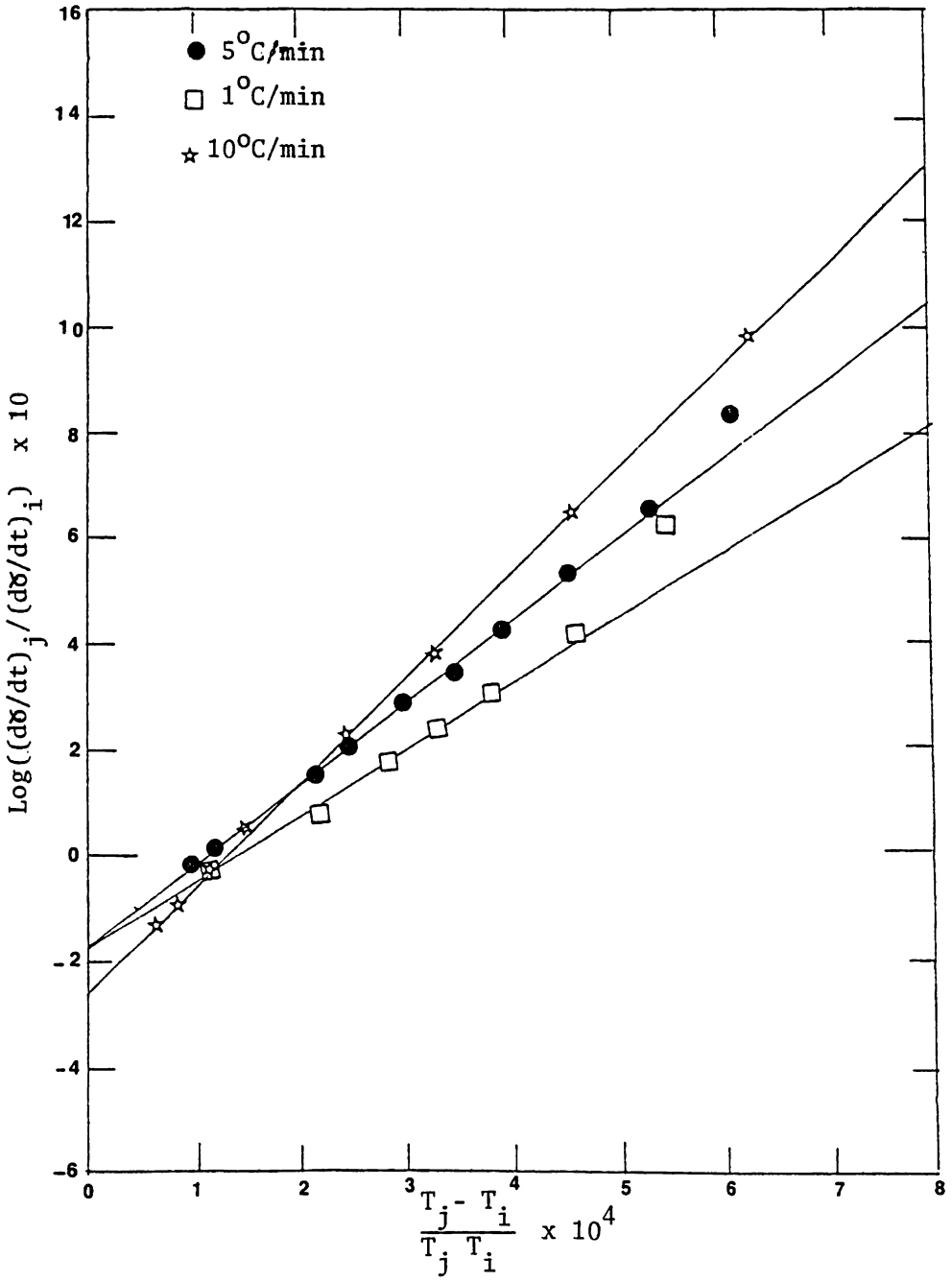

Figure 8-10 :Straight lines obtained by ratio method for crude oil at different heating rates (peak 1)

Table 8-2:
Activation energy and order of the treaction obtained from heating of Iola crude oil at different heating rates

Heating Rate °C/Min	P E A K #1		P E A K #2		P E A K #3	
	Reaction order	Activation Energy Cal/gm mole	Reaction Order	Activation Energy Cal/gm mole	Reaction Order	Activation Energy Cal/gm mole
1	2.21	6131.9	1.7	41184.55	1.2	45760.61
5	2.21	6800.0	1.7	41184.55	1.2	45760.61
10	3.28	9094.9	2.4	43760.61	1.9	54912.73

Δq_s= Y-axis range setting in mV/cm.

H = Heat values in j/gm

The peak area was determined as follows; a base line was drawn. The base line is the line which corresponds to the portion of the DSC curve where Δq_s approximately zero. Base line shifting occures due to the change in specific heat as well as bulk density of the sample. In our experiment it is unavoidable since gas is produced during the reaction therefore, the mass and the composition of the sample is continously changing. So, the peak area will be the area of that portion of the DSC curve which departs from and subsequently returns to the base line. The area was measured using a planemeter from Burrell Corporation, Pittsburgh, Pa, USA.

To calculate the amount of the sample reacted during each exothermic reaction, the onset and the final temperatures are determined. The onset temperature is the point of intersection of the tangent drawn at the point of greatest slope on the leading edge of the peak with the extrapolated base line. This temperature will be the temperature at which the reaction starts. To determine the end temperature, the temperature at which the reaction ends, the minimum point between two distinct peaks, at which the point of intersection between the base line and the DSC curve, was found. It should be mentioned here that in case of two peaks, the end temperature of the first peak will be the onset temperature of the second peak. From the TG curve of the sample in study, one can get the weight loss at this range of temperature.

The value of the time base setting, B, in equation 8-1 was kept constant at 5 min/cm during all DSC runs. Also Y axis range setting,

Δq_s, was kept constant at 20 mV/cm for all the DSC runs. A sample calculation to show how to calculate heat values from the produced DSC thermograms is given in Appendix E.

To get a numerical value for the cell calibration coeffecient E, the caliberation curve of Figure C-1 Appendix C was used. The E values obtained from this figure correspond to the onset temperature of each DSC thermogram.

Table 8-3 shows the results obtained for all runs performed by the DSC. The average heat value is defined as the heat produced per unit mass of crude oil loss in the range of exothermic reaction.

The results of Table 8-3 show that the addition of clay or silica powder to the crude oil or crude oil and sand mixtures have an effect on the DSC thermograms. The major effect was a shifting of a larger amount of heat produced from a higher to a lower temperature range. For peak number 1 of 100% oil and 80% sand - 20% oil DSC thermograms produced heat values of 460 - 660 cal/gm. While for peak number 1 of 80% clay - 20% oil, 80% silica powder - 20% oil, and 40% clay - 40% sand - 20% oil the heat value of the crude oil was between 1350 - 1600 cal/gm. For peak number 1 of 40% sand - 40% silica powder - 20 % oil a value of 1061 cal/gm was obtained, which is between the value of the clay runs, the oil runs, and the oil and sand runs.

The heat values of the oil in the second peaks of the DSC thermograms, show that 80% clay - 20% oil produced the largest heat amount (2680 cal/gm) while 80% silica powder - 20% oil produced only 1737 cal/gm which is even less than crude oil heat values produced when oil was burned by itself (2065 cal/gm).

From the calculated activation energies, a significant reduction due to addition of clay to the crude oil is a definite indication of catalytic and/or surface area effect on crude oil combustion/cracking reactions. Also, the addition of clay and silica powder to the crude oil mixture shifted a portion of the total heat of reactions from a higher to a lower temperature range.

Table 8-3:

Heat Of Reactions Produced From DSC Thermograms

Figure #	Sample Tested	Average Heat Value Cal/gm	Heat Values of Individual Peaks Cal/gm			
			Temp. Range °C	Peak #1 Heat Value	Temp. Range °C	Peak #2 Heat Value
7-22	100% crude oil	1499.3	262.5 - 370	662.7	370 - 550	2065
7-23	80% sand/20% oil	1374.6	275 - 387.5	464.9	387.5 - 550	2095.8
7-25	80% clay/20% oil	1846.6	265 - 387.5	1527.8	387.5 - 550	2680.8
7-24	80% silica powder/20% oil	1926.6	250 - 400	1615.3	400 - 550	1737.5
7-27	40% clay/40% sand/40% oil	1574.9	270 - 287.5	1353.5	287.5 - 550	1995.3
7-26	40% silica powder/40% sand/ 20% oil	1328.2	270 - 385	1061.2	385 - 500	1498.5

CHAPTER 9

Conclusions And Recommendations

9-1 Conclusions

Major conclusions derived from this study can be summarized as follows:

1- Three distinct regions, namely distillation and two combustion/cracking regions were observed in all TGA thermograms.

2- The addition of kaolinite clay or IMSIL silica powder changed the shape of the crude oil TGA/DSC thermograms significantly while sand and ground sand had no effect. The major effect on DSC thermograms was shifting of the large amount of heat produced from a higher to a lower temperature range.

3- The average heat value increased from around 1400 cal/gm of oil to 1900 cal/gm of oil when clay or silica powder was included in sand matrix.

4- Crude oil weight loss under a constant heating rate and flowing air atmosphere was larger in the presence of clay than in its absence, which is an indication of the clay effect on the chemical reactions occuring.

5- Due to the absorption of the crude oil on the clay particles, its weight loss under a constant heating rate and flowing nitrogen became smaller in the presence of clay than in its absence.

6- The activation energy of the distillation peak varied between 6000 - 7000 cal/g-mole and was unaffected by the presence of clay or silica powder in the mixture.

7- The activation energies of the two combustion/cracking peaks calculated from TGA thermograms were significantly lower for the clay/crude oil mixture than for the crude oil or crude oil/sand mixture.

8- Reduction of activation energy due to the addition of kaolinite clay to the crude oil indicates a catalytic and/or a surface area effect on combustion/cracking reactions.

9- Reaction order was equal to 2.2 for distillation peaks but varied between 1 and 2 for combustion/cracking peaks.

9-2 Recommendations

1- More TGA/DSC runs should be performed using lower amounts of clay (5-20%) to investigate whether clay, when used in small amounts, possesses the same effects on the crude oil burning or not. If clay reduces the activation energy, this will be a definite indication of its catayltic effect.

2- Runs using activated clay should be investigated to determine whether the activation energy will be effected or not. If activation energy decreases, then this will be another positive indication of clay catalytic effects on the process.

3- Future studies on the clay effects should include other types of common clays, such as, illite and montmorillonite which have a larger and more reactive surface area than the kaolinite clay used in this study.

4- To investigate the accuracy of the calculated results, another kinetic model can be applied, and a comparison of the generated kinetic parameters should be made.

5- Analysis for the exhaust gases is needed to identify the amount of oil that undergoes cracking, distillation, and burning, so the three regions of the TGA thermograms could be studied in more detail.

6- Similar study can be repeated using different heating rates ($1^{o}C$/min or $10^{o}C$/min) to investigate the effects of heating rates on the generated kinetic parameters.

REFERENCES

1. "Enhanced Oil Recovery Potential in the United States" Library of Congress Card Number 77-600063, Congress of the United States, Office of Technology Assessment, Washington, D.C., 1978.

2. Kuhn, C.S., and Roch, R.L., "In Situ Combustion Newest Method of Oil Recovery", Oil & Gas Journal, Vol 52 (August 10, 1953), p. 92.

3. Tadema, H.J., "Mechanism of Oil Production by Underground Combustion", Proceedings, Fifth World Petorleum Congress, Section II (1959) p.279.

4. Wu, C.H., "An Experimental Study on the Oil and Water Behavior in Porous Media Under Stepwise - Approximately Isothermal Conditions with Multi-phase Fluid Flow" , Ph.D Dissertation, School of Engineering, University of Pittsburgh (1968).

5. Fuchita, T., "Laboratory and Field Experiments on Fire Flood Recovery Method", Produces Monthly. Vol. 23, No. 9 (1959), p.30.

6. Alexander, V.D., Martin, W.L. and Dew, J.N., "Factors Affecting Fuel Availability and Combustion During In-situ Combustion", J. Pet. Tech. (Oct 1962) p.225.

7. Penberthy, W.L. and Ramey, H.J., "Design and Operation of Laboratory Combustion Tubes", Society of Petorleum Engineers Journal (june 1966) p. 183.

8. Showalter, W.E., "Combustion Drive Tests", Society of Petorleum Engineers of AIME, Transactions, Vol. 228 (1963), p.53.

9. Grant, B.F., and Szasz, S.E., "Development of An Underground Heat Wave for Oil Recovery", Society of Petorleum Engineers of AIME, Transactions, Vol. 210 (1954), p. 108.

10. Moss, J.T., White, P.D., and McNeil, J.S. , Jr., "In-Situ Combustion Process - Results of Fire Well Field Experiment in Southern Oklahoma", Society of Petorleum Engineers of AIME, Transactions, Vol. 213 (1959). pp. 55-64.

11. Parrish, D.R., Rausch, R.W., and Beaver, H.W., "Underground Combustion in the Shannon Pool, Wyoming", Society of Petroleum Engineers of AIME, Transactions, Vol. 225 (1962), pp.197-205.

12. Emery, W.L., "Results from a Multi-Well Thermal Recovery Test in Southwestern Kansas", Society of Petroleum Engineers of AIME, Transactions, Vol. 225 (1962), pp. 671-678.

13. Copperman, P., "Some Criteria for the In-Situ Combustion of Crude Oil", Journal of Applied Physics, Vol. 30, No. 9 (September, 1959) pp. 1376-1380.

14. Gottfried, B.S., "A Mathematical Model of Thermal Oil Recovery in Linear Systems", Society of Petorleum Engineers of AIME, Transactions, Vol. 234 (1965).

15. Bailey, H.R. and Larkin, B.K., "Conduction-Convection in Underground Combustion", Society of Petorleum Engineers of AIME, Transactions, Vol. 219 (1960), p. 321.

16. Chu, C., "The Vaporization-Condensation Phenomena in a Linear Heat Wave", Society of Petroleum Engineers Journal, Vol. 4, No. 2(June 1964) pp. 85-95.

17. Chu, C., "Two Dimensional Analysis of a Radial Heat Wave", Journal of Petorleum Technology, Vol. 15 (1963), pp. 1137-1144.

18. Wilson, L.A., Wygal, R.J., Reed, D.W., Gergins, R.L., and Henderson, J.H., "Fluid Dynamics During an Underground Combustion Process", Society of Petorleum Engineering of AIME, Transactions, Vol. 213 (1958), pp. 146-154.

19. Thomas, G.W., "A Study of Forward Combustion in a Radial System Bounded by Permeable Media", Society of Petorleum Engineers of AIME, Transactions, Vol. 228(1963) p. 1145.

20. Vogel, L.C. and Kureger, R.F., "An Analog Computer for studying Heat Transfer During a Thermal Recovery Process", Society of Petorleum Engineers of AIME, Transactions, Vol. 204 (1955), p. 208.

21. Partington, J.R., "Origins and Development of Applied Chemistry", Longmans Green, London, (1935), pp. 8-36.

22. Keattch, C., "An Introduction to Thermogravimetry", Heyden and Son LTD, publisher, Library of Congress Catalog Card No. 69-19569.

23. Duval, C.L., "Inorganic Thermogravimetric Analysis", Elsevier Publishing Company, (1953).

24. Wendlondt, W.W., "Hand-book of Commercial Scientific Instruments", Volume 2 of Thermoanalytical Techniques Series, Marcel Dekker, Inc., New York (1974).

25. Wendlondt, W.W., "Thermal Methods of Analysis",Second Edition, A Wiley-Interscience Publication, Vol. 19, (1974).

26. Brown A.H. Jr., Penski, E.C., and Callahan, J.J., "An Apparatus for High Pressure Thermogravimetry", Thermochimica Acta, 3, (1972), pp. 271-276.

27. Feldmand, R.F., and Ramachandarn, V.S., "Modified Thermal Analysis Equipment and Technique for Study Under Controlled Humidity Conditions", Thermochimica Acta, 2 (1971), pp. 293-403.

28. Stone, R.L., "Apparatus for Differential Thermal Analysis under Controlled Partial Pressure of H_2O, CO_2, or other gasses". J. Am. Ceram. Soc. (1952), pp. 35,76.

29. Stone, R.L., "Differential Thermal Analysis of Kaolin Group Minerals Under Controlled Pressure of H_2O", J. Am. Ceram. Soc,(1952) pp. 35-90

30. Borchandt, H.J., and Daniels, F., "Differential Thermal Analysis of Inorganic Hydrates", J. Phys. Chem., Vol 61, P. 917

31. Newkirk, A.E., "Thermogravimetric Measurements", Talanta, Vol 13, (1966) P.1401

32. Coats, A.W., and Redfern, J.P., "Kinetic Parameters from Thermogravimetric Data", nature, Vol. 201, (January 4, 1964) p. 68.

33. Freeman, E.S., and Carroll, B., "The Application of Thermoanalytical Techniques to Reaction Kinetics", J. Phys. Chem., Vol 62, (1958) P. 394.

34. Horowitz, H.H., and Metzger G., "A New Analysis of Thermogravimetric Traces", Anal. Chem., Vol 35, (1963) P.1464.

35. Mickelson, R.W., Einhorn, I.N., "The Kinetics of Polymer Decomposition through Thermogravimetric Analysis", Thermochimica Acta, Vol 1, (1970) P. 147.

36. Doyle, C.D., "Kinetic Analysis of Thermogravimetric Data", J. of Applied Polymer Science, Vol. V., Issue No. 15 (1961) pp. 285-292.

37. Ozawa, T.J., "Kinetic Analysis of Derivative Curves in Thermal Analysis", J. Thermal Analysis, Vol 2, (1970) P. 301.

38. Satava, V., "Mechanism and Kinetics from Non-Isothermal TG Traces", Thermochemica Acta, Vol 2, (1971) pp. 423-428.

39. Zsako, J., "Kinetic Analysis of Thermogravimetric Data", J. Phys. Chem., Vol 72, (1968) P. 2406.

40. Wieckowska, J. and Bogdanow, H., "Initial Investigation of the Thermal Decomposition Kinetics of the Vacuum-Distillation Residue of Crude Oil", J. Thermal Anal., Vol 17, 1979.

41. Carroll Benjamin, "Kinetic Analysis of Chemical Reactions for Non- Isothermal Procedures", Thermochemica Acta,Vol 3,(1972) pp. 449-459.

42. Sharp, J.H., and Wentworth, S.A., "Kinetic Analysis of Thermogravimetric Data", Anal. Chem., Vol 41, (1969) P. 2060.

43. Ellerstein, S.M., Porter, R.S., and Johnson, J.F. (Eds), "Analytical Calorimetry", Plenum Press, 1968 pp. 279-287.

44. Vachuska, J. and Voboril, M., "Kinetic Data computation from Non-Isothermal Thermogravimetric Curves of Non-Uniform Heating Rate", Thermochimica Acta,Vol 2,(1971) pp. 379-392.

45. sestack, J., "Errors of Kinetic Data obtained from Thermogravimetric Curves at Increasing Temperature", Talanta, Vol 13, (1966) pp 567-579.

46. Burger, J.G. and Sahuquet, B.C., "Chemical Aspects of In-Situ Combustion-Heat of Combustion, and Kinetics", SPE J., Vol 12, (Oct. 1972) P. 410.

47. Bae, J.H., "Characteristics of Crude Oil for Fire Flooding Using Thermal Analysis Methods", SPE paper number 6173, presented at the 51st Annual Fall Technical conference and exhibition of the Society of Petroleum Engineers of AIME, held in New Orleans, Oct. 3-6,(1976).

48. Hardy, W.D., Raiford, J.D., "In-Situ Combustion in a Bartlesville Sand Allen County, Kansas", Proceedings of the Tertiary Oil Recovery Conference, Wichita, Kansas, Published by Tertiary Oil Recovery Project, Institute of Mineral Resources Research, University of Kansas (contribution No.2), October 1975, p. 24.

49. Adonyi, Z., "Investigation of Evaporation by Thermogravimetry", Thermal Analysis, Vol. I, (1971), P. 255.

50. Dyszel, S.M., "A Thermogravimetric Method for Distinguishing Alaskan Crude Oil from that of other World Sources", Thermochimica Acta, Vol 38, (1980) pp. 229-310.

51. Lonvik, K., Rajeshawr, K., and Bubow, J.B., "New Observation on Chemical and Structural Transformations in Green River Oil Shales", Thermochimica Acta, Vol 42, (1980) pp. 11-19.

52. Grim, R.E., "Applied Clay Mineralogy", International Series in the Earth Sciences, McGraw Hill Publisher, 1962.

53. Shabaker, H.A., "Process of Acid-Activating Kaolin Clay", United States Patent Office, 2477664, (1949).

54. Mills, G., "Process of Activating Koalin Clay", United States Patent Office, 2477639, (1949).

55. Dart, J.C., Savage, R.T., and Kirkbride, C.G., "Regeneration Characteristics of Clay Cracking Catalyst", Chemical Engineering Progress, Vol. 45, (Feb. 1949) P. 102.

56. Bousaid, I.S., "Oxidation of Crude Oil in Porous Media", Ph.D. Dissertation, Texas A&M University, College Station, Texas, (1967).

57. Dabbous, M.K., "In-Situ Oxidation of Crude Oils in Porous Media", Ph.D. Dissertation, University of Pittsburgh, School of Engineering, (1971).

58. Guvenier, I.M., "The Development of an Automated In-Situ Combustion Assembly to study Effects of Clay on the Dry Forward In-Situ Combustion Process", Ph.D. Dissertation, University of Kansas, School of Engineering, (1980).

59. Fassihi, R., Ramey, N.J., Jr., "The Frontal Behavior of In-Situ Combustion", SPE 8907 presented at the 50th Annual California Regional meeting of the Society of Petroleum Engineers of AIME held in Las Angeles, California, April 9-11,(1980).

60. Vossoughi, S., Willhite, G. P., El-Shoubary Y., and Bartlett, G. "Study of the Clay Effect on Crude Oil Combustion by the mehtod of Thermogravimetric Analysis (TGA) and Differential Scanning Calorimetry (DSC)", Proceedings of the eleventh North American Thermal Analysis Society (NATAS) conference, Vol.2, (1981), pp. 391-399.

61. Johnson, R. and Smith, J., " Simultaneous DTA - TGA - EGA for Oil Shale and Solid Feuls" United States Rep. of The Interior, Burea of Mines, (Sep. 1970).

62. DuPont Instruments Instruction Manual, issued September 1980, DuPont Analytical Instruments Division, serial number 910037-000.

Appendix A

In this appendix an in-depth study for both Freeman and Carrol, and the ratio method is presented.

The foundation for the calculations of kinetic data from a thermogram in both methods is based on the formal kinetic equation:

$$-\frac{d\gamma}{dt} = K\,\gamma^{n} \qquad \text{----------} \quad (A\text{-}1)$$

where;

t = Time

γ = Fraction remaining = $(w-w_f)/(w_o-w_f)$

w = Weight at any time

w_f = Final weight

w_o = Initial wieght

n = Order of the reaction

K = Specfic rate constant.

The specific rate constant K may be related to temperature by Arrhenius' equation:

$$K = A\,\mathrm{Exp}\,(-E/RT) \qquad \text{----------} \quad (A\text{-}2)$$

A = Frequency factor (Arrhenius constant)

E = Activation Energy

R = Gas law constant

T = Absolute temperature

Combining equation A-1 and A-2;

$$-\frac{d\gamma}{dt} = A \, Exp \, (-E/RT) \, \gamma^n \quad \text{------} \quad (A\text{-}3)$$

Time can be eliminated from equation (A-3) by using the following relationship

$$T = T_o + bt$$

Where;

T_o = Initial temperature

b = Heating rate

then equation (A-3) can be written in this form

$$-\frac{d\gamma}{dT} = \frac{A}{b} Exp \, (-E/RT) \, \gamma^n \quad \text{----------} \quad (A\text{-}4)$$

This is a power-law type kinetic model which will be used as a base for both Freeman and Carrol and ratio methods.

A-1 Freeman and Carrol method [33]

Freeman and Carrol method was the first method used for determining the kinetic parameters. This method required taking the logrithm of both sides of equation (A-4), differentiating once to eliminate the frequency factor, and dividing by the differential of the logrithm of γ. Their results are presented by equation (A-5)

$$\frac{d \log (-d\gamma/dT)}{d\log \gamma} = \frac{E}{2.303 \, R} \left(\frac{dT}{T^2 \, d\log \gamma} \right) + n \quad (A\text{-}5)$$

If

$$\frac{d \log (-d\gamma/dT)}{d \log \gamma} \quad \text{is plotted against} \quad \frac{dT}{T^2 \, d\log \gamma}$$

a straight line will be obtained. From the intersection with the Y axis the reaction order can be determined, and from the slope of the line the activation energy can be calculated. Thus, from a single thermogram obtained for one constant rate of heating, the kinetic parameters can be ascertained.

A-2 Ratio method (Mickelson and Einhorn method) [35]

The rate of decomposition of any material with respect to time and the fraction remaining can be determined at any temperature i so that,

$$\left(\frac{-d\gamma}{dt}\right)_i = A \, \text{Exp} \, (-E/RT_i) \, \gamma_i^n \quad \text{----------} \quad (\text{A-6})$$

Repeating the same procedure at any other point of temperature j

$$\left(\frac{-d\gamma}{dt}\right)_j = A \, \text{Exp} \, (-E/RT_j) \, \gamma_j^n \quad \text{----------} \quad (\text{A-7})$$

Dividing equation (A-6) and equation (A-7) one can get,

$$((-d\gamma/dt)_i/(-d\gamma/dt)_j) = \left(\text{Exp} \left(\frac{-E}{R} \, \frac{T_j - T_i}{T_j T_i}\right)\right) \times \left(\frac{\gamma_i}{\gamma_j}\right)^n$$

Taking the log of each side,

$$\log ((-d\gamma/dt)_i/(-d\gamma/dt)_j) = \frac{-E}{2.303 \, R} \left(\frac{T_j - T_i}{T_j T_i}\right) + n \log \frac{\gamma_i}{\gamma_j}$$

If γ_i/γ_j remains constant, then a plot of

$$\log((-d\gamma/dt)_i/(-d\gamma/dt)_j) \quad \text{versus} \quad \frac{T_j - T_i}{T_j T_i}$$

will yield a straight line and the reaction order can be determined from the intercept with the Y axis and the activation energy can be calculated from the slope of the line. It should be noted here that the choice of ratio (γ_i/γ_j) dictates the number of points used in the kinetic analysis. Ratios quite near to unity will require a very precise measurment of the temperature and the slope of the thermogram if any straight line is to be expected.

If one were to use different values of ratio, in another words to eleminate the requirment of constant ratio, then a plot of

$$\frac{\log((-d\gamma/dt)_i/(-d\gamma/dt)_j)}{\text{Log } \gamma_i/\gamma_j} \quad \text{versus} \quad \frac{T_j - T_i}{T_j T_i} \Big/ \text{Log } (\gamma_i/\gamma_j)$$

would yield a straight line. In this case one can use as many points as needed.

It is obvious that this method depends on the accuracy of the reading of ($d\gamma/dt$) which can be obtained from the DTG curve directly. This method does not require the determination of two more slopes as is necessiated by the method of Freeman and Caroll which makes it simpler to apply. The entire thermogram or a portion of the curve can be used for analyzing the kinetic parameters. This mostly depends on the choice of ratio.

APPENDIX B

In this appendix the formula suggested in DuPont instructional manual to calculate ΔH from the DSC curves will be discussed.

The heat of reaction (ΔH) is porportional to the area under the curve (peak area)

$$\Delta H \propto A \qquad (B\text{-}1)$$

Where

A = Peak area

ΔH = Heat of reaction

Then,

$$\Delta H = A \times C_1 \qquad (B\text{-}2)$$

Where, C_1 is a proportionality constant

$$C_1 = B\ E\ \Delta q_s \qquad (B\text{-}3)$$

Where,

B = Time base sitting in min/cm

E = Cell calibration coefficient at the temperature of experiment mW/mV see Appendix C

Δq_s = Y-axis range setting in mV/cm.

DuPont apparatus has the capability to get Δq_s and B directly from the X-Y plotter.

To get ΔH in mcal/mg then we divide the right hand side of equation B-2 by m where, m is the weight of the sample in mg. therefore, the final equation will become

$$\Delta H = \left(\frac{A}{m}\right) (60 \; B \; E \; \Delta q_s) \qquad (B\text{-}4)$$

Note the 60 appears in equation (B-4) due to the change from the minute base to the second base.

APPENDIX C

In this appendix the calibration curves used in this study will be shown.

Table C-1 presents the results of the DSC calibration coefficient obtained from three experimental runs using three different elements as recommended by the DuPont instructional manual. These results are plotted in Figure C-1.

Figure C-2 presents the rotameter calibration curve. The rotameter used for this study is a precision bore flowmeter (made by Fischer and Porter). The rotameter was calibrated using an a gas burrette.

Figures C-3 and C-4 present the DSC curves for Indium and Zinc used to calculate the calibration coefficient (E) respectively. The same procedures which were mentioned in DuPont-instruction manual were taken to calculate E.

Table C-1 Values of calibration coefficient for the elements used to caliberate the DSC module.

Element	Temperature °C	Calibration Coefficient x 10^3 (E mW/mV x 10^3)
Indium	156	112
Zinc	419	120
Antimony	615	126

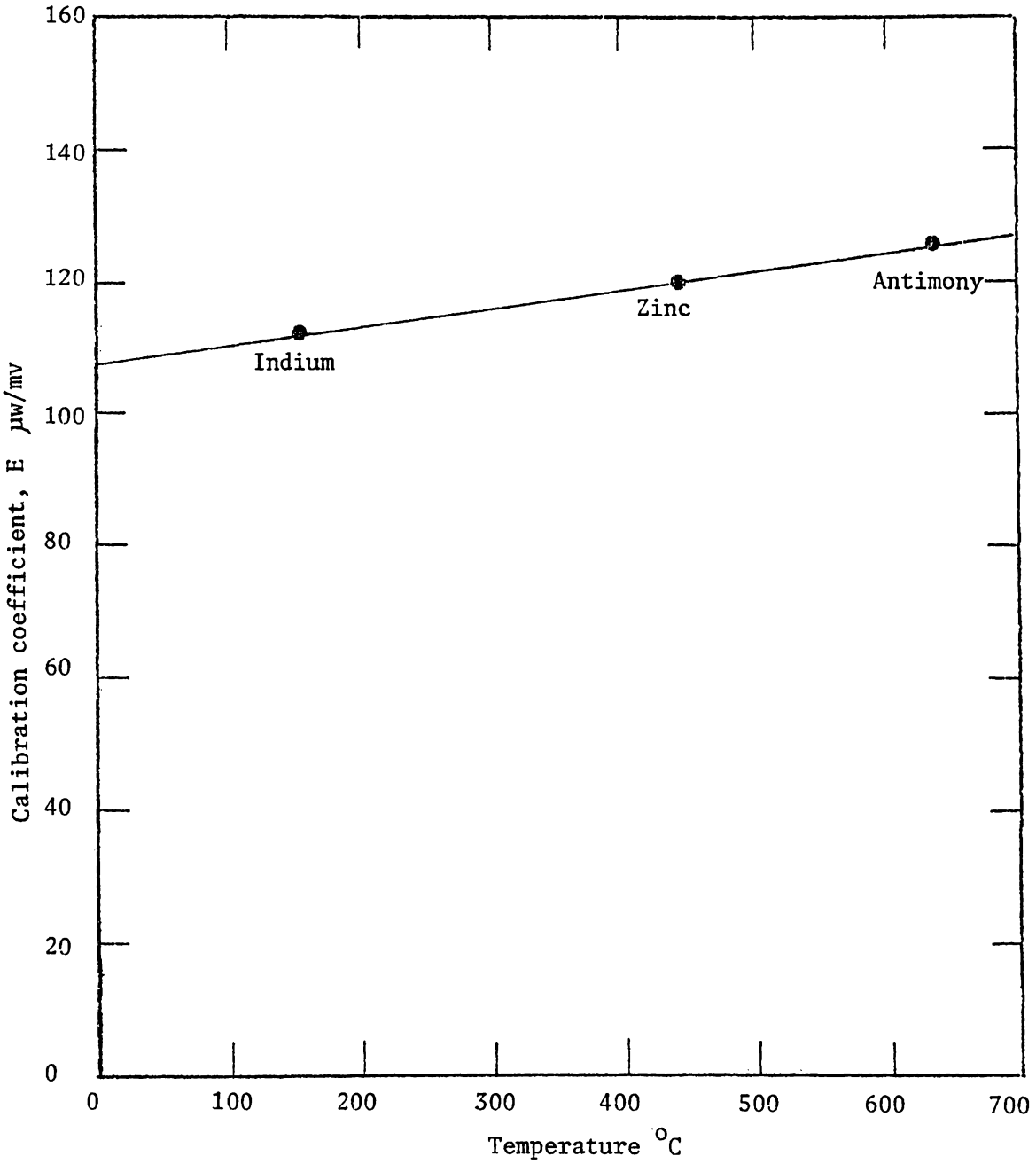

Figure C-1. DSC calibration curve

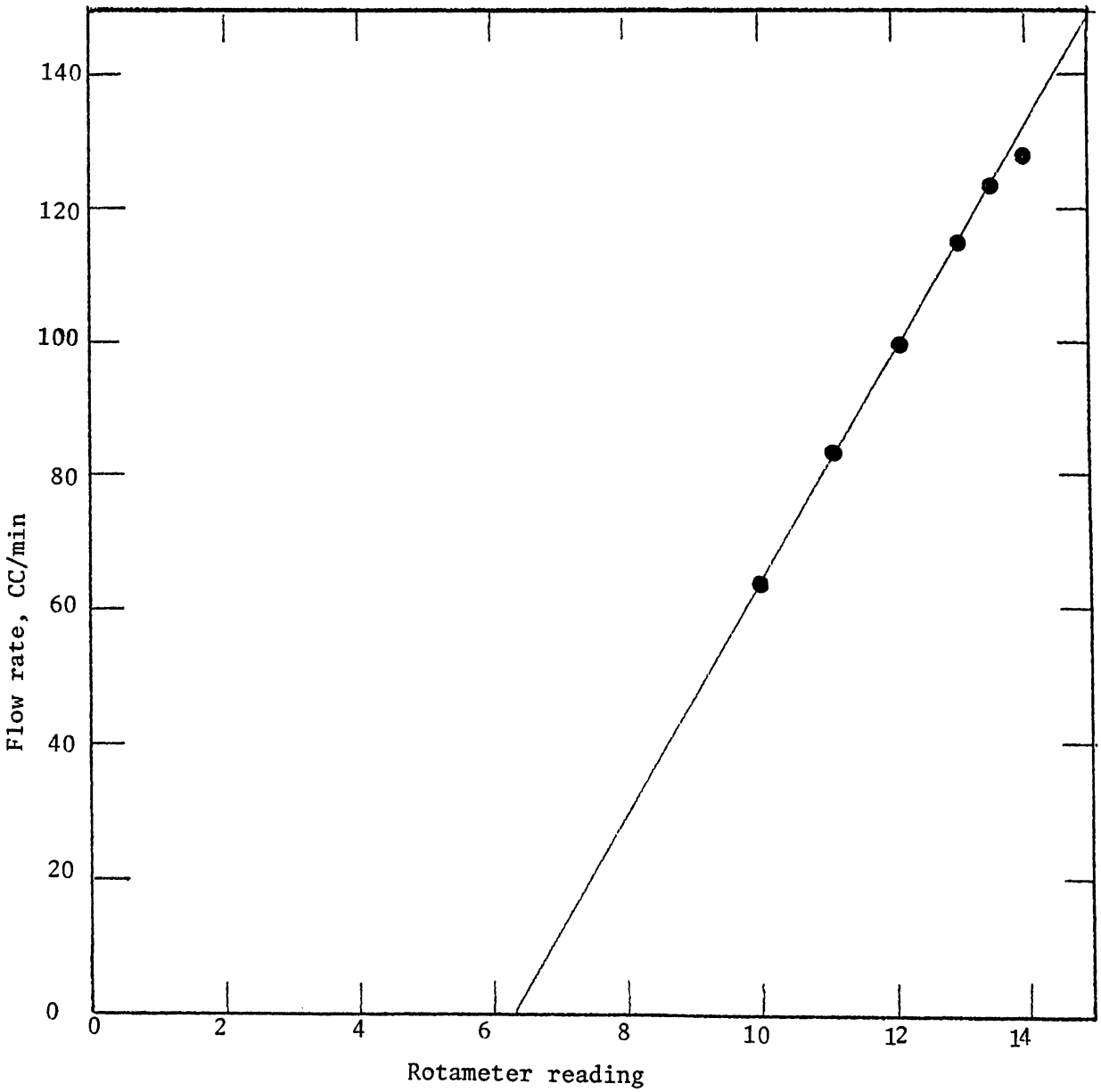

Figure C-2 Rotameter calibration curve

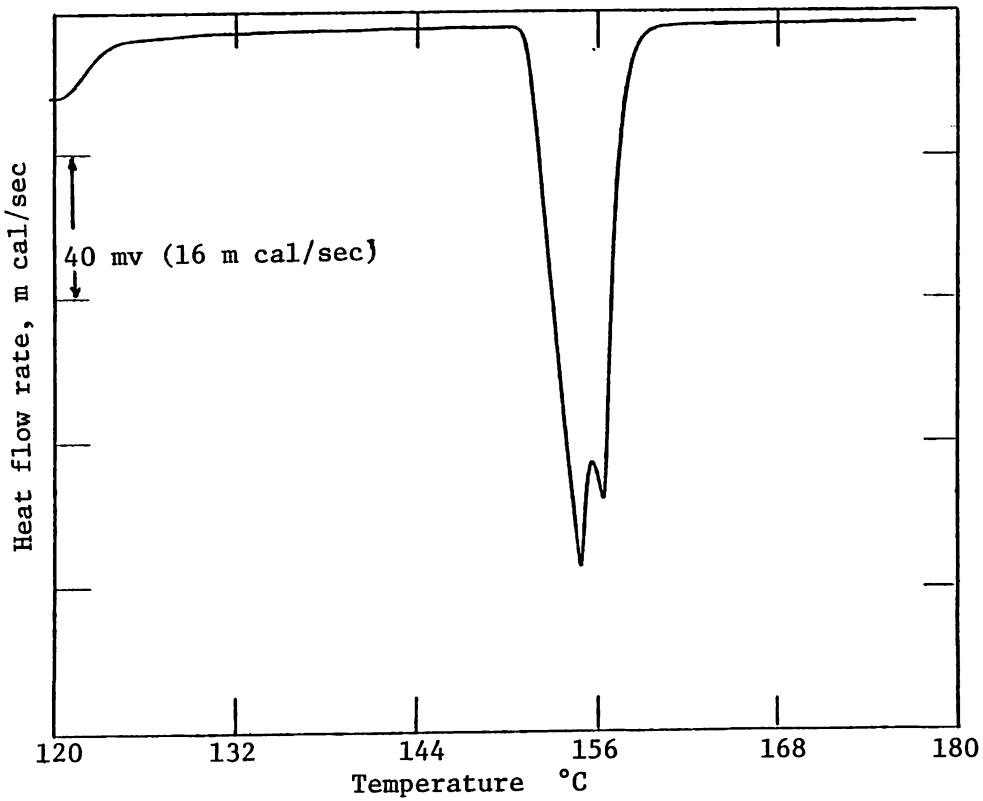

Figure C-3 DSC thermogram of indium

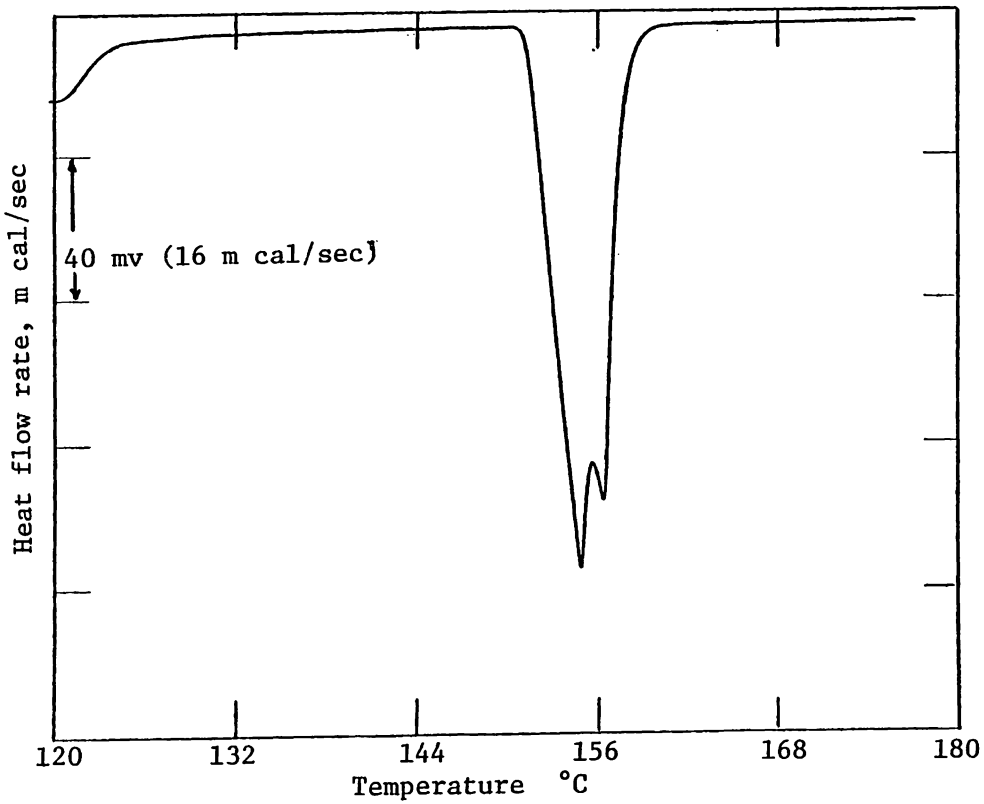

Figure C-3 DSC thermogram of indium

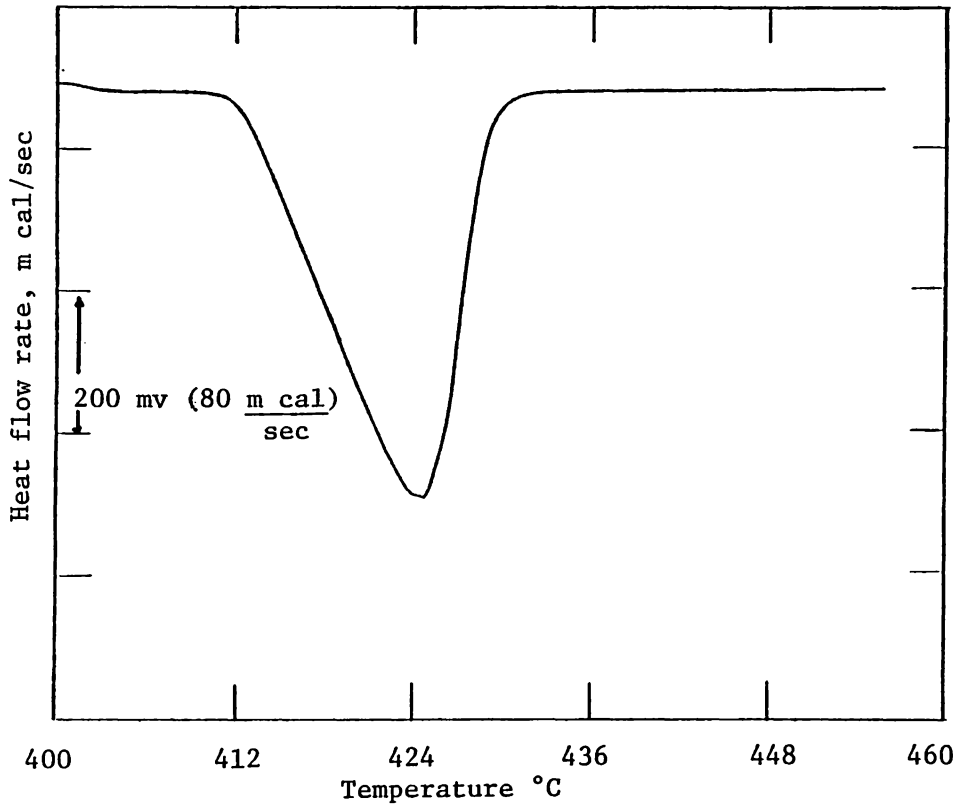

Figure C-4 DSC thermogram for zinc

Sample calculation of E for Indium

$$E = \frac{\Delta H\ m}{60\ A\ B\ \Delta q_s}$$

ΔH = 28.4 J/gm 'given in DuPont instruction manual'

m = 12.1 mg

A = 20.4 cm^2 'area under the curve measued by planemeter'

Δq_s = .25 mV/cm 'Experiment setting'

B = 10 min/cm 'experiment setting'

then

E = 0.1123 mv/mW or E =112 μV/mW

note:

This E corresponds to the onset temperature of 156°C as given in DuPont instruction manual[62].

APPENDIX D

In this appendix the Arrhenius-type plots constructed for each thermogram peak using the ratio method are given in Figures D-1 to D-19. The order of the reaction as well as the activation energy for each plot are presented in the corresponding figure. The final as well as intermediate values required to plot these figures are tabulated in tables D-1 to D-25.

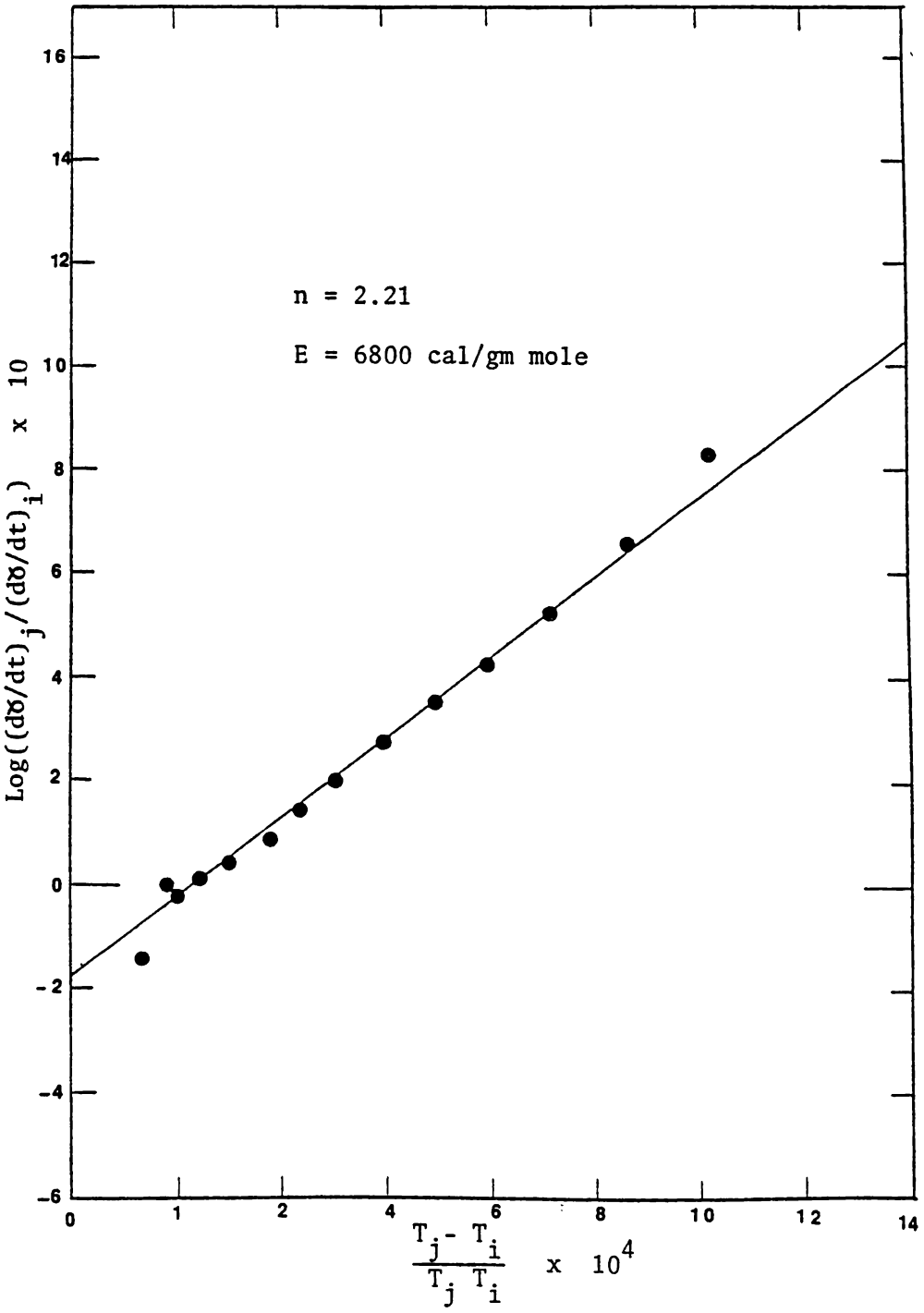

Figure D-1 Straight line constructed by ratio method for 100% crude oil (peak 1)

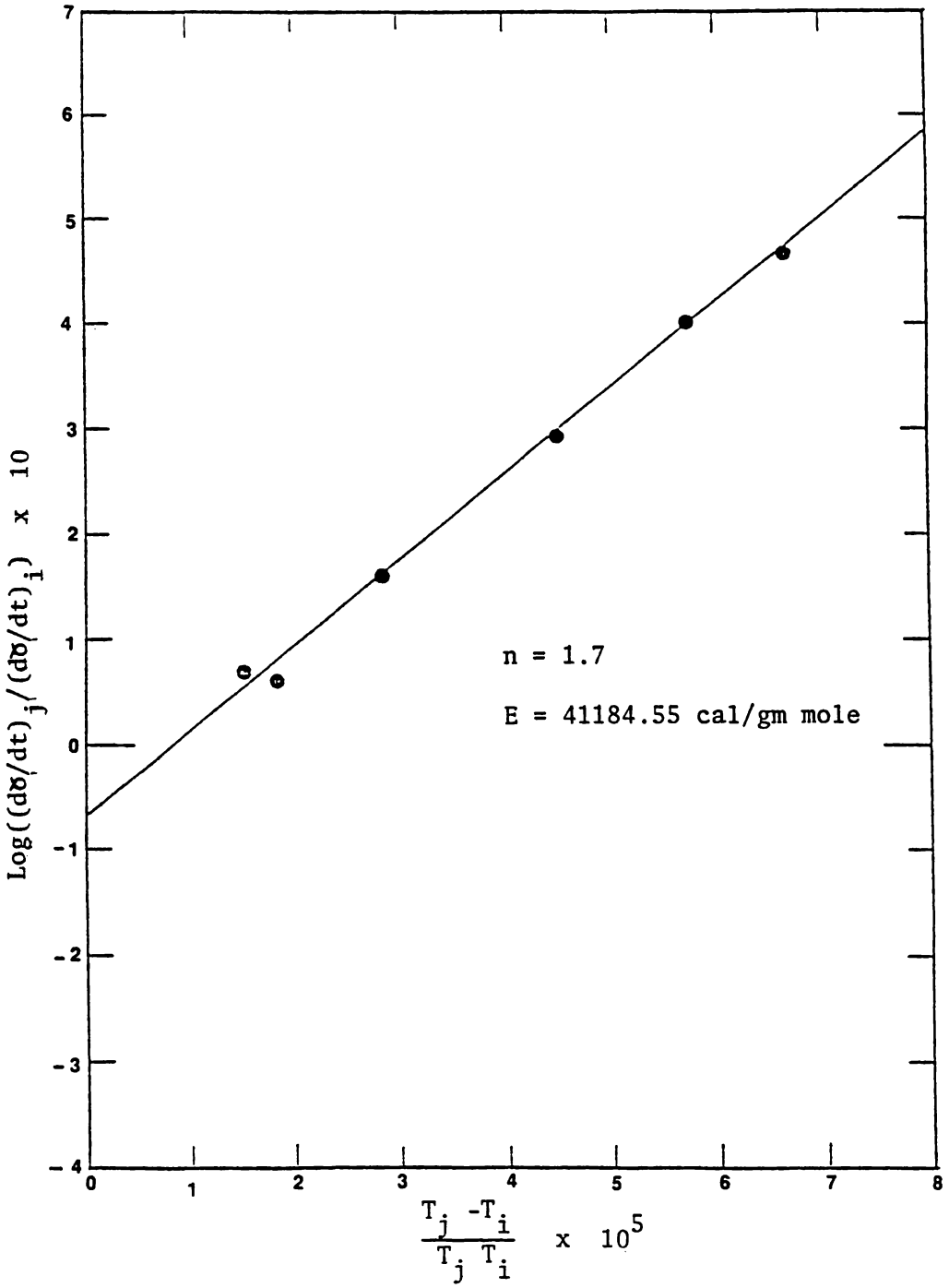

Figure D-2 Straight line constructed by ratio method for 100% crude oil (peak 2)

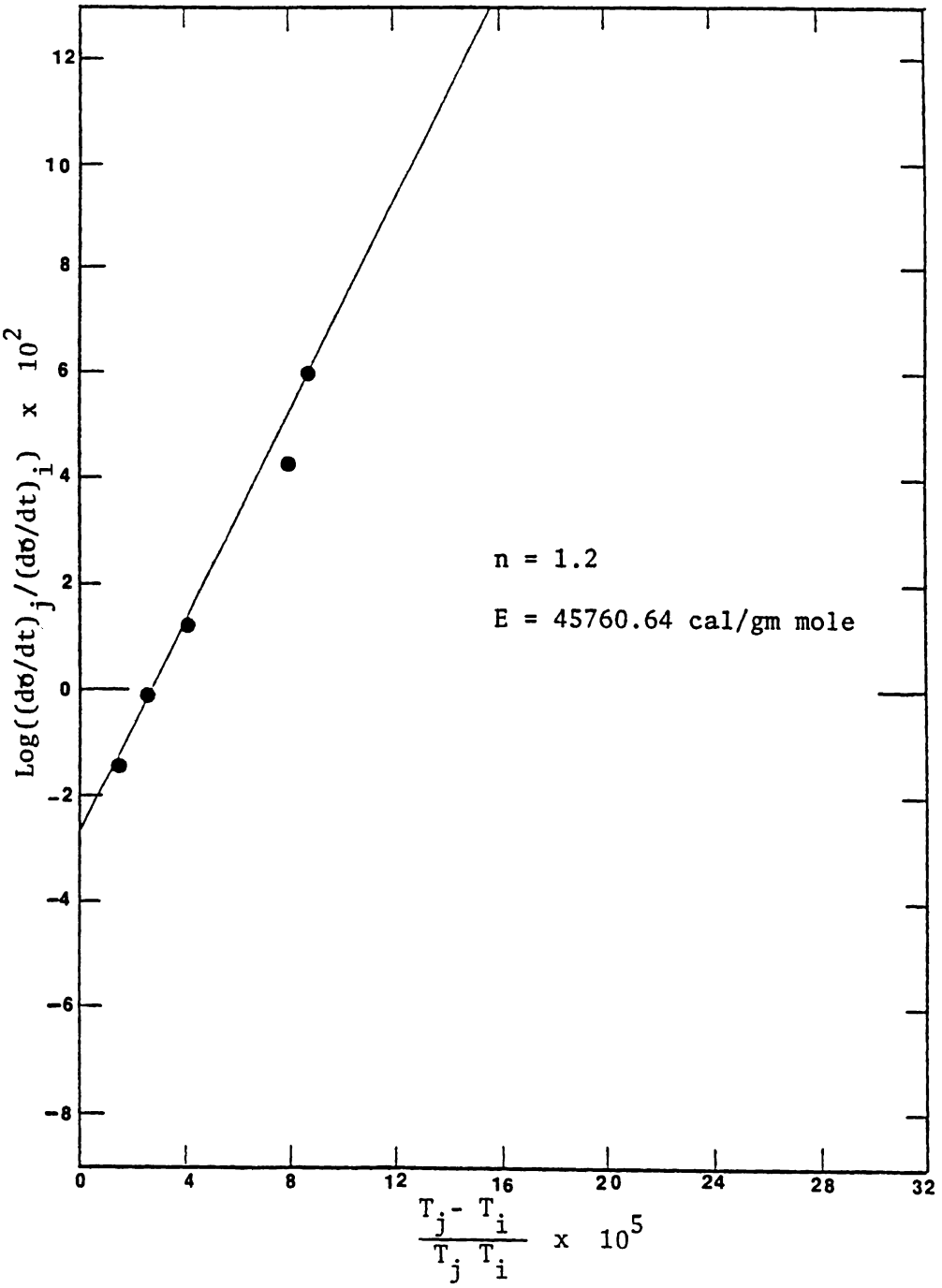

Figure D-3 Straight line constructed by ratio method for 100% crude oil (peak 3)

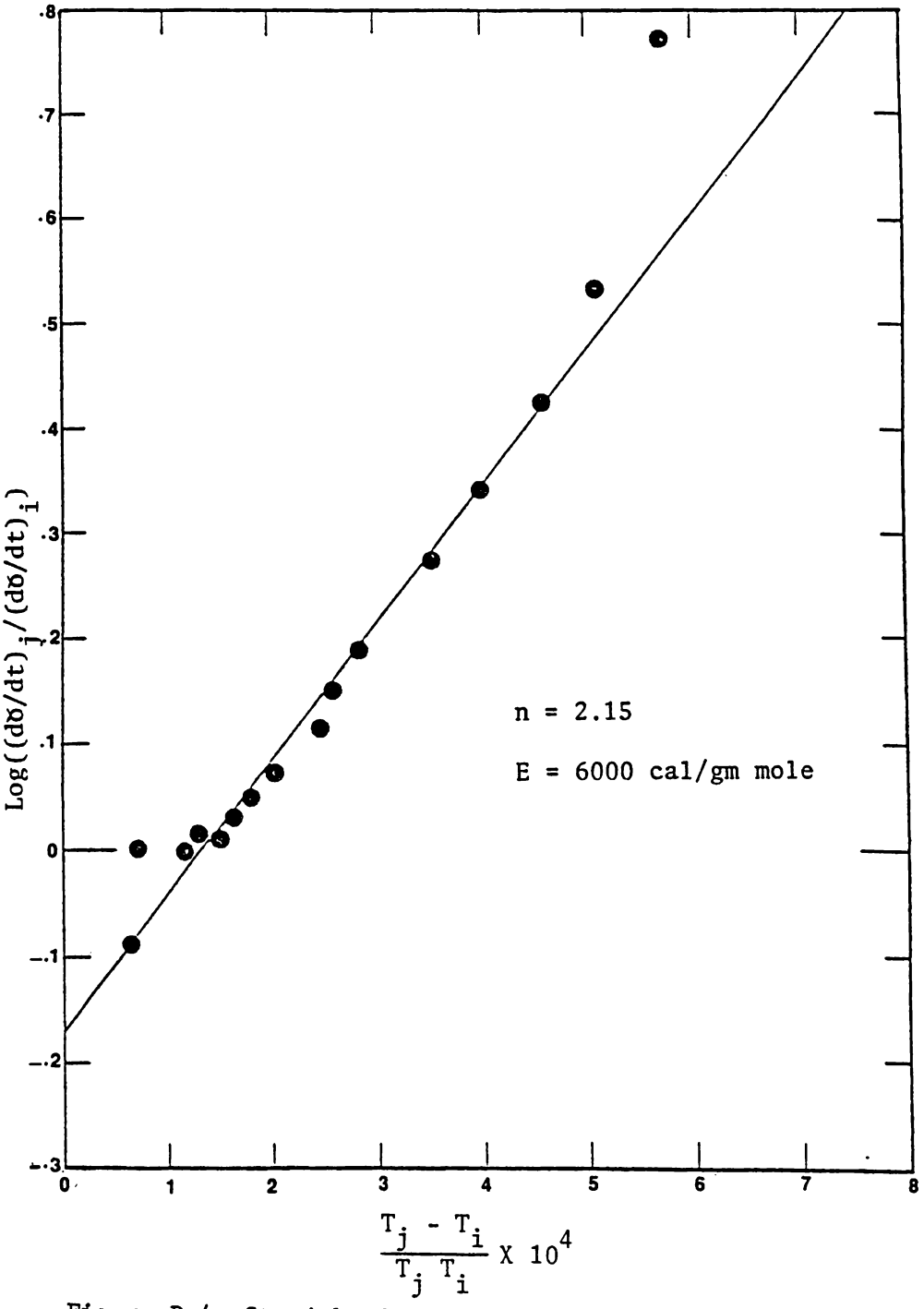

Figure D-4 Straight line constructed by ratio method for 80% sand - 20% oil (peak 1)

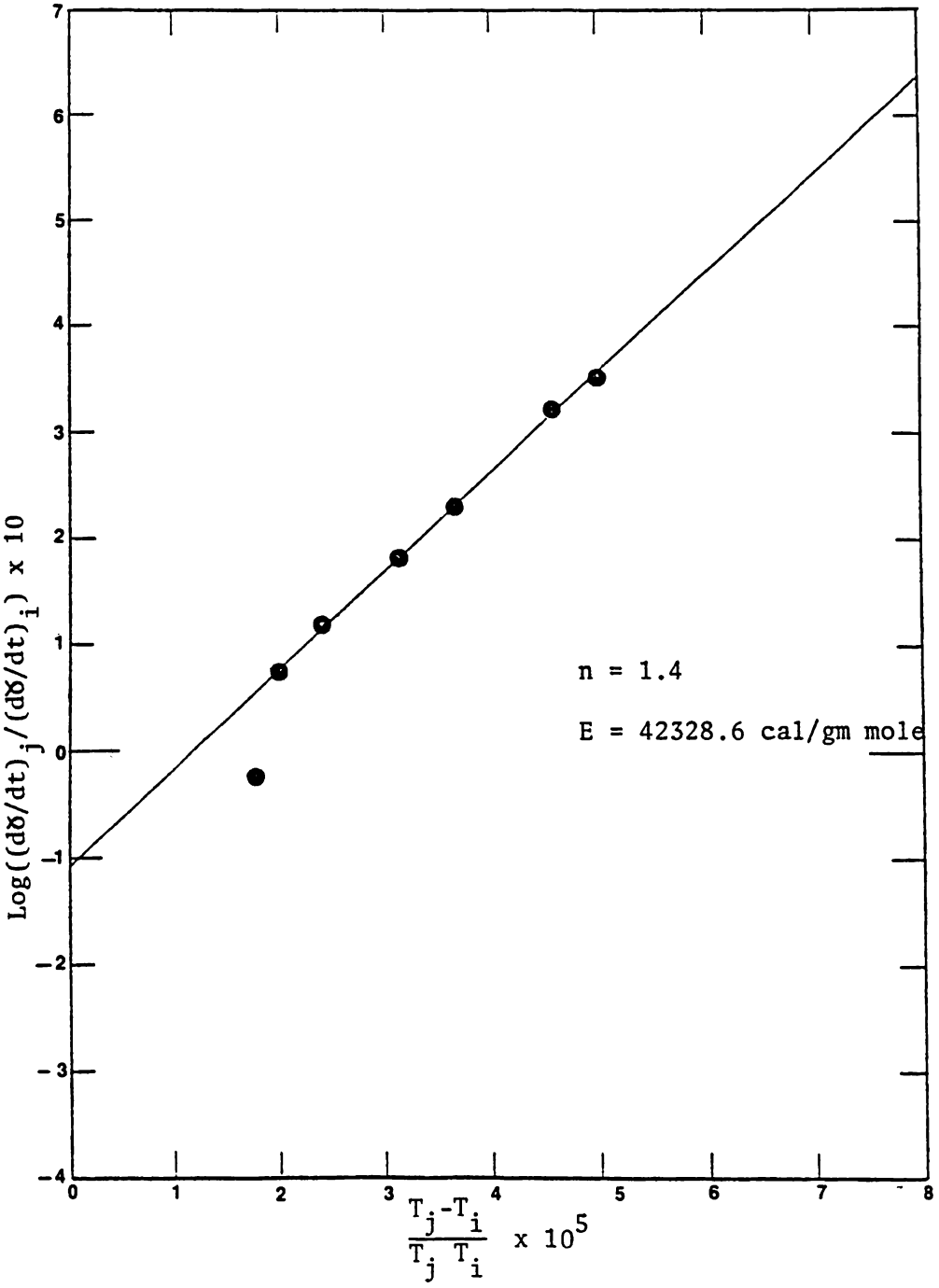

Figure D-5 Straight line constructed by ratio method for 80% sand - 20% oil (peak 2)

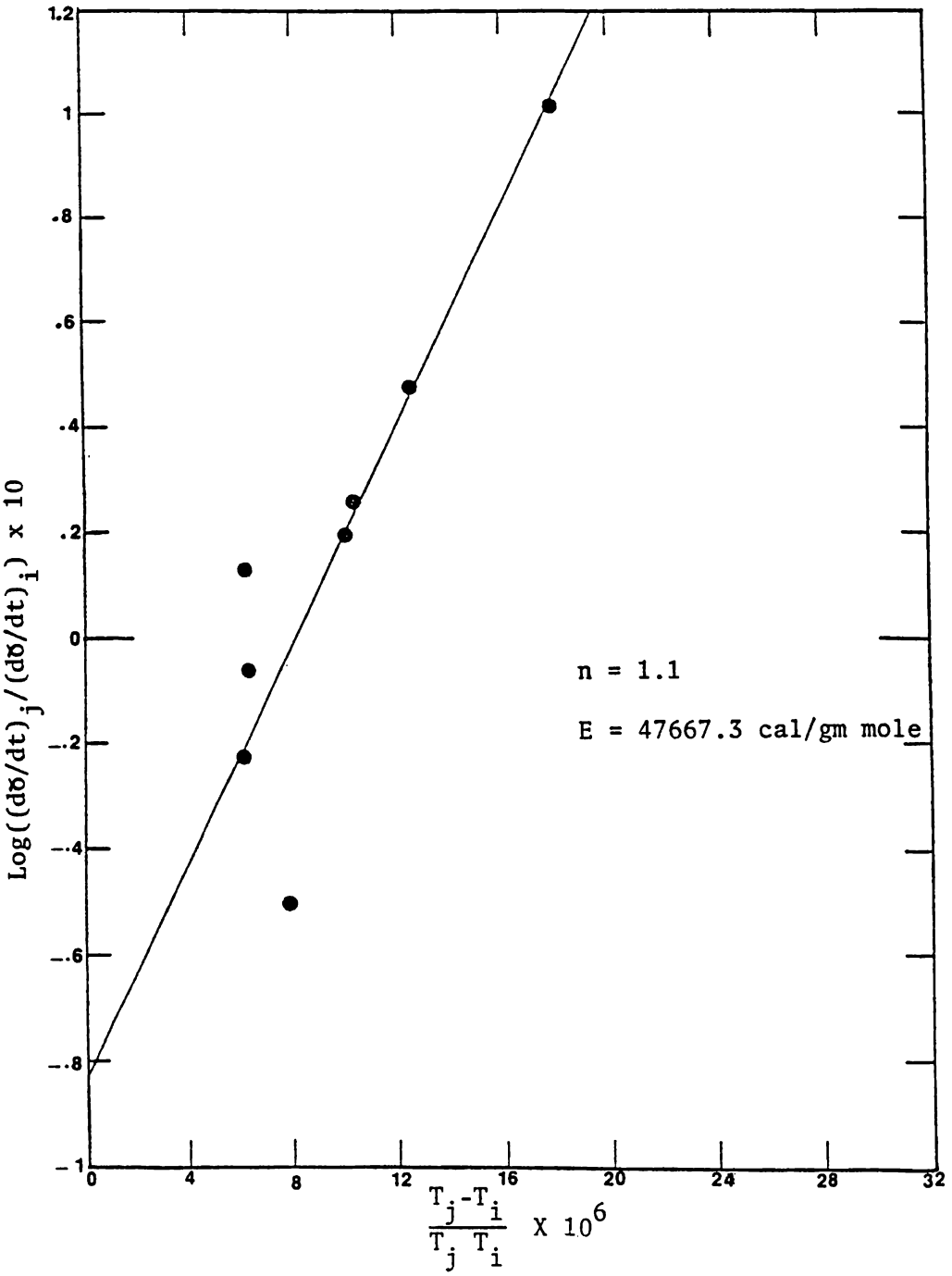

Figure D-6 Straight line constructed by ratio method for 80% sand - 20% oil (peak 3)

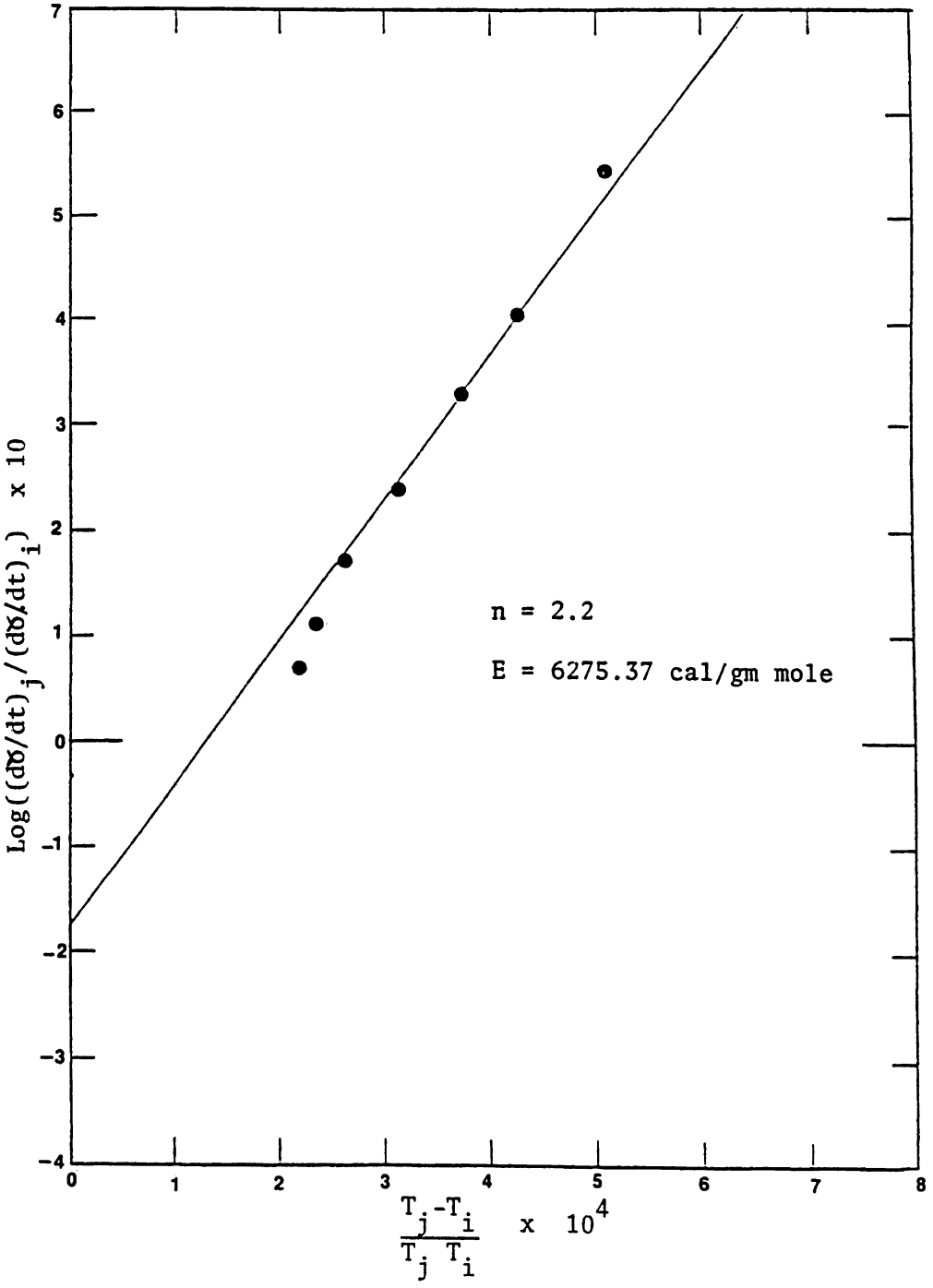

Figure D-7 Straight line constructed by ratio method for 80% fine silica - 20% oil (peak 1)

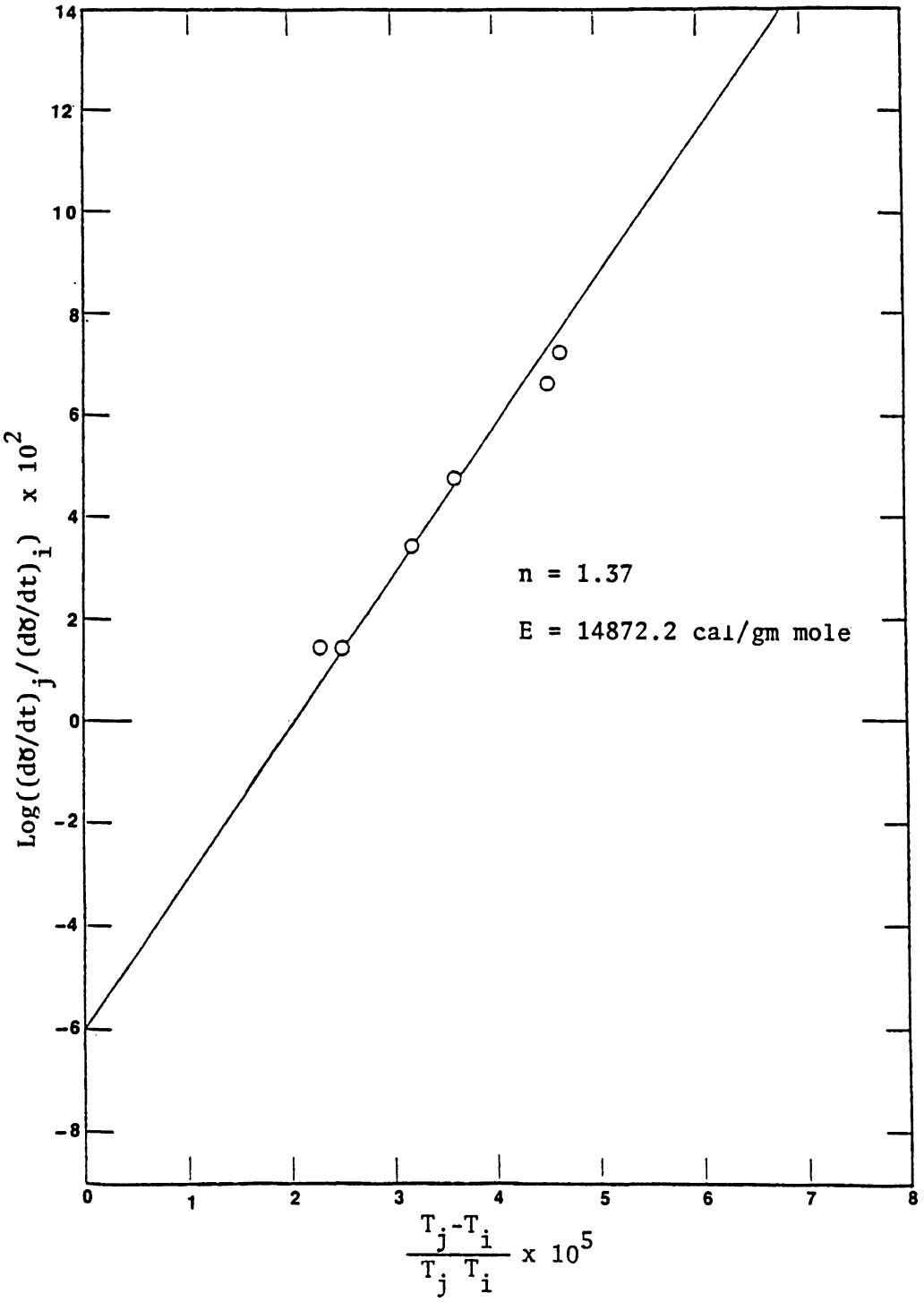

Figure D-8 Straight line constructed by ratio method for 80% fine silica - 20% oil (peak 2)

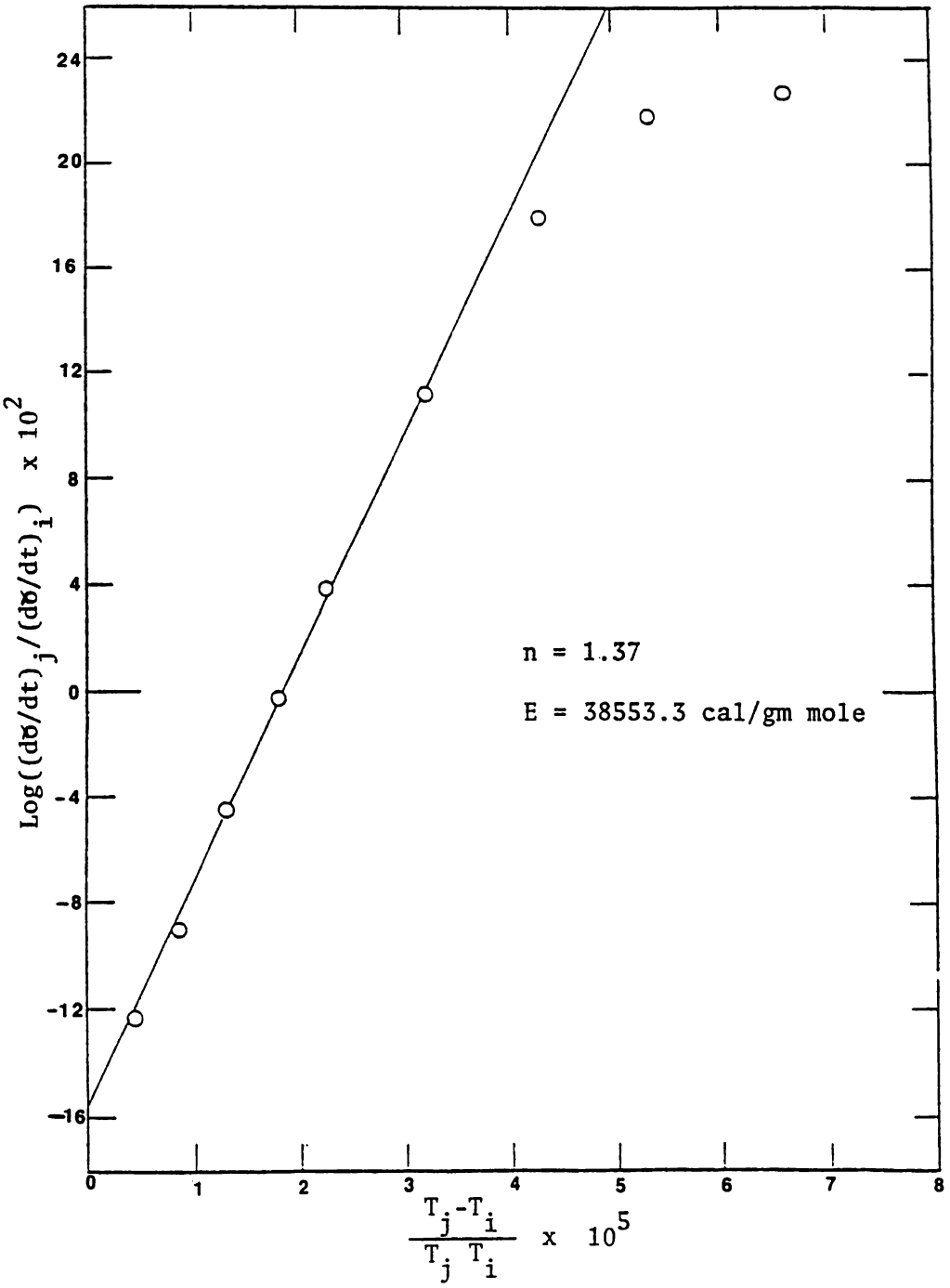

Figure D-9 straight line constructed by ratio method for 80% fine silica - 20% oil (peak 3)

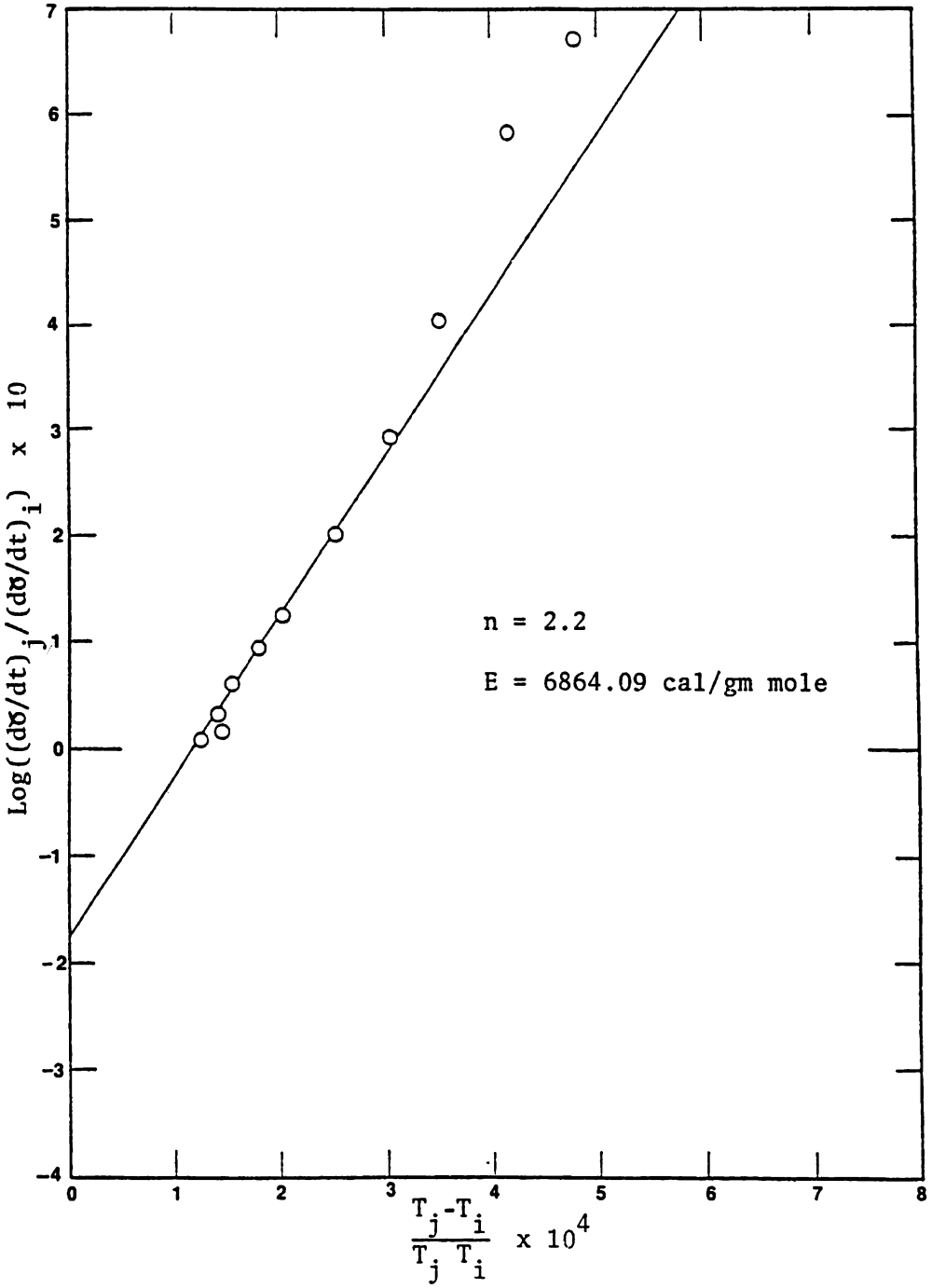

Figure D-10 Straight line constructed by ratio method for 80% clay - 20% oil (peak 1)

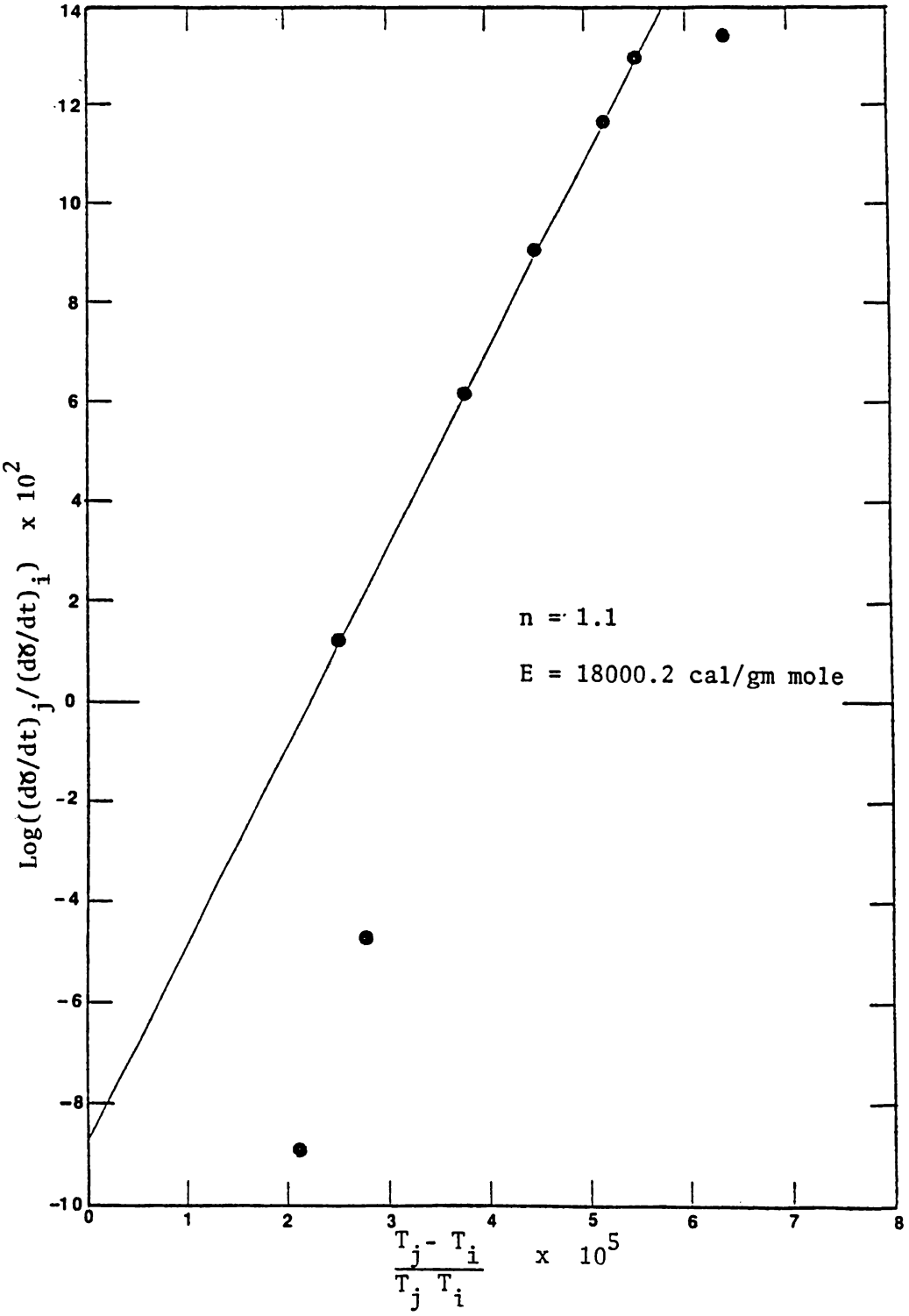

Figure D-11 Straight line constructed by ratio method for 80% clay - 20% oil (peak 2)

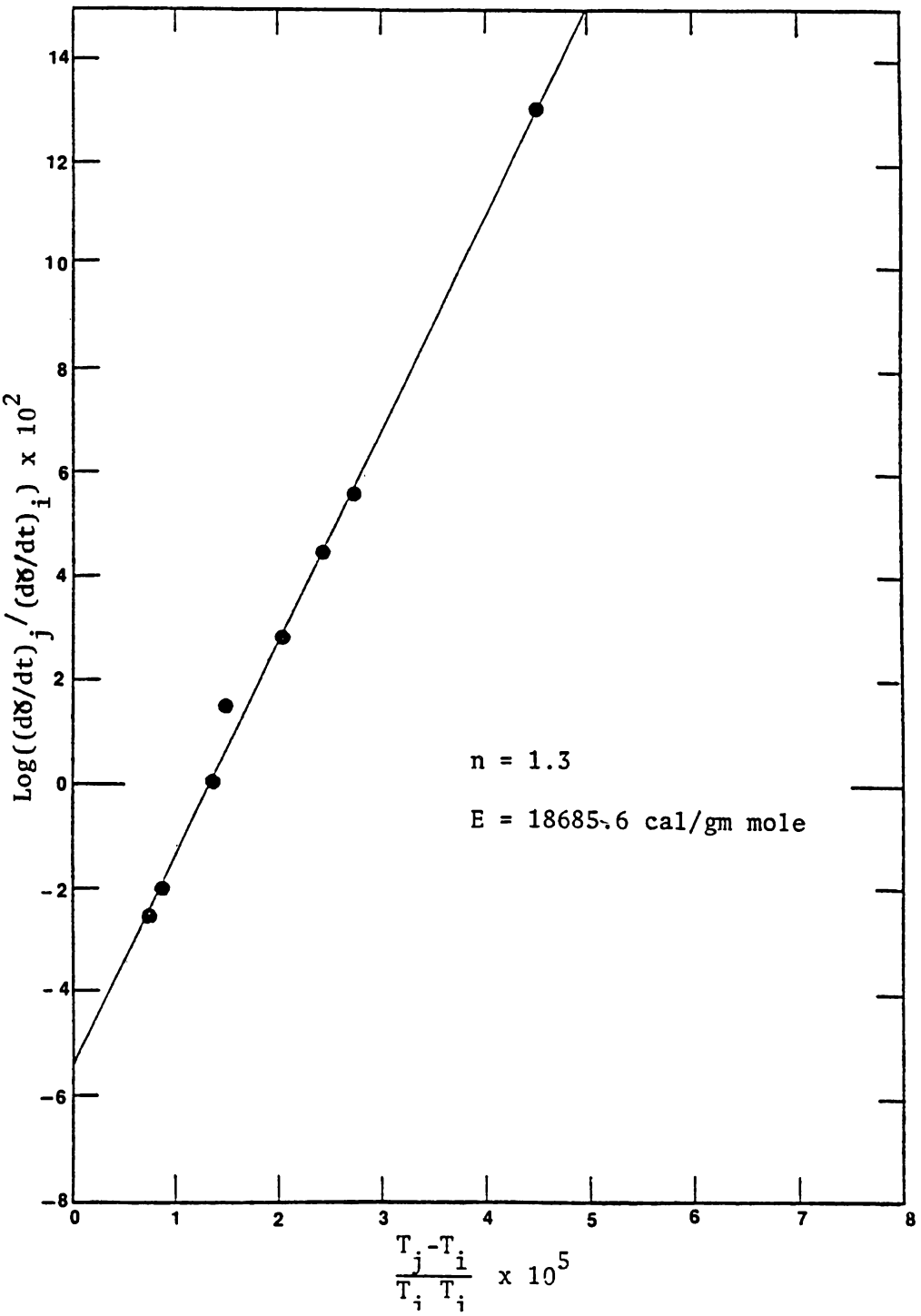

Figure D-12 Straight line constructed by ratio method for 80% clay - 20% oil (peak 3)

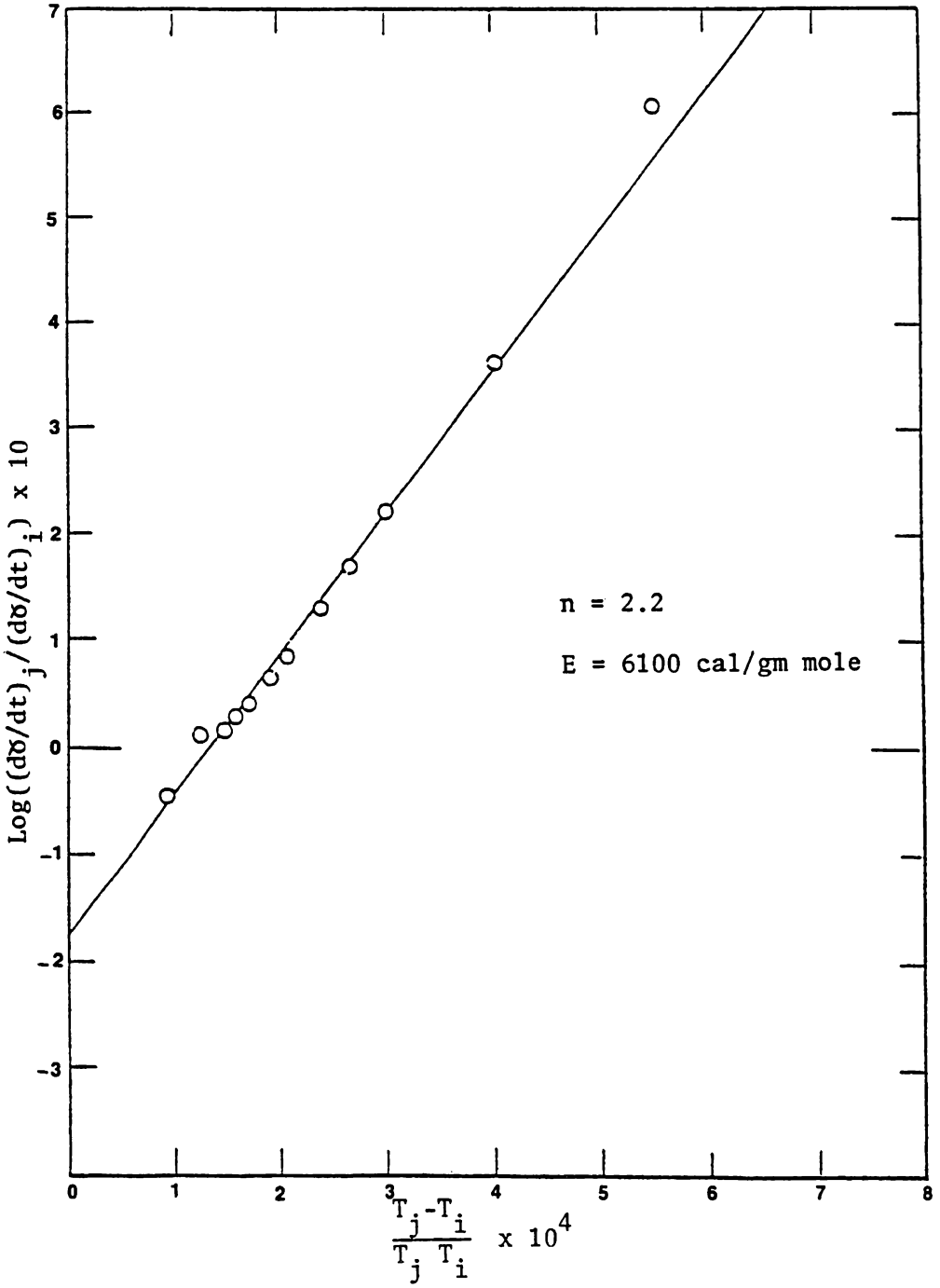

Figure D-13 Straight line constructed by ratio method for 40% silica powder - 40% sand - 20% oil (peak 1)

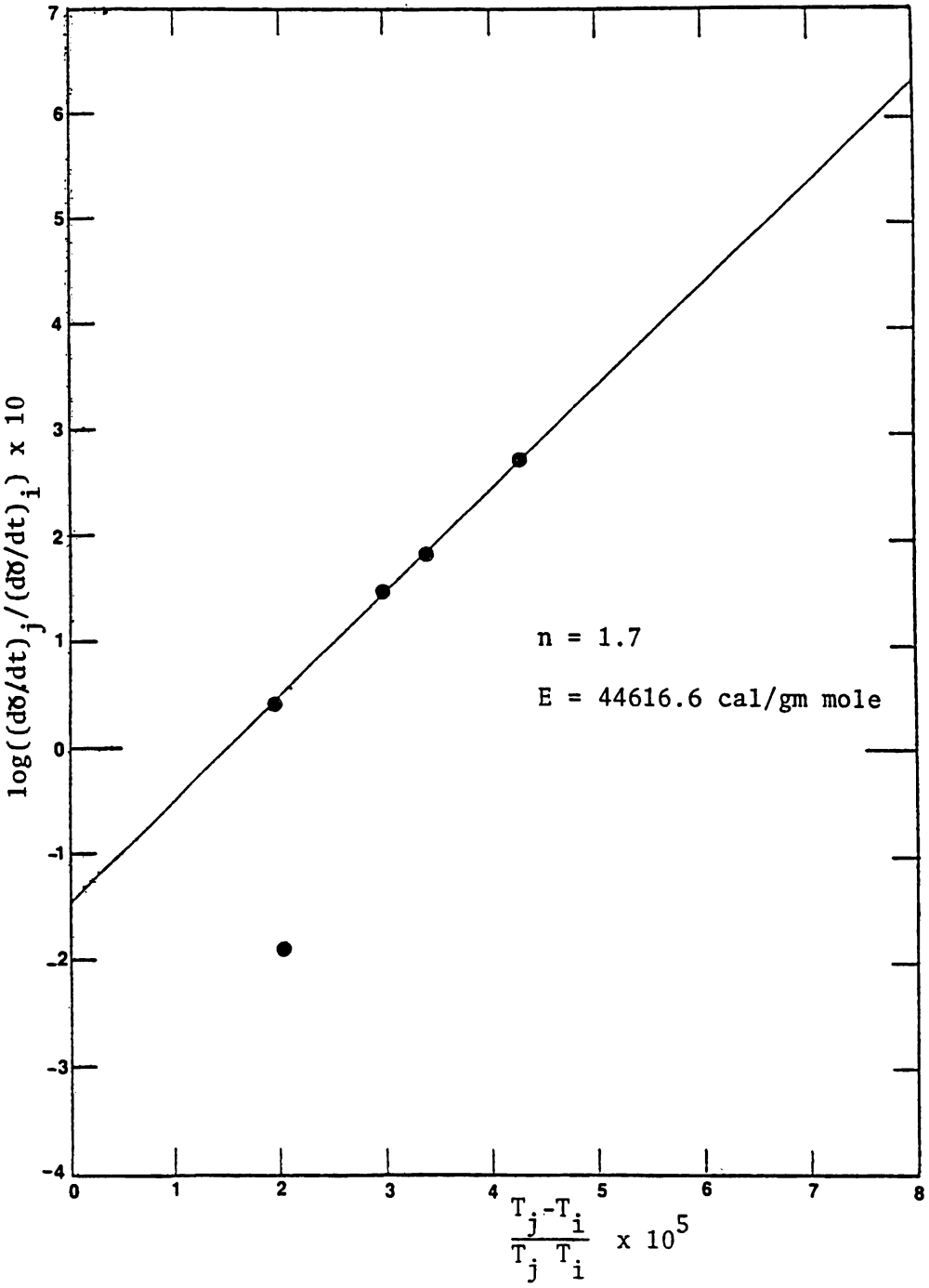

Figure D-14 Straight line constructed by ratio method for 40% silica powder - 40% sand - 20% oil (peak 2)

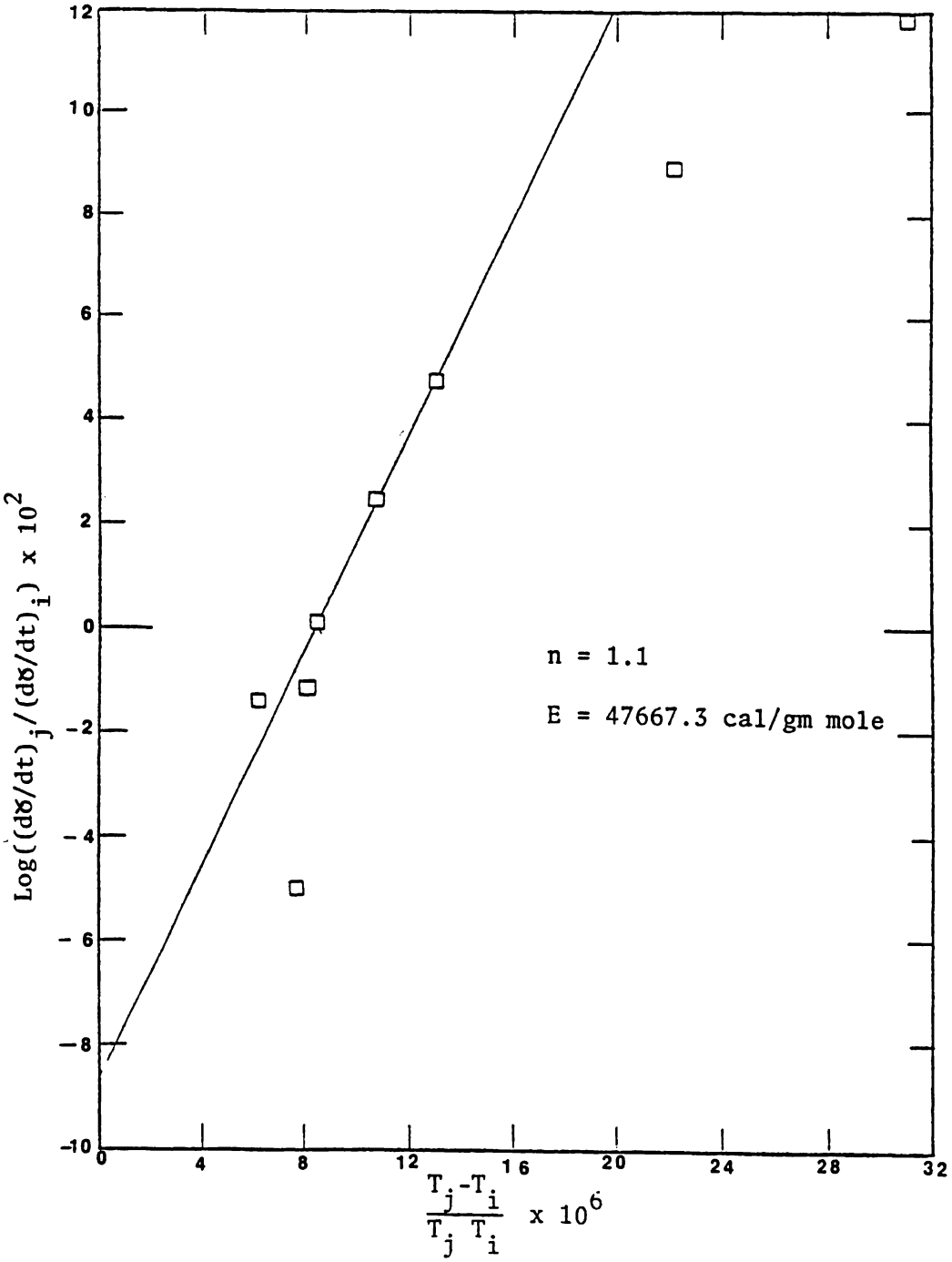

Figure D-15 Straight line constructed by ratio method for 40% silica powder - 40% sand - 20% oil (peak 3)

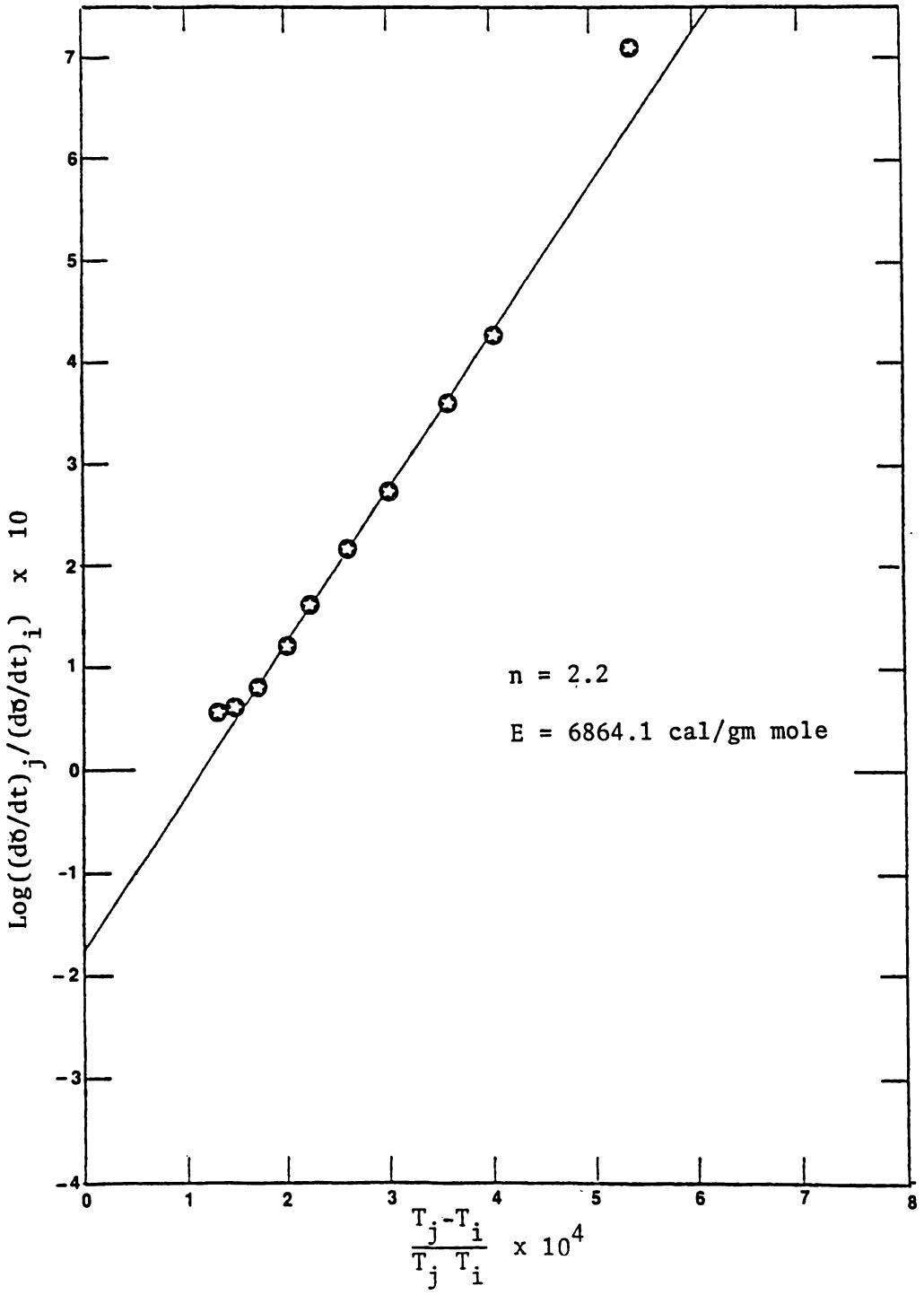

Figure D-16 Straight line constructed by ratio method for 40% clay - 40% sand - 20% oil (peak 1)

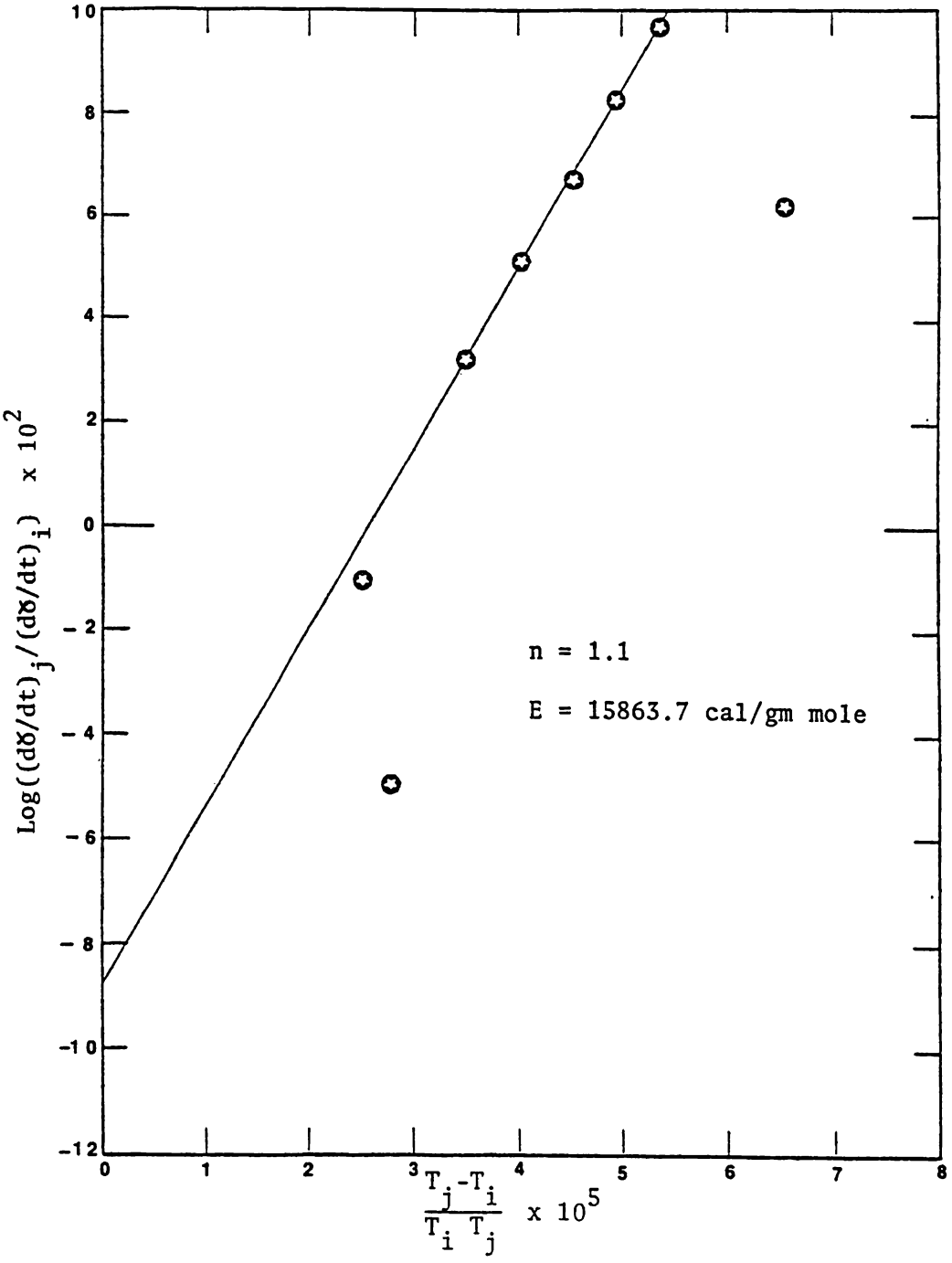

Figure D-17 Straight line constructed by ratio method for 40% clay - 40% sand - 20% oil (peak 2)

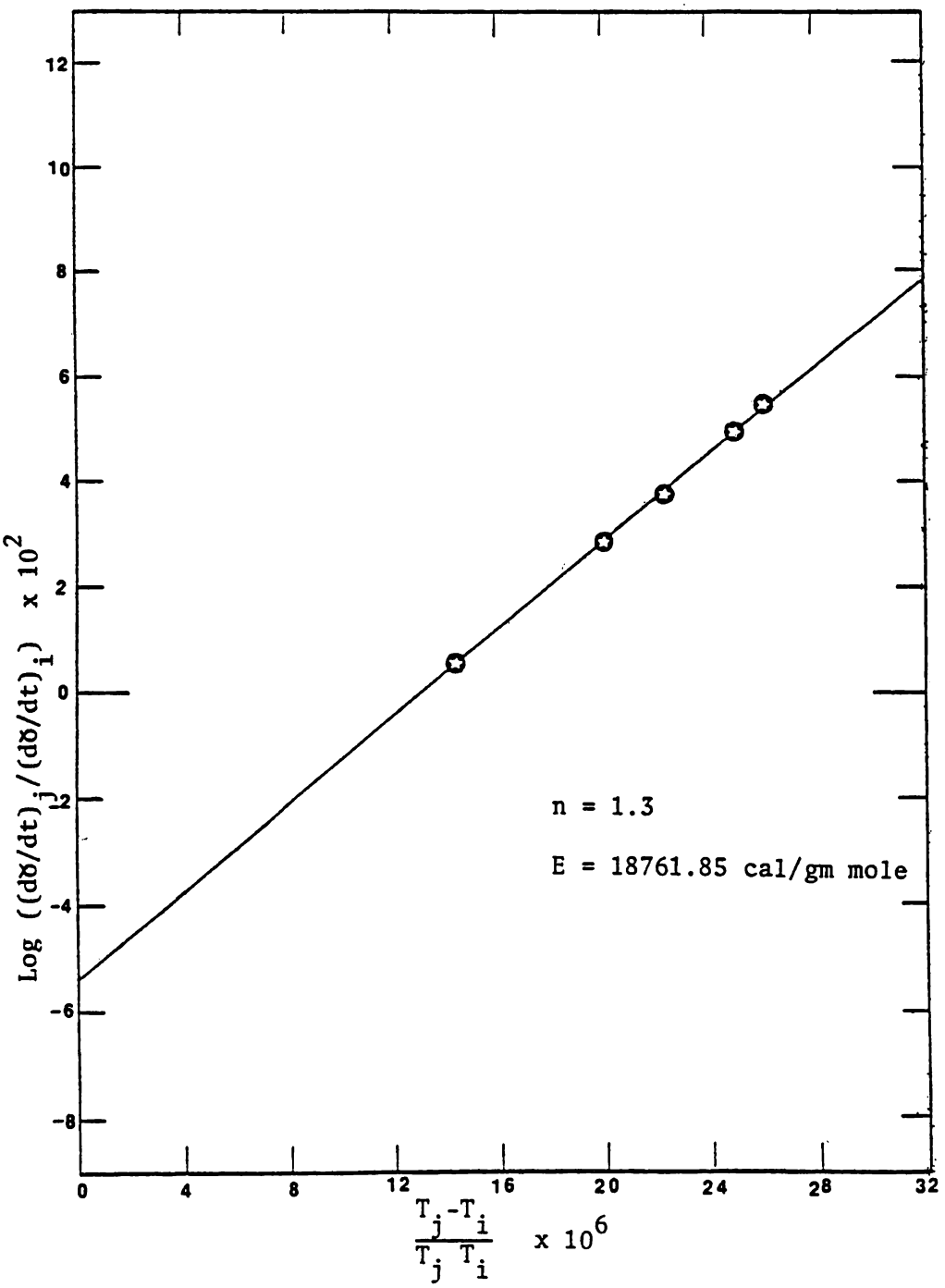

Figure D-18 Straight line constructed by ratio method for 40% clay - 40% sand - 20% oil (peak 3)

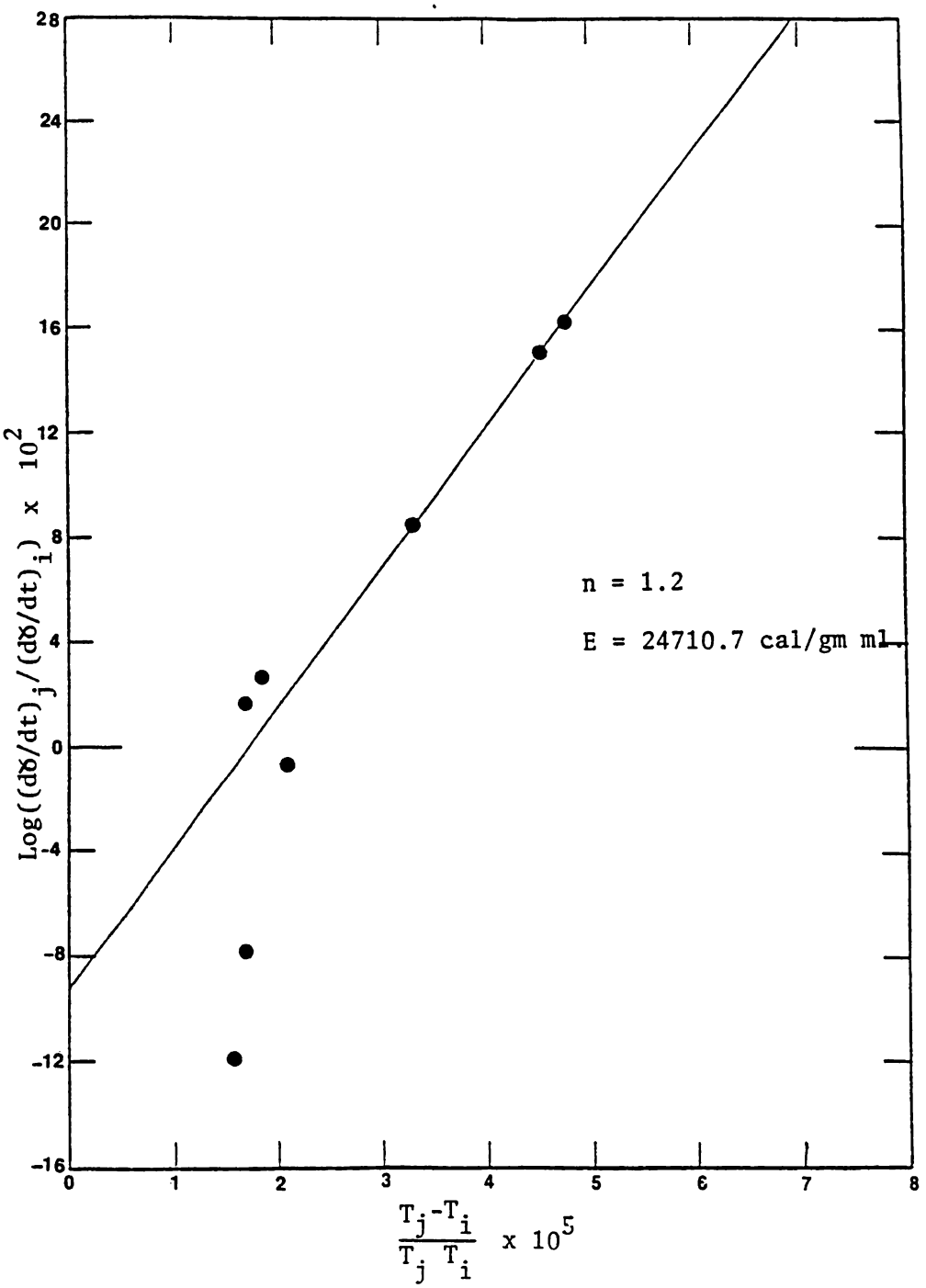

Figure D-19 Straight line constructed by ratio method for 80% burned clay - 20% oil (peak 3)

Table D-1 Data points for 100 Crude Oil, Peak # 1 (Heating rate = $5^{o}C/min$)

Point #	γ_i	γ_j	T_i °C	T_j °C	T_i °K	T_j °K	$(d\gamma/dt)_i$	$(d\gamma/dt)_j$	$\text{Log}\frac{(d\gamma/dt)_j}{(d\gamma/dt)_i}$	$\frac{T_j - T_i}{T_j T_i} \times 10^5$
1	.992	.826	100	210	373	483	1.7	11.6	.836	.611
2	.986	.822	112.5	212.5	385.5	485.5	2.6	11.8	.657	.534
3	.976	.813	125	215	398	488	3.6	12.1	.526	.4634
4	.964	.803	137.5	217.5	410.5	490.5	4.6	12.3	.427	.3973
5	.948	.79	150	222.5	423	495.5	5.74	12.6	.341	.3459
6	.9308	.776	162.5	227.5	435.5	500.5	7.0	12.7	.2587	.2982
7	.908	.757	175	232.5	448	505.5	8.3	12.8	.188	.2539
8	.882	.735	187.5	240	460.5	513	9.6	13	.1316	.222
9	.851	.709	200	247.5	473	520.5	10.8	13.1	.0835	.193
10	.778	.648	225	266.25	498	539.25	12.5	13.8	.041	.1536
11	.698	.5813	250	285	523	558	13.2	13.7	.0162	.1199
12	.617	.514	275	307.5	548	580.5	13.7	13.4	-.0144	.1022
12	.5362	.447	300	330	573	603	13.5	13.5	0.0	.087
14	.4596	.383	325	350	598	623	13.5	9.8	-.139	.0671

Note Ratio = 1.2

Point #	γ_i	γ_j	T_i °C	T_j °C	T_i °K	T_j °K	$(d\gamma/dt)_{cm_i}$	$(d\gamma/dt)_{cm_j}$	$\text{Log } \frac{(d\gamma/dt)_j}{(d\gamma/dt)_i}$	$\frac{T_j - T_i}{T_j\ T_i} \times 10^5$
1	.34	.31	387.5	417.5	660.5	690.5	2.2	6.3	.457	.658
2	.326	.3	400	427.5	673	700.5	2.6	6.5	.4	.583
3	.316	.287	412.5	432.5	685.5	705.5	3.7	7.2	.29	.416
4	.3	.273	425	438.75	698	711.75	5.5	8	.1627	.277
5	.278	.253	437.5	445	710.5	718	6.9	8.3	.08022	.147
6	.24	.22	450	460	723	733	8.9	10.2	.059	.189

Note Ratio = 1.1

Table D-3 : Data points for 100% Crude oil, Peak # 3 (Heating rate = $5^{o}C/min$)

Point #	γ_i	γ_j	T_i °C	T_j °C	T_i °K	T_j °K	$(d\gamma_{cm}/dt)_i$	$(d\gamma_{cm}/dt)_j$	$\text{Log} \frac{(d\gamma/dt)_j}{(d\gamma/dt)_i}$	$\frac{T_j - T_i}{T_j T_i} \times 10^5$
1	.17	.16	487.5	492.5	760.5	765	6.7	7.7	.06045	.86
2	.146	.14	500	502.5	773	775.5	9.6	9.9	.01336	.42
3	.1	.095	512.5	517.5	785.5	790.5	13	14.3	.0413	.81
4	.064	.061	525	526.5	798	799.5	11.5	11.5	0	.24
5	.024	.023	537.5	538.75	810.5	811.75	5.7	5.5	-.0155	.19

Note Ratio = 1.05

Table D-4 Data points for 100% Crude oil, Peak # 1 (Heating rate = 10^{o}C/min)

Point #	γ_i	γ_j	T_i °C	T_j °C	T_i °K	T_j °K	$(d\gamma/dt)_i$	$(d\gamma/dt)_j$	Log $\frac{(d\gamma/dt)_j}{(d\gamma/dt)_i}$	$\frac{T_j - T_i}{T_j T_i} \times 10^5$
							cm	cm		
1	.992	.827	100	210	373	483	1.2	11.6	.958	.61
2	.978	.815	125	215	398	488	2.8	12	.632	.4634
3	.956	.796	150	220	423	493	5.2	12.4	.3774	.3357
4	.908	.757	175	232.5	448	505.5	7.9	13.3	.2262	.254
5	.825	.71	200	247.5	473	520.5	10.7	13.9	.0945	.193
6	.78	.65	225	265	498	538	12.9	14.2	.042	.1493
7	.7	.583	250	285	523	558	14	14	0.0	.12
8	.616	.5133	275	305	548	578	14.1	13.9	-.006	.0947

Note Ratio = 1.2

Table D-5 Data points for 100% crude oil, Peak # 2 (Heating rate = 10^{o}C/min)

Point #	γ_i	γ_j	T_i °C	T_j °C	T_i °K	T_j °K	$(d\gamma_{cm}/dt)_i$	$(d\gamma_{cm}/dt)_j$	Log $\frac{(d\gamma/dt)_j}{(d\gamma/dt)_i}$	$\frac{T_j - T_i}{T_j T_i} \times 10^5$
1	.3084	.28	400	427.5	673	700.5	2.3	4.5	.29	.583
2	.3	.273	412.5	432.5	685.5	705.5	2.9	4.35	.176	.414
3	.285	.26	425	442.5	698	715.5	4.1	5.7	.133	.35
4	.2692	.245	437.5	450	710.5	723	5.4	7.3	.131	.2433
5	.22	.2	450	461.25	723	734.25	7.3	10.5	.1579	.212
									.0215	.137

Note Ratio' = 1.1

Table D-6 Data points for 100% crude oil, Peak # 3 (heating rate = 10 C/min)

Point #	γ_i	γ_j	T_i °C	T_j °C	T_i °K	T_j °K	$(d\gamma/dt)_{cm_i}$	$(d\gamma/dt)_{cm_j}$	$\text{Log} \frac{(d\gamma/dt)_j}{(d\gamma/dt)_i}$	$\frac{T_j - T_i}{T_j T_i} \times 10^5$
1	.138	.1314	512.5	517.5	785.5	790.5	5.5	6.4	.066	.81
2	.116	.11	525	528.75	798	801.75	7.8	8.35	.03	.59
3	.088	.084	537.5	540	810.5	813	10.15	10.6	.19	.38
4	.048	.046	550	551.75	823	824.75	11.5	11.3	-.0076	.26
4										

Note Ratio = 1.05

Table D-7 Data points for 100% crude oil, Peak #1 (heating rate = $1^{o}C/min$)

Point #	γ_i	γ_j	T_i °C	T_j °C	T_i °K	T_j °K	$(d\gamma/dt)_{cm_i}$	$(d\gamma/dt)_{cm_j}$	$\text{Log}\frac{(d\gamma/dt)_j}{(d\gamma/dt)_i}$	$\frac{T_j - T_i}{T_j T_i} \times 10^5$
1	.982	.81	75	155	348	428	.95	4.15	.64	.5371
2	.968	.8	87.5	160	360.5	433	1.6	4.25	.424	.4645
3	.95	.792	100	162.5	373	435	2.1	4.3	.31	.3848
4	.926	.772	112.5	170	385.5	443	2.6	4.45	.233	.3367
5	.902	.75	125	177.5	398	450.5	3.15	4.45	.1501	.2928
6	.832	.69	150	195	423	468	4	4.5	.052	.2273

Note Ratio = 1.2

Table D-8 Data points for 100% crude oil, Peak # 2 (Heating rate = $1^{o}C$/min)

Point #	γ_i	γ_j	T_i °C	T_j °C	T_i °K	T_j °K	$(d\gamma_{cm}/dt)_i$	$(d\gamma_{cm}/dt)_j$	$\text{Log}\frac{(d\gamma/dt)_j}{(d\gamma/dt)_i}$	$\frac{T_j - T_i}{T_j\ T_i} \times 10^5$
1	.326	.27	375	395	648	668	.9	2.1	.367	.462
2	.31	.28	387.5	402.5	660.5	675.5	1.6	2.6	.211	.336
3	.284	.26	400	412.5	673	685.5	2.2	3	.14	.271
4	.258	.235	412.5	420	685.5	693	3.1	3.6	.064	.158
5	.224	.204	425	432.5	698	705.5	4.1	3.7	-.044	.152

Note Ratio = 1.1

Table D-9 Data points for 100% crude oil, Peak # 3 (heating rate = 1 ^{o}C/min)

Point #	γ_i	γ_j	T_i °C	T_j °C	T_i °K	T_j °K	$(d\gamma/dt)_{cm})_i$	$(d\gamma/dt)_{cm})_j$	Log $\frac{(d\gamma/dt)_j}{(d\gamma/dt)_i}$	$\frac{T_j - T_i}{T_j T_i} \times 10^5$
1	.16	.15	450	452.5	723	725.5	3.4	3.55	.0187	.48
2	.12	.114	462.5	464.25	735.5	737.25	4.3	4.35	.005	.32
3	.07	.0667	475	476.75	748	749.75	5	5	0.0	.31

Note Ratio = 1.05

Table D-10 Data points for 80%sand-20%oil, Peak # 1

Point #	γ_i	γ_j	T_i °C	T_j °C	T_i °K	T_j °K	$(d\gamma/dt)_i$	$(d\gamma/dt)_j$	$\text{Log}\frac{(d\gamma/dt)_j}{(d\gamma/dt)_i}$	$\frac{T_j - T_i}{T_j T_i} \times 10^5$
1	.9889	.8241	100	202.5	373	475.5	.7	4.15	.7729	.5779
2	.9778	.815	112.5	207.5	385.5	480.5	1.2	4.2	.544	.513
3	.971	.81	125	212.5	398	485.5	1.6	4.35	.434	.453
4	.956	.794	137.5	217.5	410.5	490.5	2.0	4.45	.347	.397
5	.934	.778	150	222.5	423	495.5	2.45	4.48	.262	.346
6	.9165	.674	162.5	225	435.5	498	2.9	4.55	.1956	.288
7	.8901	.74	175	235	448	508	3.3	4.65	.1489	.264
8	.8637	.72	187.5	242.5	460.5	515.5	3.65	4.7	.11	.232
9	.839	.699	200	250	473	523	4.05	4.72	.0664	.202
10	.804	.67	212.5	260	485.5	533	4.3	4.77	.045	.184
11	.77	.64	225	270	498	543	4.45	4.8	.032	.166
12	.736	.613	237.5	280	510.5	553	4.6	4.8	.018	.151
13	.7032	.586	250	287.5	523	560.5	4.7	4.65	.0136	.1279
		[illegible]	262.5	297.5	535.5	570.5	4.75	4.95	.018	.1146

Table D-10 (cont'd)

Point #	γ_i	γ_j	T_i °C	T_j °C	T_i °K	T_j °K	$(d\gamma_{cm}/dt)_i$	$(d\gamma_{cm}/dt)_j$	$\text{Log} \frac{(d\gamma/dt)_j}{(d\gamma/dt)_i}$	$\frac{T_j - T_i}{T_j T_i} \times 10^5$
15	.626	.522	275	310	548	583	4.8	4.97	.01511	.1096
16	.5538	.462	300	327.5	573	600.5	4.9	4.95	.00441	.0799
17	.4725	.393	325	350	598	623	4.9	4.8	-.0089	.0671
18	.429	.357	337.5	365	610.5	638	4.95	2.5	-.296	.0706

Table D-11 Data points for 80%sand-20%oil, Peak # 2

Point #	γ_i	γ_j	T_i °C	T_j °C	T_i °K	T_j °K	$(d\gamma_{cm}/dt)_i$	$(d\gamma_{cm}/dt)_j$	$\text{Log} \frac{(d\gamma/dt)_j}{(d\gamma/dt)_i}$	$\frac{T_j - T_i}{T_j T_i} \times 10^5$
1	.3077	.256	425	450	698	723	2	4.5	.3522	.495
2	.2967	.247	431.25	455	704.25	728	2.35	5	.3288	.463
3	.2879	.2399	437.5	456.25	710.5	729.25	2.95	5.05	.233	.362
4	.275	.22	443.75	460	716.75	733	3.65	5.65	.1897	.309
5	.257	.214	450	462.5	723	735.5	4.5	6	.1249	.235
6	.242	.2	456.25	467.5	729.25	740.5	5.1	6	.0705	.208
7	.2142	.1785	462.5	472.5	735.5	745.5	5.5	5.2	-.02	.182

Note Ratio = 1.2

Table D-12: Data points for 80%sand-20%oil, peak # 3

Point #	γ_i	γ_j	T_i °C	T_j °C	T_i °K	T_j °K	$(d\gamma/dt)_{cm_i}$	$(d\gamma/dt)_{cm_j}$	$\text{Log}\frac{(d\gamma/dt)_j}{(d\gamma/dt)_i}$	$\frac{T_j - T_i}{T_j T_i} \times 10^5$
1	.1604	.1337	481.25	487.5	754.25	760.5	2.95	3.1	.0215	.109
2	.138	.1154	487.5	497.5	760.5	770.5	3.1	4	.111	.171
3	.1275	.1062	493.75	500	766.75	773	3.85	4.1	.0273	.105
4	.1063	.0886	500	507.5	773	780.5	4.15	4.65	.0494	.124
5	.0989	.0824	506.25	510	779.25	783	4.7	4.85	.0136	.061
6	.077	.064	512.5	516.25	785.5	789.25	5.0	4.95	-.004	.06
7	.055	.046	518.75	522.5	791.75	795.5	5.1	4.85	-.0218	.06
8	.033	.027	525	530	798	803	4.65	4.1	-.05	.078
9	.022	.018	531.25	535	804.25	808	3.5	2.2	-.2	.058

Note Ratio = 1.2

Table D-13 Data points for 80% silica powder-20%oil, peak # 1

Point #	γ_i	γ_j	T_i °C	T_j °C	T_i °K	T_j °K	$(d\gamma_{cm}/dt)_i$	$(d\gamma_{cm}/dt)_j$	$\text{Log} \frac{(d\gamma/dt)_j}{(d\gamma/dt)_i}$	$\frac{T_j - T_i}{T_j T_i} \times 10^5$
1	.981	.816	100	187.5	373	460.5	1.35	4.95	.5642	.51
2	.965	.804	112.5	190	385.5	463	1.95	5.05	.413	.4342
3	.951	.793	125	195	398	468	2.4	5.15	.331	.3758
4	.934	.778	137.5	200	410.5	473	3	5.25	.243	.322
5	.906	.755	150	205	423	478	3.6	5.3	.168	.272
6	.883	.736	162.5	212.5	435.5	485.5	4.15	5.35	.110	.2365
7	.85	.705	175	225	448	498	4.7	5.45	.064	.2241

Note ratio = 1.2

Table D-14: Data points for 80%silica powder-20%oil, Peak# 2

Point #	γ_i	γ_j	T_i °C	T_j °C	T_i °K	T_j °K	$(d\gamma_{cm}/dt)_i$	$(d\gamma_{cm}/dt)_j$	$\text{Log}\frac{(d\gamma/dt)_j}{(d\gamma/dt)_i}$	$\frac{T_j - T_i}{T_j T_i} \times 10^5$
1	.5856	.532	262.5	277.5	535.5	550.5	6.3	7.2	.058	.509
2	.5622	.511	268.75	282.5	541.75	555.5	6.6	7.85	.075	.457
3	.537	.488	275	287.5	548	560.5	7.1	8.3	.0678	.407
4	.519	.472	281.25	292.5	554.25	565.4	7.7	8.6	.048	.359
5	.49	.445	287.5	297.5	560.5	570.5	8.35	9	.0325	.313
6	.465	.423	293.75	302.5	566.75	575.5	8.7	9	.0147	.268
7	.436	.396	300	307.5	573	580.5	9.1	8.6	-.0245	.225
8	.41	.369	306.25	315	579.25	588	8.7	7	-.0944	.257

Note: ratio = 1.1

Table D-15: Data points for 80%silica powder-20%oil, peak # 3

Point #	γ_i	γ_j	T_i °C	T_j °C	T_i °K	T_j °K	$(d\gamma/dt)_{cm_i}$	$(d\gamma/dt)_{cm_j}$	$\text{Log}\frac{(d\gamma/dt)_j}{(d\gamma/dt)_i}$	$\frac{T_j - T_i}{T_j T_i} \times 10^5$
1	.222	.171	412.5	445	685.5	718	1.9	3.2	.222	.66
2	.202	.1556	425	452.5	698	725.5	2.25	3.7	.216	.543
3	.185	.142	437.5	460	710.5	733	2.7	4.05	.176	.432
4	.1634	.126	450	467.5	723	740.5	3.4	4.4	.112	.327
5	.138	.106	462.5	475	735.5	748	4.2	4.6	.0395	.227
6	.105	.081	475	485	748	758	4.6	4.55	-.0047	.176
7	.076	.058	487.5	495	760.5	768	4.5	4.1	-.0404	.128
8	.0467	.036	500	505	773	778	3.6	2.9	-.093	.083
9	.027	.021	512.5	515	785.5	788	1.4	1.06	-.121	.04

Note Ratio ≠ 1.3

Table D-16 data points for 80%clay-20%oil, Peak # 1

Point #	γ_i	γ_j	T_i °C	T_j °C	T_i °K	T_j °K	$(d\gamma/dt)_{cm})_i$	$(d\gamma/dt)_{cm})_j$	Log $\frac{(d\gamma/dt)_j}{(d\gamma/dt)_i}$	$\frac{T_j - T_i}{T_j T_i} \times 10^5$
1	.954	.795	100	180	373	453	.9	4.4	.689	.0004735
2	.9463	.7886	112.5	185	385.5	458	1.15	4.5	.621	.0004106
3	.93	.7744	125	190	398	463	1.85	4.8	.414	.0003527
4	.9073	.756	137.5	195	410.5	468	2.45	4.9	.303	.0002993
5	.883	.736	150	200	423	473	3.1	5.0	.207	.0002499
6	.854	.711	162.5	205	435.5	478	3.9	5.2	.1249	.0002042
7	.822	.68	175	215	448	488	4.4	5.5	.09691	.000183
8	.78	.65	187.5	222.5	460.5	595.5	4.75	5.5	.064	.0001534
9	.732	.61	200	235	473	508	5.1	5.5	.0328	.0001457
10	.6878	.573	212.5	245	485.5	518	5.4	5.5	.0079	.0001292
11	.646	.538	225	262.5	498	535.5	5.5	5.7	.0155	.0001406

Note Ratio = 1.2

Table D-17 Data points for 80%clay-20%oil, peak # 2

Point #	γ_i	γ_j	T_i °C	T_j °C	T_i °K	T_j °K	$(d\gamma_{cm}/dt)_i$	$(d\gamma_{cm}/dt)_j$	$\text{Log} \frac{(d\gamma/dt)_j}{(d\gamma/dt)_i}$	$\frac{T_j - T_i}{T_j T_i} \times 10^5$
1	.554	.461	275	295	548	568	6.1	8.3	.1337	.643
2	.53	.4431	281.25	297.5	554.25	570.5	6.7	8.8	.1184	.514
3	.5	.417	287.5	305	560.5	578	7.2	9.7	.1294	.54
4	.4634	.386	293.75	308.5	566.75	581.5	8.15	10.1	.093	.448
5	.439	.366	300	312.5	573	585.5	9.1	10.5	.062	.373
6	.4024	.3354	306.25	315	579.25	588	10	10.3	.012	.257
7	.361	.3	312.5	322.5	585.5	595.5	9.5	8.5	-.048	.287
8	.33	.275	318.75	327	591.75	600	9.25	7.5	-.09	.246

Note ratio = 1.2

Table D-18 Data points for 80%clay-20%oil, Peak # 3

Point #	γ_i	γ_j	T_i °C	T_j °C	T_i °K	T_j °K	$(d\gamma_{cm}/dt)_i$	$(d\gamma_{cm}/dt)_j$	$\text{Log}\frac{(d\gamma/dt)_j}{(d\gamma/dt)_i}$	$\frac{T_j - T_i}{T_j T_i} \times 10^5$
1	.2073	.1885	387.5	407.5	660.5	680.5	2.7	3.65	.1309	.445
2	.1707	.155	400	412.5	673	685.5	3.3	3.75	.0555	.271
3	.1552	.1411	412.5	422.5	685.5	695.5	3.75	4.0	.028	.21
4	.134	.1219	425	432.5	698	705.5	4.25	4.4	.015	.152
5	.0952	.087	437.5	450	710.5	723	4.65	5.15	.0443	.243
6	.07312	.0665	450	457.5	723	730.5	5.15	5.15	0.0	.143
7	.04878	.0443	462.5	467.5	735.5	740.5	5	4.77	-.0205	.092
8	.012	.011	475	480	748	753	3.6	3.4	-.0248	.089

Note: Ratio=1.1

Table D-19 Data points for 40%sand-40%silica powder-20%oil, Peak # 1.

Point #	γ_i	γ_j	T_i °C	T_j °C	T_i °K	T_j °K	$(d\gamma/dt)_{cm_i}$	$(d\gamma/dt)_{cm_j}$	Log $\frac{(d\gamma/dt)_j}{(d\gamma/dt)_i}$	$\frac{T_j - T_i}{T_j T_i} \times 10^5$
1	.98	.82	100	195	373	468	1.1	4.55	.617	.5442
2	.959	.799	125	200	398	473	2	4.65	.366	.3984
3	.92	.765	150	212.5	423	423	3	4.9	.213	.3043
4	.897	.7474	162.5	220	435.5	493	3.5	5.1	.163	.2678
5	.866	.722	175	230	448	503	3.9	5.2	.125	.2441
6	.835	.696	187.5	237.5	460.5	510.5	4.4	5.35	.085	.2127
7	.804	.67	200	247.5	473	520.5	4.65	5.35	.061	.193
8	.773	.644	212.5	255	485.5	528	4.9	5.45	.046	.166
9	.732	.61	225	267.5	498	540.5	5.15	5.55	.032	.1579
10	.693	.577	237.5	277.5	510.5	550.5	5.35	5.6	.0198	.1423
11	.66	.55	250	285	523	558	5.35	5.55	.01594	.1199
12	.588	.49	275	305	548	578	5.5	5.7	.0155	.0947
13	.505	.42	300	325	573	598	5.6	5.2	-.032	.073

Note Ratio = 1.2

Table D-20 Data points for 40%sand-40%silica powder-20%oil, Peak # 2

Point #	γ_i	γ_j	T_i °C	T_j °C	T_i °K	T_j °K	$(d\gamma/dt)_{cm_i}$	$(d\gamma/dt)_{cm_j}$	$\text{Log}\frac{(d\gamma/dt)_j}{(d\gamma/dt)_i}$	$\frac{T_j - T_i}{T_j T_i} \times 10^5$
1	.3814	.32	400	419	673	692	4.4	2	.2798	.429
2	.361	.3	406.5	422.5	679.5	695.5	5.9	8.8	.17	.339
3	.34	.238	412.5	426.5	685.5	699.5	5.9	8.5	.1736	.292
4	.319	.266	418.75	428	691.75	701	7	7.6	.035	.191
5	.28	.24	425	435	698	708	8.7	5.6	-.34	.202

Note Ratio = 1.2

Table D-21: Data points for 40%sand-40%silica powder-20%oil, Peak # 3

Point #	γ_i	γ_j	T_i °C	T_j °C	T_i °K	T_j °K	$(d\gamma/dt)_{cm})_i$	$(d\gamma/dt)_{cm})_j$	$\text{Log} \frac{(d\gamma/dt)_j}{(d\gamma/dt)_i}$	$\frac{T_j - T_i}{T_j T_i} \times 10^5$
1	.196	.163	462.5	480	735.5	753	2.9	3.8	.11738	.316
2	.175	.146	475	487.5	748	760.5	3.5	4.3	.0893	.22
3	.146	.122	487.5	495	760.5	768	4.3	4.8	.048	.128
4	.1134	.094	500	505	773	778	4.98	5	.0017	.083
5	.074	.061	512.5	517.5	785.5	790.5	5.1	4.95	-.012	.081
6	.041	.034	525	530	798	803	4.4	3.9	-.0523	.078
7	.13	.11	493.75	500	766.75	773	4.7	4.98	.025	.105
8	.093	.077	506.25	510	779.25	783	5.1	5	-.013	.061

Note Ratio = 1.2

Table D-22: Data points for 40%sand-40%clay-20%oil, Peak # 1

Point #	γ_i	γ_j	T_i °C	T_j °C	T_i °K	T_j °K	$(d\gamma_{cm}/dt)_i$	$(d\gamma_{cm}/dt)_j$	$\text{Log}\ \frac{(d\gamma/dt)_j}{(d\gamma/dt)_i}$	$\frac{T_j - T_i}{T_j\ T_i} \times 10^5$
1	.9785	.815	100	195	373	468	.75	3.9	.716	.5442
2	.955	.796	125	202.5	398	475.5	1.65	4.35	.421	.4095
3	.938	.782	137.5	210	410.5	483	2.0	4.55	.356	.3657
4	.92	.7658	150	212.5	423	485.5	2.45	4.65	.2783	.3043
5	.9	.75	162.5	217.5	435.5	490.5	2.8	4.7	.2249	.2575
6	.869	.72	175	225	448	498	3.4	4.9	.1587	.2241
7	.836	.696	187.5	235	460.5	508	3.8	5.05	.1235	.203
8	.81	.675	200	240	473	513	4.27	5.25	.089	.1648
9	.7658	.638	212.5	250	485.5	523	4.65	5.5	.73	.1477
10	.72	.6	225	260	498	533	4.9	5.7	.065	.1319

Note Ratio = 1.2

Table D-23: Data points for 40%sand-40%clay-20%oil, peak # 2

Point #	γ_i	γ_j	T_i °C	T_j °C	T_i °K	T_j °K	$(d\gamma_{cm}/dt)_i$	$(d\gamma_{cm}/dt)_j$	Log $\frac{(d\gamma/dt)_j}{(d\gamma/dt)_i}$	$\frac{T_j - T_i}{T_j T_i} \times 10^5$
1	.519	.433	281.25	302	556.25	577	6.2	7.15	.0619	.651
2	.495	.413	287.5	305	562.5	580	6.2	7.75	.096	.54
3	.471	.393	293.75	310	568.75	585	6.7	8.1	.0825	.492
4	.44	.367	300	315	575	590	7.1	8.3	.067	.445
5	.417	.347	306.25	320	581.25	595	7.8	8.8	.052	.4
6	.381	.317	312.5	325	587.5	600	8.3	8.5	-.012	.357
7	.357	.298	318.75	327.5	593.75	602.5	8.9	8.2	-.0356	.246
8	.3095	.26	325	335	600	610	8.5	7.5	-.0543	.275

Note Ratio = 1.2

Table D-24 : Data points for 40%sand-40%clay-20%oil, peak # 3

Point #	γ_i	γ_j	T_i °C	T_j °C	T_i °K	T_j °K	$(d\gamma_{cm}/dt)_i$	$(d\gamma_{cm}/dt)_j$	$\text{Log} \frac{(d\gamma/dt)_j}{(d\gamma/dt)_i}$	$\frac{T_j - T_i}{T_j T_i} \times 10^5$
1	.862	.784	412.5	425	685.5	698	2.2	2.5	.05552	.261
2	.86	.782	425	437.5	698	710.5	2.5	2.8	.049	.252
3	.854	.7764	437.5	449	710.5	722	2.8	3.05	.037	.224
4	.85	.773	450	457.5	723	730.5	3.1	3.15	.0069	.142
5	.846	.7691	462.5	475	735.5	748	2.95	3.2	.036	.227
6	.842	.7655	475	495	748	768	3	1.2	-.39	.348

Note Ratio = 1.1

Table D-25: Data points for 80%burned clay-20%oil, Peak # 3

Point #	γ_i	γ_j	T_i °C	T_j °C	T_i °K	T_j °K	$(d\gamma_{cm}/dt)_i$	$(d\gamma_{cm}/dt)_j$	$\text{Log} \frac{(d\gamma/dt)_j}{(d\gamma/dt)_i}$	$\frac{T_j - T_i}{T_j T_i} \times 10^5$
1	.225	.1875	425	447.5	698	720.5	1.95	2.75	.15	.447
2	.206	.172	437.5	462.5	710.5	735.5	2.4	3.45	.157	.478
3	.1863	.1553	450	467.5	723	740.5	2.9	3.6	.093	.327
4	.167	.14	462.5	472.5	735.5	745.5	3.5	3.75	.0299	.182
5	.1373	.114	475	485	748	758	4.1	4.25	.0156	.176
6	.098	.082	487.5	500	760.5	773	4.3	4.2	-.01022	.213
7	.0784	.065	500	510	773	783	4.2	3.5	-.0792	.165
8	.049	.041	512.5	522.5	785.5	795.5	3.1	2.3	-.129	.16

Note Ratio = 1.2

Appendix E

In this Appendix a sample calculation will be presnted for applying the Ratio method to the produced TGA thermograms. The Ratio method will be applied for a matrix which showed a weight loss with temperature, as well as for the matrix which did not show any weight loss with temperature. also, a sample calculation will be presented for appling the DSC equation for the DSC produced thermograms.

E-1 Sample calculation for matrix which did not show any weight loss with temperature

The following sample calculation can be applied to any matrix which did not show weight loss with temperature such as,

fine silica powder, sand, or a mixture of both. Also, for burning crude oil alone the following procedure was applied:

1- A choice of ratio was selected - the choice of the value of the ratio depends on the temperature range in which the peak occurs. Narrow peaks require a small ratio to get as many points on the thermogram as possible, while wide peaks require a relatively large value of ratio. Ratio was kept constant for each peak.

2- Figure E-1 presents a TG and DTG sample thermogram. The procedure of calculation was as follows:

   a- Choose any point, I, on the thermogram where the temperature is T_i.

   b- Measure the length, K, which will present the value of $(dy/dt)_i$.

   c- From the TG curve obtain the readings, B and A, which correspond to the weight loss at point I, and the total weight loss due to the complete burning of the crude oil.

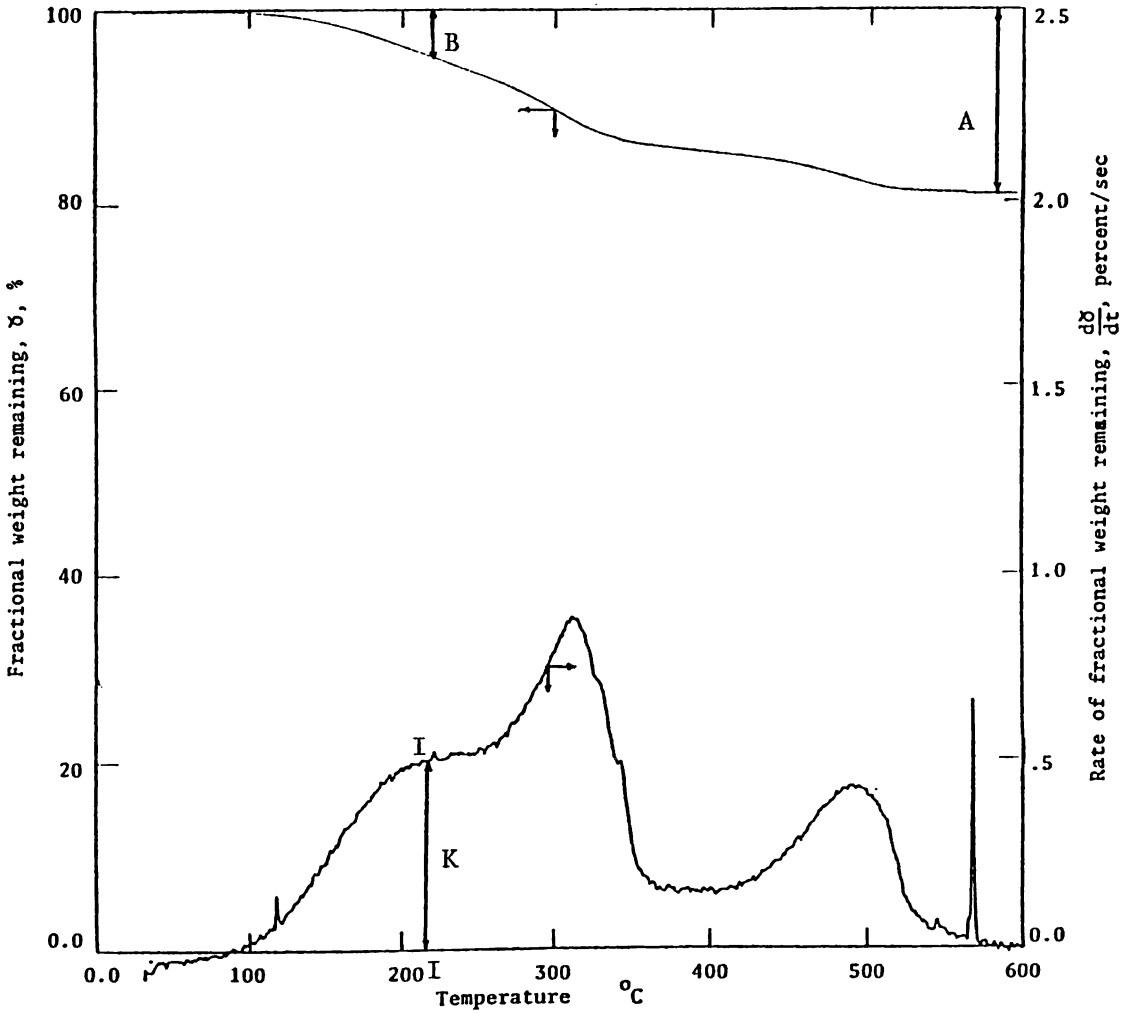

Figure E-1 TG and DTG curves for heating of crude oil in the presence of matrix with no weight loss with temperature

d- Calculate the γ_i fraction remaining as follows:

$$\gamma_i = \frac{A - B}{A}$$

e- Obtain γ_j by dividing γ_i by the previously selected ratio.

f- Determine weight loss, C, at point J on the thermogram as follows:

$$\gamma_j = \frac{A - C}{C}$$

g- Find the length C on the TG curve and determine T_j.

h- Obtain the reading of $(d\gamma/dt)$ at point j from the DTG thermogram.

For simpelicity the new value of $d\gamma/dt$ is designated as M.

i- Repeating the same procedure several times, a plot of

$$\log (M/K) \quad \text{VS.} \quad \frac{(T_j + 273) - (T_i + 273)}{(T_j + 273)\ (T_i + 273)}$$

will yield a straight line.

E-2 Sample calculation for a matrix which shows weight loss with temperature

This sample calculation can be applied for any matrix which shows weight loss with temperature such as, clay. In this case, the curves from the TGA run of heating the matrix was overlapped on the curve from the TGA run of the matrix mixed with oil. Figure E-2 presents a sample overlapped thermograms. The same procedure as in part A was applied, but the readings between the two corresponding curves were taken.

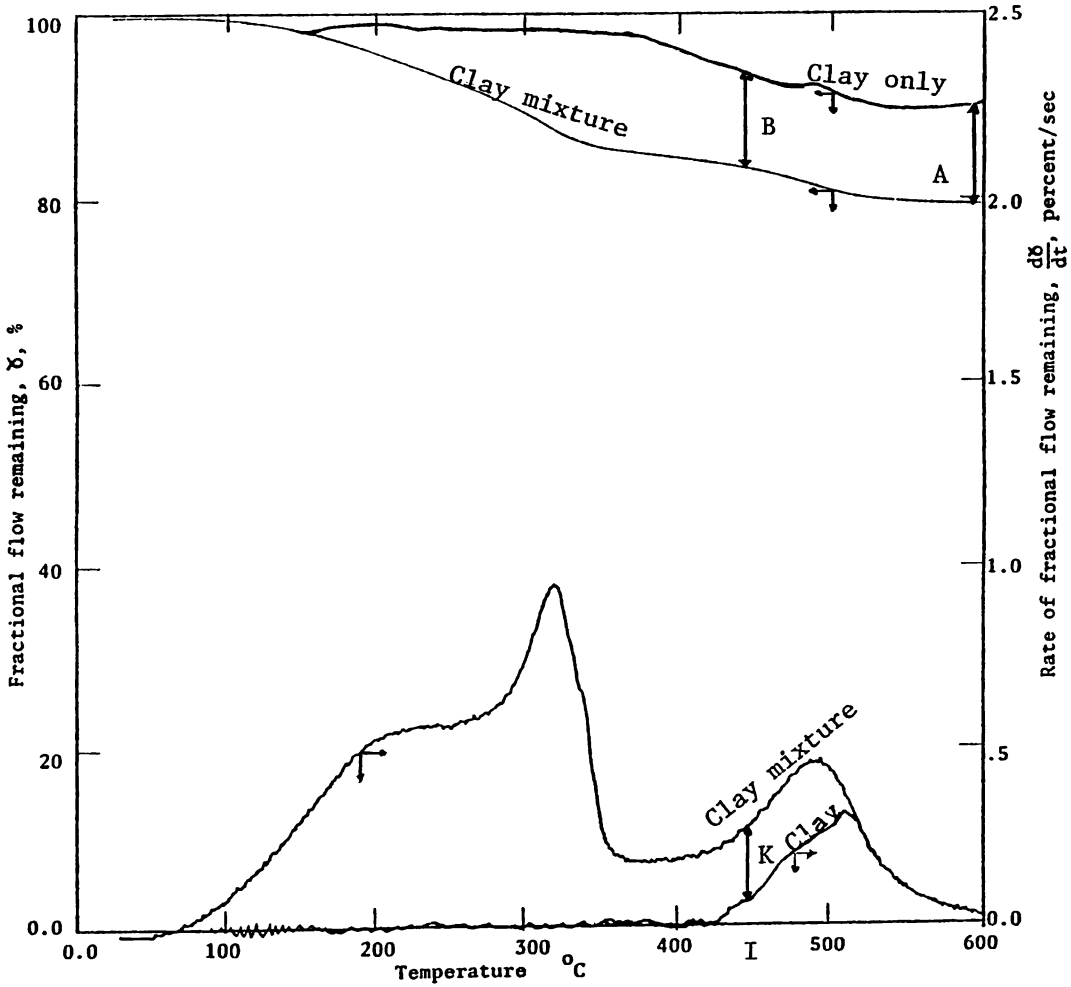

Figure E-2 Overlapped TG and DTG thermograms for heating of clay and crude oil in the presence of clay

E-3 Sample calculation for calculating heat values from DSC thermograms

The heat value for Figure 7-23 (80% sand - 20% oil) peak number 1 will be calculated.

1- From Figure 7-23

onset temperature = $275^{o}C$

end temperature = $387.5^{o}C$

area under peak #1 = 2.77 cm^2

Total amount of oil in the sample = oil weight % X total sample wt.

= 0.2 X 17.2

= 3.44 mg

2- From Figure 7-4 (80% sand - 20% oil), TGA run, the percentage of weight loss corresponding to the temperature range ($275^{o}C$ - 387.5^{o}) = 28.6 %. Therefore,

Amount of oil lost at this peak = .98 mg.

B = 5 min/cm from experimental setting.

E = .115 mw/mv from Figure C-1 Appendix C.

Δq_s = 20 mv/cm from experiment setting.

This E value corresponds to the temperature of $275^{o}C$ which is considered to be the onset temperature of the reaction peak.

Then, by using equation (B-4)

$$\Delta H = \frac{2.77}{.98} \quad (60 \text{ X } 5 \text{ X } .115 \text{ X } 20)$$

= 1946.03 J/gm

= 464.93 cal/gm